Universitetet
i Stavanger

FACULTY OF SCIENCE AND TECHNOLOGY

MASTER'S THESIS

Study programme/specialization: Petroleum Engineering/Well Engineering	Spring semester, 2020 Open
Author: Beate Aas	…………………………………… (signature of author)
Faculty supervisor: Bernt Sigve Aadnøy External supervisor: Thor Paulsen - Equinor	
Title of master's thesis: Dynamic Acceptance Criteria for Periodic Testing of Downhole Safety Valves	
Credits: 30	
Keywords: DHSV Acceptance Criteria Leakage Test Interface Fiber Optics Echo Sounding	Number of pages: 96 + supplemental material/other: 13 Stavanger, 15.06.2020

(Page left intentionally blank)

Acknowledgements

First, I would like to thank my supervisor in Equinor, Thor Paulsen. He was the one who provided the idea and the problem for the thesis. Throughout the semester he has also shown to be of great support and provide good feedback all the way. I am grateful for all his help.

Then I would like to thank my supervisor at the University of Stavanger, Bernt Sigve Aadnøy. He has provided me with great support throughout the semester and have had a lot of good ideas that improved the thesis. I am grateful for all his help.

I would also like to thank Håkon Sunde Bakka in Equinor. I am grateful for all his help regarding the Fiber Optic sections in the thesis and for providing the initial idea that formed the MATLAB code.

Then I would like to thank another professor at the University of Stavanger, Kjell Kåre Fjelde. He provided a lot of good ideas regarding the MATLAB code developed for the thesis and provided great support to form the code.

I would also like to thank Morten Kvernvold, CEO of ScanWell, for providing me with useful data needed for the Echo Sounding sections.

Then I would like to thank my colleagues in Equinor. They have been of great assistance and support throughout the semester. They have provided me with good ideas, and some have helped a lot regarding data gathering and evaluation of data.

Finally, I would like to thank my friends, family, and fellow students for believing in me and supporting me both prior to and throughout the thesis work. I would especially like to thank my partner for always supporting and believing in me.

(Page left intentionally blank)

Abstract

Downhole Safety Valves (DHSVs) are periodically leak tested as part of the preventative maintenance program on an oil and gas producing facility. The last couple of years, the oil and gas industry on the Norwegian Continental Shelf (NCS) has experienced too high failure fractions on the periodic leak testing of DHSVs. From this result it is believed that refining the way the acceptance criteria is calculated today might reduce this failure fraction. The thesis work therefore investigates the possibility of implementing a more accurate, more representative and more time-efficient method to calculate the acceptance criteria compared to the method used today. This is done by defining a Dynamic Acceptance Criteria (DAC) which includes the effect of gas and liquid variations in the testing volume.

The research methods used to investigate the thesis problems are divided into three main parts. The first part is the derivation of two equations that can be used to calculate DAC. One for testing volumes with high gas fractions, and another for testing volumes with high liquid fractions. For the second part, a code is developed to find the depth of the interface between gas and liquid in the well based on given input. Results from the code are further used to calculate the different gas or liquid fractions. The third part investigates the use of different measurement methods. The methods are evaluated based on their potential of locating the gas and liquid interface in the well. These methods are Fiber Optics and Echo Sounding.

A small study is performed to investigate the impact of using DAC. The method of using DAC proved to have a great potential for reducing the failure fraction of DHSV leakage tests. There are, however, a lot of uncertainties regarding the method. Further research combined with a more representative study is recommended.

From the research methods, the use of the DAC is concluded to be more representative for the periodic leak tests of DHSVs. This is compared to the acceptance criteria used to evaluate DHSV leakage tests today. Further, it is concluded that using DAC will result in a more time-effective operation for the testing procedure of the DHSV. Finally, it is unclear whether the DAC is more accurate or not compared to the acceptance criteria used today. The accuracy of DAC must therefore be further researched before DAC can be implemented to evaluate real periodic DHSV leakage tests.

(Page left intentionally blank)

Table of Contents

List of Tables

List of Figures

List of Appendix Figures

List of Abbreviations

API	American Petroleum Institute
ASV	Annulus Safety Valve
CAPEX	Capital Expenses
DAC	Dynamic Acceptance Criteria
DAS	Distributed Acoustic Sensing
DTS	Distributed Temperature Sensing
DHSV	Down Hole Safety Valve
ESCSSV	Electric Surface Controlled Subsurface Safety Valve
HC	Hydrocarbon
HMV	Hydraulic Master Valve
ID	Inner Diameter
ISO	International Organization for Standardization
LAN	Local Area Network
LL	Liquid Level
NCS	Norwegian Continental Shelf
NORSOK	The Norwegian shelf‘s competitive position
OD	Outer Diameter
OPEX	Operational Expenses
PM	Preventative Maintenance
PSA	Petroleum Safety Authority
PVT	Pressure-Volume-Temperature
PWV	Production Wing Valve
RKB	Rotary Kelly Bushing
RNNP	Trends in Risk Level in the Petroleum Activity
SAC	Static Acceptance Criteria
SCSSV	Surface Controlled Subsurface Safety Valve
SPM	Side Pocket Mandrel
SSCSSV	Subsurface Controlled Subsurface Safety Valve
SV	Swab Valve
TH	Tubing Hanger
TRSV	Tubing Retrievable (Surface Controlled Subsurface) Safety Valve
WBE	Well Barrier Element
WBS	Well Barrier Schematic
WH	Wellhead
WRSV	Wireline Retrievable (Surface Controlled Subsurface) Safety Valve
XO	Crossover
XT	Christmas Tree

1 Introduction

The thesis investigates the use of acceptance criteria during Down Hole Safety Valve (DHSV) leakage tests. Calculations of the acceptance criteria today is based on a gas filled volume above the DHSV. The thesis will introduce a gas-liquid ratio into these calculations. Relevant and important theory is presented to fully understand the thesis work. The main part consists of calculations and coding in order to research the thesis problem. As the gas-liquid ratio is not applicable for water injection wells, this well type is not discussed in this thesis.

1.1 Background

The oil and gas industry is an evolving industry. It started off with drilling shallow wells and has evolved into drilling deep wells in harsh environments. This development increases the risks related to the operations. Hence, it increases the importance and awareness of safety.

It is no secret that there have been some major accidents in the oil and gas industry. Some well-known accidents are for instance Macondo and Piper Alpha. In both cases there where unfortunately loss of human lives and a spill to the environment. Smaller accidents and major accidents like these will result in an increased focus on safety. Today there are also an increasing focus for more environmentally friendly operations. This affects how safety regulations, standards and guidelines have evolved over the years.

For the Norwegian oil and gas industry, the NORSOK standard is important to ensure safe and cost-effective operations on the Norwegian Continental Shelf (NCS). Originally, NORSOK is the abbreviation for "The Norwegian shelf's competitive position" [1]. This standard provides guidelines or references to other standards, such as International Organization for Standardization (ISO) standards and American Petroleum Institute (API) standards. The NORSOK standard was first published in 1994 and has since been an important part of the Norwegian oil and gas industry. It currently consists of 79 different standards. One of them, NORSOK D-010 rev. 4, is the one used in the thesis. All references to NORSOK throughout the thesis are directed at this one. A new revision of this standard is to be published during 2020. [1]

A key element to ensure safe operations of a well is to understand the important aspect of barriers. Figure 1.1 illustrates a simple well barrier schematic (WBS) figure of a well in operation (to the left) and a well during drilling operation (to the right). The barrier philosophy

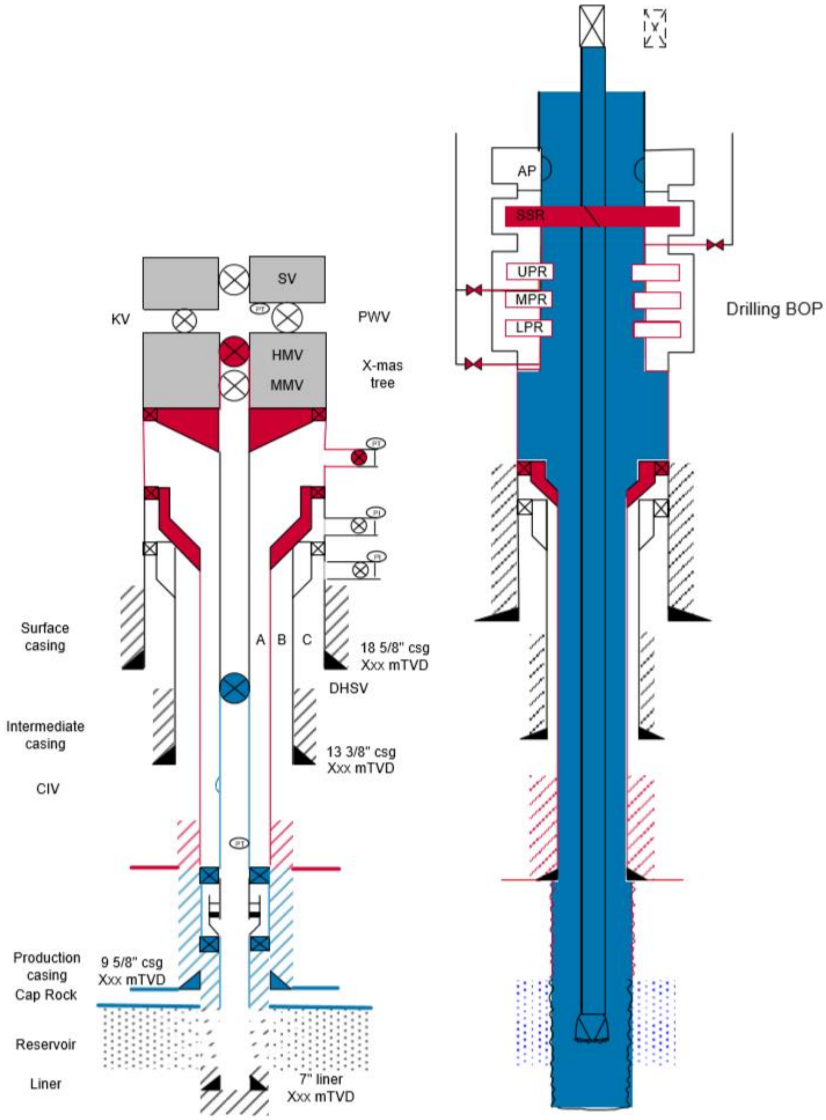

Figure 1.1 WBS figure for production phase – left,
WBS figure for drilling phase – right [2]

is to always have two barriers for every phase of the life cycle of the well. This means that there is a separate WBS for drilling operation, production phase, intervention activities and for Plug and Abandonment (P&A) operation. The barriers are marked in the figure as blue for primary barrier, and red for secondary barrier. These barriers consist of different well barrier elements (WBE). The barriers are referred to as barrier envelopes. Examples of typical WBEs can for instance be cement, tubing, casing, BOP, drilling fluid or the DHSV. As seen to the left in Figure 1.1, the DHSV is a part of the primary barrier. Hence it is a part of the first barrier envelope to stop uncontrolled release of production fluid from the well. [2, 3]

1.2 Motivation

All petroleum related operations on the NCS and offshore Norway are regulated by the Norwegian Petroleum Safety Authority (PSA). This includes both offshore and land facilities in addition to subsea pipelines. This means that PSA follows up on all activities performed on the NCS and provide guidelines and frames regarding safety of all operations. They are responsible for the working environment, safety, security and preparedness for emergencies for the Norwegian oil and gas industry. [4]

The PSA annually publishes a report referred to as RNNP. This report is called *Trends in risk level in the petroleum activity*, and the abbreviation RNNP is a result of the Norwegian name *Risikonivå i norsk petroleumsvirksomhet*. The report is based on data collection and analysis and has since 1999 been used to measure the development of risk level in the Norwegian oil and gas industry. The report covers both technical risks and risks to humans. It is important for the PSA regarding further planning and development of regulations. There are several contributors for this report. Amongst them are the PSA and the operating companies on the NCS. The operating companies provides data from their facilities. [5]

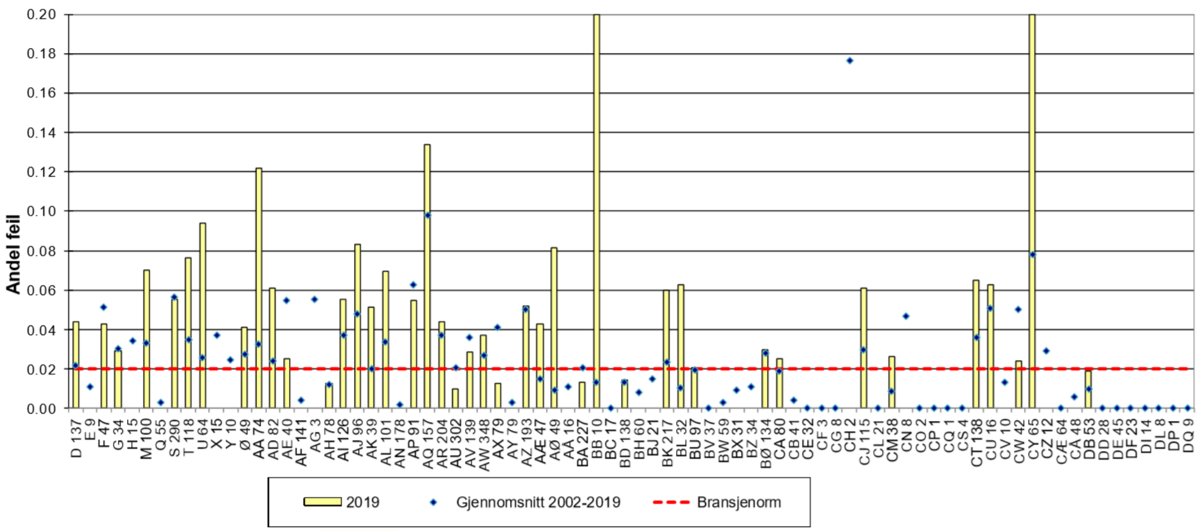

Figure 1.2 Failure fraction of DHSVs per facility (reproduced with permission) [6]

The results from the RNNP report forms the motivation for the thesis. The latest RNNP report (*RNNP 2019*) was published in April 2020. Some of the results from this report is presented here in Figure 1.2. This figure is the same as Figure 7-18 in the *RNNP 2019* report. The figure illustrates failure fraction of DHSVs on different installations. The failure fraction represent the number of DHSV tests performed, with results outside the acceptance criteria, divided by total number of performed tests on that specific installation. The failure fraction scale is plotted as the y-axis in the figure. The yellow bars illustrate failure fraction of DHSVs per installation for 2019. The blue dots illustrate the average failure fraction of DHSVs per installation from 2002 to 2019. The red line marked along 0.02 illustrates the 2% limit of reliability for the DHSV. The DHSV is a safety critical vale and shall therefore not have a failure rate above this red line [3]. This will be further explained in Chapter 2.1. From Figure 1.2 it is clear to see that several installations have a higher failure rate of DHSVs than desired. In fact, the graph shows that 35 of the 80 installations were above the 2% limit in 2019. 38 of the 80 installations were above the 2% limit for average failed valves from 2002 to 2019. This shows that just below 50% of all the installations has DHSV failures above the 2% limit. [6]

The *RNNP 2019* report illustrates too high failure rate of DHSVs. This proves that the failure rate of DHSVs are too high, and that this is a problem for the Norwegian oil and gas industry in general. This is therefore the main motivation for looking closer at the DHSV testing. Too high failure rate affects the reliability of the barrier hence the safety of the operation. When looking closer at reasons for possible DHSV fails, there are many different aspects to be investigated. Therefore, the thesis only focuses on one of these aspects. Namely the acceptance criteria. The NORSOK D-010 standard, Rev 4, states on page 72 that: "The liquid/gas composition above the valve(s) to be tested should be known. If the composition is not known, the worst case composition scenario shall be used. For gas-liquid combinations special calculation formulas should be developed." [3]. The most common method today is to use the worst-case scenario from NORSOK, where the volume above the valve is 100% gas filled. The thesis investigates if the method used to calculate the acceptance criteria today is too strict or too conservative and can be the reason for some of the failed DHSV tests. This will all be investigated in a form that has digitalization of these tests as a main goal. This means that the effect of liquid and gas ratio will be introduced.

1.3 Thesis Problem

The thesis work investigates the possibility to use an acceptance criteria where the effect of gas-liquid ratio in the well during the DHSV test is included. The thesis work is based on the acceptance criteria today and investigates the following:

- If a dynamic acceptance criteria will improve the accuracy of periodic testing of downhole safety valves
- If a dynamic acceptance criteria will result in a more cost-effective operation

- If it is possible to construct a dynamic acceptance criteria that is more representative for each test compared to the static acceptance criteria used today

1.4 Thesis Layout

The thesis is built up by six different parts. The layout of the thesis is illustrated in Figure 1.3. Part one contains information regarding the DHSV. It includes mainly information about the design and function of different DHSVs and how the DHSV is tested against leaks. The next section, part two, explains the acceptance criteria. It explains and illustrates how the acceptance criteria is used today and introduces the concept of Dynamic Acceptance Criteria (DAC). The DAC is the acceptance criteria where gas-liquid ratio is introduced. Part three contains information about different measurement methods. The main idea behind the use of measurement methods is that these can be used to locate the interface between gas and liquid in the well. Part four is about fluids. It explains different fluid behaviors and fluid properties involved in the calculations used today, but also in the calculations using DAC. Part five is the calculation section. The DAC calculations are investigated and performed in this section. The final part, part six, is about locating the interface in the well. Both calculating the depth and measuring the depth of the interface is investigated. Part five and six are therefore the main problem-solving sections of the thesis where the thesis problem is investigated, while the first four sections forms the basis.

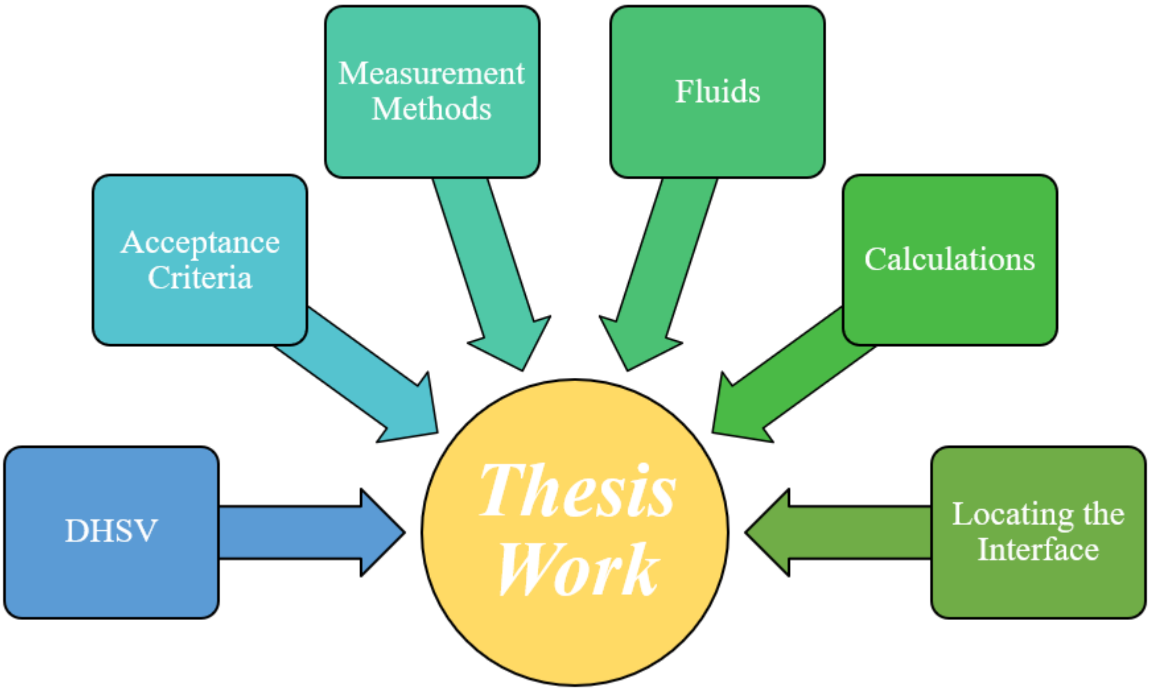

Figure 1.3 Thesis layout

(Page left intentionally blank)

2 Downhole Safety Valves, DHSV

The main objective of the thesis work is to investigate the possibility of improving the periodic tests of DHSVs. To understand the methods used later in the thesis, it is important to understand the function and design of the valve itself. It is also important to understand how the testing of the DHSV is performed and why the valve is such an important part of the well design. This will all be explained throughout this chapter.

2.1 Safety Critical Valve

DHSV is defined as a safety critical valve. Safety critical valves are valves that are a part of the emergency shutdown system of an installation. The valves are critical parts during an emergency. Some examples of such valves beside the DHSV is the Annulus Safety Valve (ASV), and Christmas Tree (XT) and wellhead (WH) valves, such as Hydraulic Master Valve (HMV), Production Wing Valve (PWV) and different valves serving the gas lift valve and the chemical injection line [3]. These safety critical vales are marked blue in Figure 2.1.

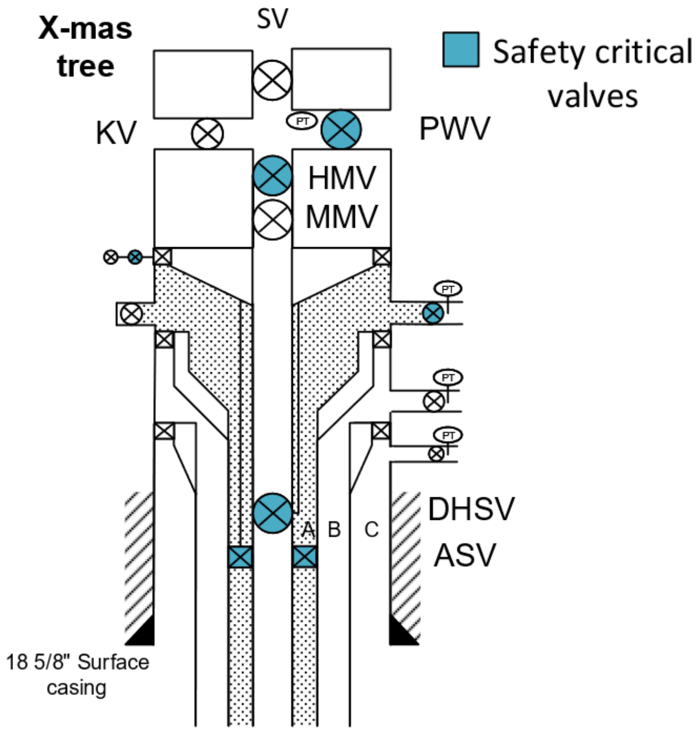

Figure 2.1 Safety critical valves

A safety critical valve is a WBE that is critical to function during an emergency. Due to this there are stricter regulations and recommendations when handling them. For instance, failure rate of safety critical valves is monitored closely. If testing reveals a failure rate of 2% on a safety critical valve type over a year on one installation, measures must be implemented in order to increase the reliability of the safety critical valve type in general [3]. This is one of the motivations of the thesis.

From a barrier envelope perspective, the DHSV is a part of the primary barrier. It is a part of the first barrier to stop the flow from the well. In a worst-case scenario where the top of the well, including WH and XT, are damaged, the DHSV might be the only valve to prevent the formation fluids from escaping the well. This is one of the reasons why the DHSV is such a safety critical part of the installation.

2.2 Design and Function

DHSV is an essential part of the well design for most wells. It is installed in the upper part of the well as a part of the completion. It is placed at least 50 m below the seabed for offshore wells [3]. If there is hydrate potential in the well, the DHSV should be installed below the potential hydrate formation depth [3]. The valve has a fail-safe mechanism that closes the valve in case of an emergency on the platform or vessel above the well [7].

The DHSV is an element that is known by several names. For simplicity, the valve will be addressed as DHSV in the thesis. It is only in this chapter, where the different types of DHSVs is explained, that other abbreviations are used. Some of the abbreviations for different DHSVs are listed in table 2.1. An explanation and simplified abbreviation used in the thesis is

Table 2.1 Overview of DHSV abbreviations

Common abbreviations	Expansions	Abbreviations used in thesis
SSC-SSSV	Subsurface Controlled Subsurface Safety Valve	SSCSSV
SC-SSSV	Surface Controlled Subsurface Safety Valve	SCSSV
ESCSSV	Electric Surface Controlled Subsurface Safety Valve	ESCSSV
TR SC-SSSV	Tubing Retrievable Surface Controlled Subsurface Safety Valve	TRSV
WR SC-SSSV	Wireline Retrievable Surface Controlled Subsurface Safety Valve	WRSV

also presented. The top three rows marked blue, in table 2.1 are three DHSV types. The bottom two rows marked white, are two different DHSVs based on retrieval method. All are explained in Chapters 2.2.1. to 2.2.4.

2.2.1 Subsurface Controlled Sub Surface Safety Valve, SSCSSV

The Subsurface Controlled Subsurface Safety Valve (SSCSSV) is installed after completion and is as the name suggest controlled from the subsurface. This means that the well flow will decide whether the valve stays open or closed. The flow velocity needed to close the valve is a predetermined parameter. If the velocity of the well flow becomes higher than the predetermined value, the valve will close. One example where the SSCSSV would close is if a failure on the surface results in an increased flow from the reservoir. [8] SSCSSV were the first kind of DHSVs used. It was developed during the 1930s. The modern safety valve was evolved from this. SSCSSV was in the beginning used in wells during hurricane season in the Gulf Coast. Since the valve was used during storms it was sometimes referred to as “Storm Chokes”. [8]

The thesis will not go more into details of these types of DHSVs. According to NORSOK D-010, the DHSVs used today should be surface controlled [3]. Therefore, the thesis will focus on surface controlled DHSVs.

2.2.2 Surface Controlled Subsurface Safety Valve, SCSSV

The Surface Controlled Subsurface Safety Valve (SCSSV) is as the name suggest, controlled from the surface. The function of the SCSSV is illustrated in Figure 2.2. The illustration in the figure is a part of a figure created by Baker Hughes Inc to illustrate different completion equipment [9].

The SCSSV is controlled using a hydraulic control line. The hydraulic control line is as the name suggest controlling the valve. It controls whether the valve is opened or closed. The control line is connected to both the SCSSV in the well and to monitors at the surface. It is fastened to the outside of the tubing along the well using clamps. To ensure flexibility of the control line, the line is often twirled around the tubing. This means that any movements of the tubing, for instance expansion due to heat, will not affect the control line. Since the control line in this case is connected to a DHSV, it is not recommended to splice the control line to pass through a packer or valve. This is the reason why the ASV is installed deeper than the DHSV in the well. Due to the control line being such an important part of the DHSV, both the valve and the control line is pulled if the control line fails. However, it is only the control line that is replaced, not the valve itself. [8, 10]

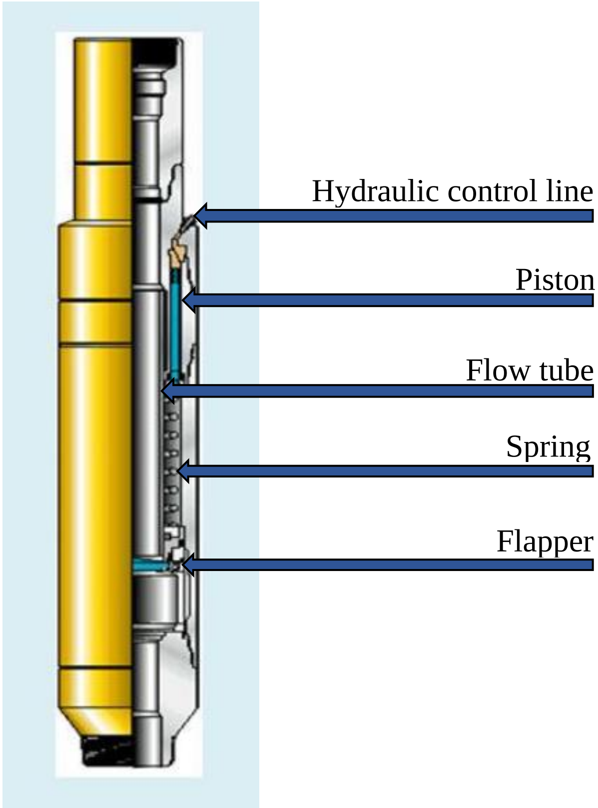

Figure 2.2 Illustration of DHSV in Closed Position [9].
The figure presented her is a part of the original figure with labels and arrows added.

The hydraulic control line is an essential part of the SCSSV. Hydraulic fluid is injected into the control line at surface when the valve is to be opened. Figure 2.2 illustrates the closed position of the valve. Pressure on the control line increases as the line fills up and injection into the line continues. The hydraulic fluid is transported from the control line and into a chamber. As this chamber fills with hydraulic fluid, it will push on a piston that results in compression of a spring. As this happens, a flow tube within the valve will start to move down. This flow tube is the part that opens the valve. The valve itself can either be a ball valve or a flapper valve. A ball valve will be opened by turning, while a flapper valve will be opened by the flow tube pushing on it. This means that the valve is opened downwards. When the valve is to be closed, the operation is reversed. Pressure on the hydraulic line is reduced to zero. This results in reduced pressure on the piston, and the spring is then decompressed, which causes the flow tube to move upwards. The valve is then closed and will not open again until the control line is pressured up and the process starts again. [8]

Opening a DHSV against reservoir flow requires high amount of hydraulic pressure. To make this easier, some DHSVs are equalizing valves. This means that the valve will not open until the pressure across the valve has been equalized. This is done by pushing the flow tube down on the flapper which opens an equalizing port. After equalization, the hydraulic pressure is increased and the flapper valve opened. [8]

2.2.3 Electric Surface Controlled Subsurface Safety Valve, ESCSSV

An electric version of the SCSSV has been desired in the oil and gas industry for several years. In 2017, an all-electric SCSSV called Electric Surface Controlled Subsurface Safety Valve (ESCSSV) was put to use and evaluated in an article regarding an all-electric well [11]. The findings of this article are presented in this section.

The ESCSSV presented in the paper function by replacing the mechanical piston driven by the hydraulic fluid pressure with an electric actuator. The actuator creates kinetic energy from electricity and provides the driving force for the valve. The mechanical fail-safe set up from conventional SCSSV is used for the ESCSSV. When the valve is commanded to, it will close. This is for instance used when the valve is leakage tested. The valve also closes during emergency situations or if it experiences loss of power. Hence, it functions in the same way as a conventional SCSSV. [11]

The advantages of using an ESCSSV compared to a conventional SCSSV are many. For instance, the ESCSSV has a position sensor installed. This sensor provides real-time data of the opening of the valve. It can tell if the valve is open, closed or in transition between opened and closed. The sensor also provides diagnostic information as for instance voltage and current of the line. Another advantage of the ESCSSV is that there is no need for hydraulic fluids. This eliminates the impact on the environment that a possible release of hydraulic fluid would have. The electric valve also has an advantage of lower costs. Both Capital Expenses (CAPEX) and Operational Expenses (OPEX) was lower for the all-electric well. This means that both the operational expenses and the maintenance and repair expenses were reduced. On the other side, the ESCSSV had a disadvantage. The paper presented this as the lack of a position indicator that was not electric. Hence an analog indicator. This is an area where the paper suggested that future advancements could be made. [11]

2.2.4 Retrievable Surface Controlled Subsurface Safety Valve

There are two types of SCSSVs regarding installation and retrieval. They are known as Tubing Retrievable Safety Valve (TRSV) and Wireline Retrievable Safety Valve (WRSV). Figure 2.3 presents the main differences between them.

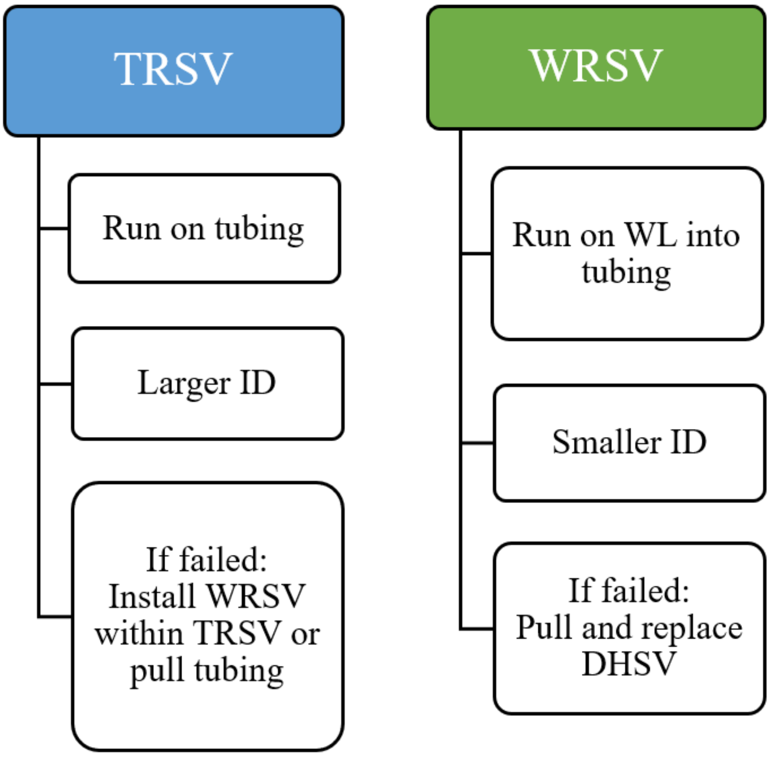

Figure 2.3 TRSV vs. WRSV

The TRSV is run on the tubing and is an integral part of it. This allows for a greater inner diameter (ID) through the valve compared to using a WRSV that is installed within the tubing. However, if the TRSV fails a WRSV can be installed within the TRSV, hence reducing the ID through the valve. Another way to deal with a failed TRSV is to retrieve the entire tubing. This means retrieving the upper completion of the well before installing the upper completion again with a new valve. Since the TRSV is a part of the tubing, it has the advantages of being more reliable and have a higher level of integrity compared to the WRSV. This is mainly due to the fact that the TRSV is integrated into the tubing, while the WRSV is held in place by a separate locking mechanism and the operation by hydraulic fluid under pressure is dependent on packer elements separating the hydraulic chamber and the wellbore. [8]

The WRSV is run on a wireline (WL) and placed within the tubing. This reduces the ID of the flow across the valve but makes it easier to replace the valve if it fails. Since the WRSV is placed within the tubing it will experience both turbulent flow and pressure drop. This leaves the valve more susceptible for scale formation which will affect the integrity of the valve. [8]

2.3 Completion Design

The completion design concerning DHSVs are composed of several factors. For instance, tubing size and setting depth. They both have an impact on the volume above the DHSV and below the XT, which is an important factor when calculating the acceptance criteria in Chapter 3. Both is therefore explained in this section.

The tubing size has an impact on the volume above the DHSV. When the tubing size increases, so does the volume. Common tubing outer diameters (ODs) on the NCS are $5^{1/2}$" and 7", and sometimes $9^{5/8}$" [12]. The effect of the different tubing sizes is illustrated in Figure 2.4. The figure shows that when the length is constant, it is only the tubing diameter that affects the volume. Different methods can be used to calculate this volume. Both tubing capacity, which is volume capacity per length, and area can be used for this. Both will give the same result. However, when calculating the volume, it is important to keep track of the units such that the volume is given in the desired unit.

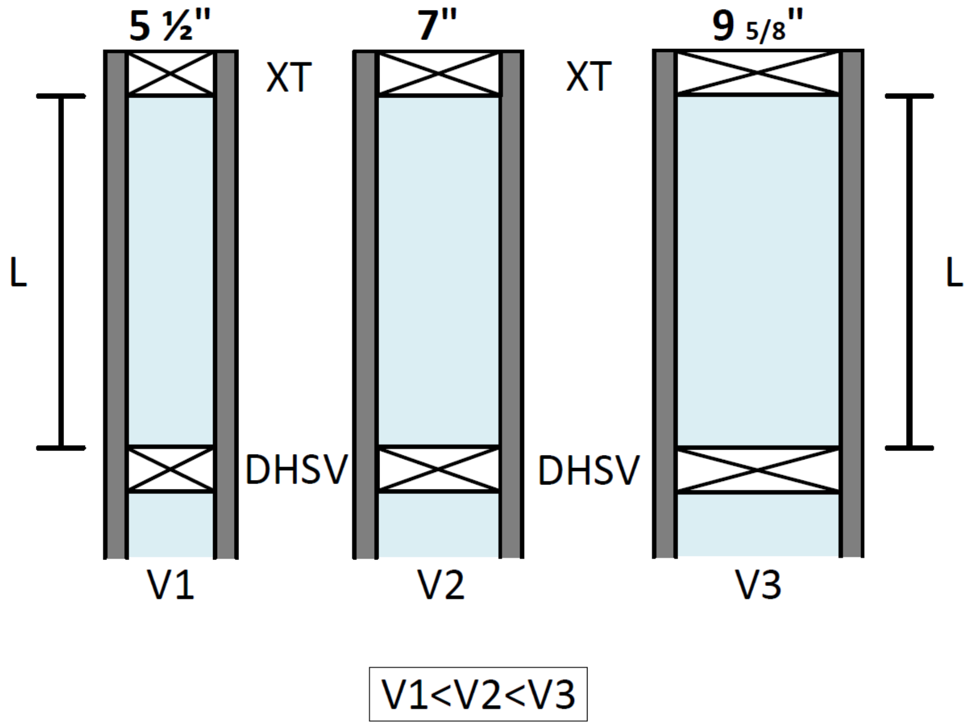

Figure 2.4 Different tubing sizes compared to volume

When determining the setting depth of the DHSV there are several parameters to consider. For instance, it shall be placed at least 50 m underneath the seabed for offshore wells, and considerations shall be taken concerning pressure and temperature with regards to hydrate formation, and wax and scale deposits [3]. In addition, NORSOK recommends that the valve is installed lower than the kick-off point in the well [3]. This is the point in the well where the inclination starts. The reason for this recommendation is to install the DHSV lower than any potential collision point from a nearby well that is being drilled. Setting depth calculations should be based on the highest density in the annulus when determining the maximum setting depth [3]. This means that the valve should not be placed too deep in the well. This is also due to fail safe functioning problems and that the volume of hydrocarbons (HCs) above the valve increases with increased depth. It also means that the valve should not be installed too shallow in the well. This is due to an increasing risk of formation of hydrates, and because the valve is the only way to close the well if something catastrophically happens to the topside facilities.

When installing the DHSV, only one valve is usually installed. However, there are some exceptions. Some wells, typical subsea wells, have two DHSVs installed after each other. Figure 2.5 shows a simplified example of the double DHSV layout. The figure is only a small cutout of a subsea well. The reason for using a double DHSV is for redundancy purpose only. This is used for wells with low accessibility for replacing a failed valve. Typically subsea wells. Although the well is installed with two DHSVs, only one is used at a time. The second one is only there in case the first valve fails. Hence, if one valve fails, it is possible to switch to the other valve without performing intervention on the well. However, using two DHSVs in one well does not increase the safety. It is purely an economical driven solution. [13]

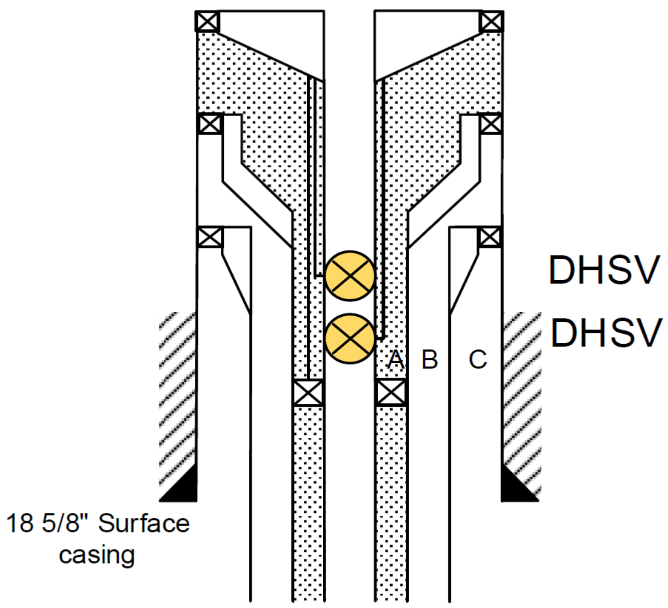

Figure 2.5 Double DHSV

2.4 Testing

Testing of WBEs is an important step to ensure integrity of the well. The WBE must be able to function properly to perform their barrier duty. This section will therefore explain the testing procedure of the DHSV element.

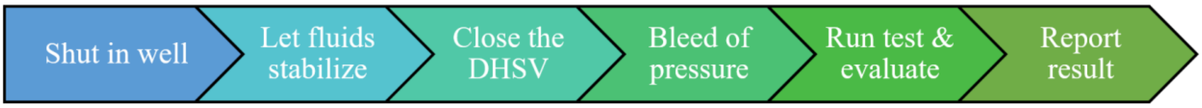

Figure 2.6 Operational testing procedure of DHSVs

The testing procedure of a DHSV is a step by step method [14]. The step by step method is illustrated in Figure 2.6. The first step is shutting in the well on the choke. This step can take around 30 minutes to avoid "shocking" the formation when shutting in the well. This stops the production, leaving the well filled with a formation fluid mix. The fluid can consist of oil, gas, or water, and it can also be a combination of them. This is illustrated in Figure 2.7. The figure illustrates the well during production, after shutting it in, and finally the stabilization process which is the next step.

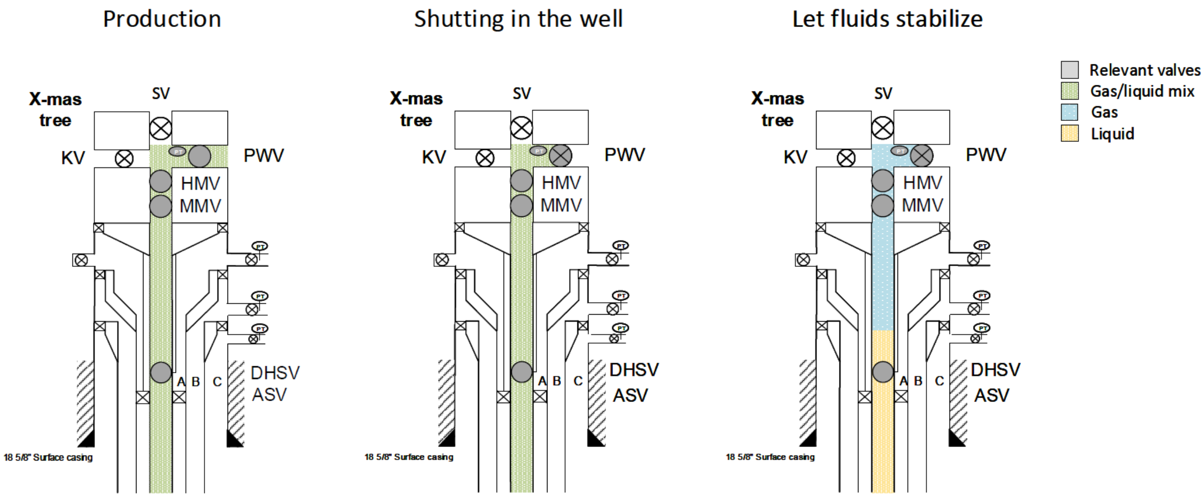

Figure 2.7 Production stage – left,
Shutting in the well – middle,
Fluid stabilization – right

During stabilization gas will accumulate at the top of the well, while any liquid will gather at the bottom. The stabilization process has no fixed time duration. It is only recommended in API RP 14B that the waiting time is minimum 5 minutes [14]. However, a longer waiting time is common. This is based on experience and can vary between 10 and 60 minutes. The stabilization stage is to ensure that the volume above the DHSV is mostly gas. This is done to ensure that the test is performed under as similar conditions as possible compared to the conditions that the acceptance criteria was calculated on, namely based on a 100% gas filled volume. However, if a more exact composition and ratio had been known there could perhaps have been a short and fixed time for this step. This shows room for improvements.

The next step of testing the DHSV is to close the valve itself. As mentioned, the control line pressure must be reduced to zero to close the valve. Closing the DHSV when the well is shut-in and the fluids in the well are mostly at rest, should only takes a couple of minutes. Although the DHSV is a safety critical valve, there is no requirements stating how quickly the valve should be able to close compared to the PWV and HMV. The closing of the DHSV is illustrated to the left in Figure 2.8.

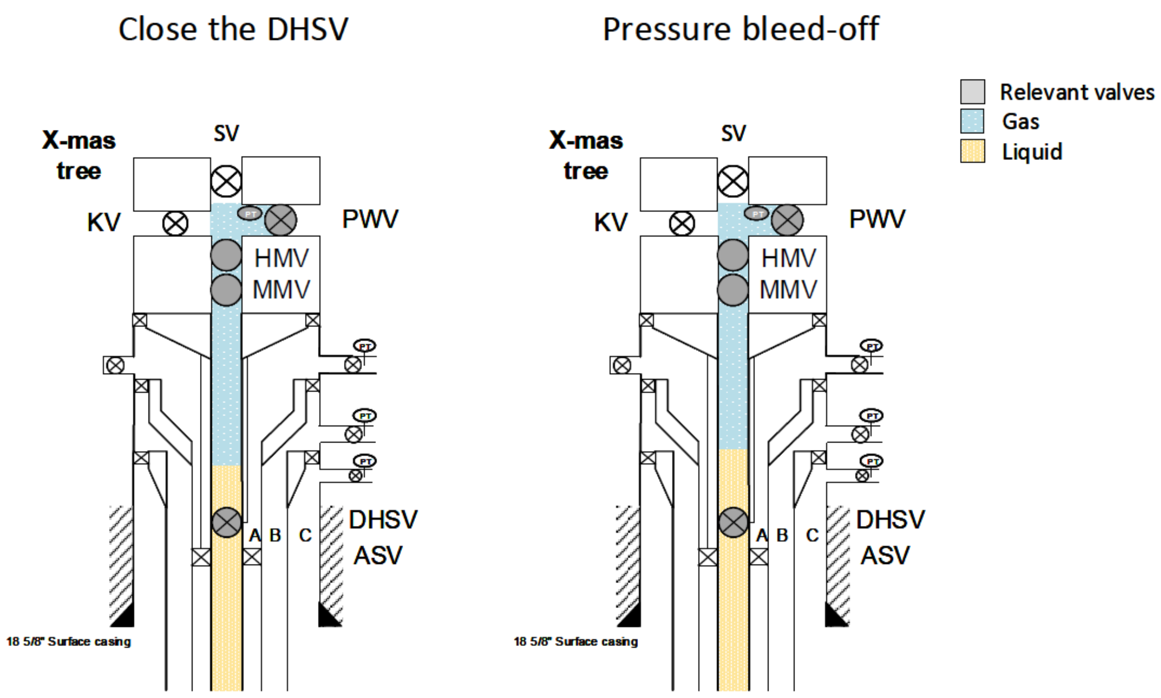

Figure 2.8 DHSV closing – left,
Pressure bleed-off – right

Closing the DHSV is followed by reducing the pressure between the DHSV and the XT. This is to create a differential pressure across the valve. Any leak through the valve will then be detected by an increase in pressure in the volume above the DHSV, measured at the WH. This is illustrated to the right in Figure 2.8. In order to create a high enough differential pressure, it is recommended in NORSOK D-010 to bleed down 70 bar to create a 70-bar differential pressure [3]. However, the DHSV can be tested with a lower differential pressure if the maximum pressure on the wellhead is below 70 bar, or if the acceptable leak rate is reduced due to reduced pressure [3]. This is recommended for all WBE that has an allowable leakage rate, such as the DHSV. Bleeding of 70 bar on a well is a time-consuming process, but a necessary process. [3] It can in some cases take up to 60 minutes to complete.

The next step, after bleeding down pressure above the DHSV, is to let the fluids stabilize again before running the leakage test. The stabilization time after bleeding off pressure will vary a lot but can in some cases take up to 30 minutes. This waiting time shows room for improvements in the same way as the previous stabilization time. Knowing the composition of the fluids in the volume can help reduce this waiting time. After the stabilization stage is finished, the leakage test of the DHSV starts. This is illustrated in Figure 2.9. Both illustrations look the same but represents different operation. The one on the left illustrates the stabilization process while the one to the right illustrates the leakage test. The testing time of the leakage test should be minimum 30 minutes according to NORSOK D-010 [3]. Sometimes it can be longer, like for instance 40 minutes instead. However, the test will be evaluated by a 30-minute testing period. During the testing period, the pressure is monitored closely for evaluation. The testing time of 30 minutes is used for HC wells. However, in the industry a testing time of 10 minutes is more common to use for water wells such as water injectors [15].

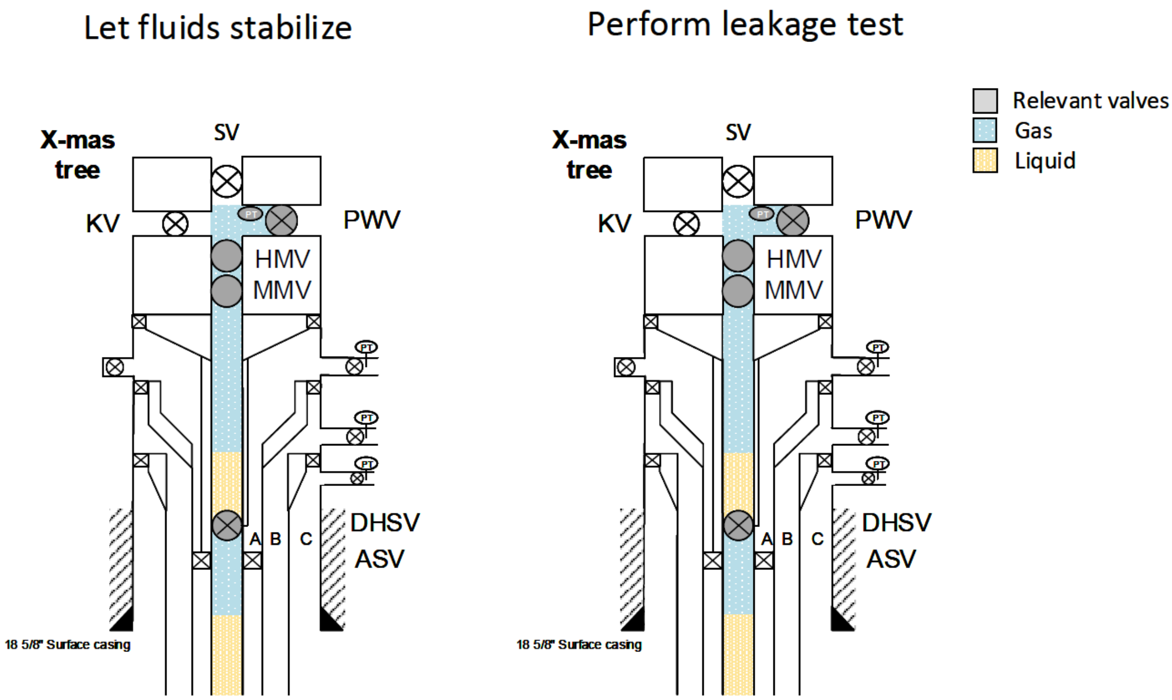

Figure 2.9 Stabilization process – left,
Leakage test – right

The evaluation of a DHSV test is based on the 30-minute testing interval. There will be a precalculated acceptance criteria that the test is evaluated against. If the acceptance criteria is given in pressure increase per 30 minutes, any pressure increase in the well can be monitored directly. If the pressure increase during the test is above the acceptance criteria, the test is failed. If the pressure increase is below the acceptance criteria, the test is approved.

There can be several reasons for a DHSV leakage test to fail. The thesis only focuses on whether the valve is leaking or not, not on problems regarding shutting the valve. Since the DHSV is a safety critical valve, special considerations are taken regarding a failed test. According to NORSOK D-010, if a DHSV valve fails, the reason for failure shall be established and actions shall be implemented to repair or replace it [3].

The final step in testing the DHSV is to report the test result. It is also important to increase the pressure above the DHSV before opening it again. This is done to remove the pressure differential across the valve. As mentioned, some DHSVs will not open if the pressure across the valve is not equalized [8]. When the pressure is equalized it is easier to open the valve against the flow direction. The equalization process is illustrated to the left in Figure 2.10. To the right in the figure the well is back on production. This marks the end of the testing procedure of a DHSV.

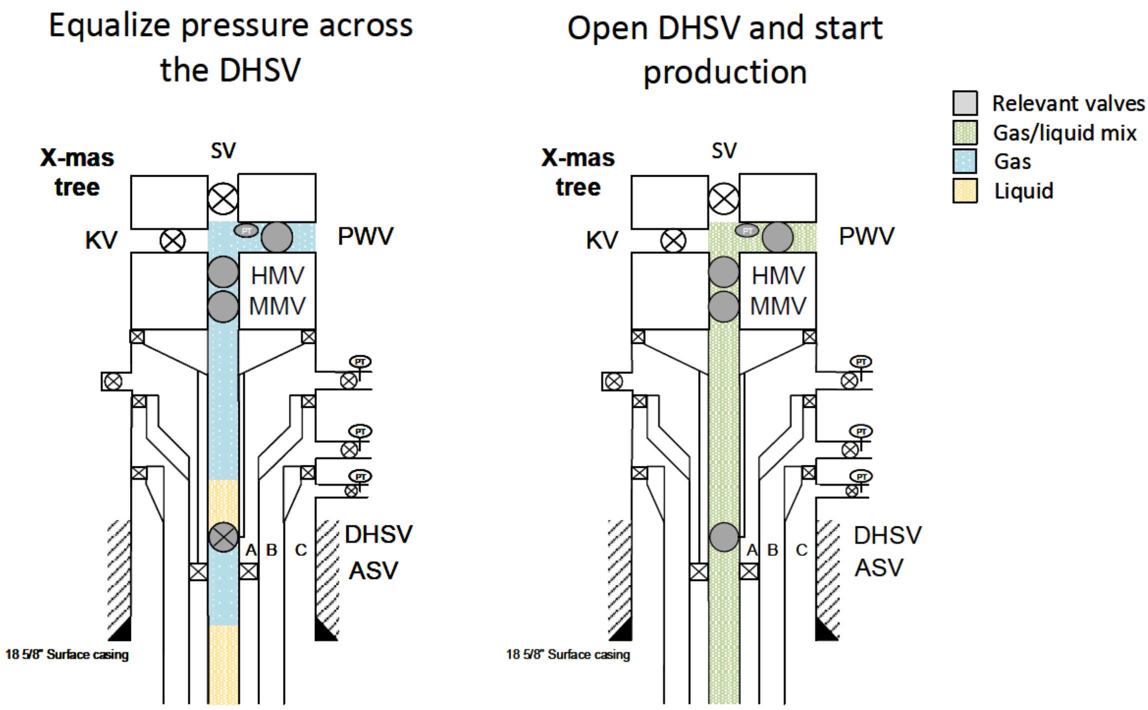

Figure 2.10 Pressure equalization across the DHSV – left, Production start – right

The DHSV shall be regularly tested. This can be referred to as periodic testing as part of a Preventative Maintenance (PM) program. NORSOK D-010 clearly states the frequency of which the tests are to be performed upon [3]. For a newly installed valve the test frequency is once a month. The monthly tests must be approved three times to move to the next test frequency. The second test frequency is testing the valve once every third month. Here, same as for the first frequency, three tests must be approved to move to the third and final test frequency. The final frequency is once every six months. This corresponds to two times a year. The explained frequencies are illustrated in Figure 2.11. The boxes in the figure represents the test frequencies with increasing frequency from left to right.

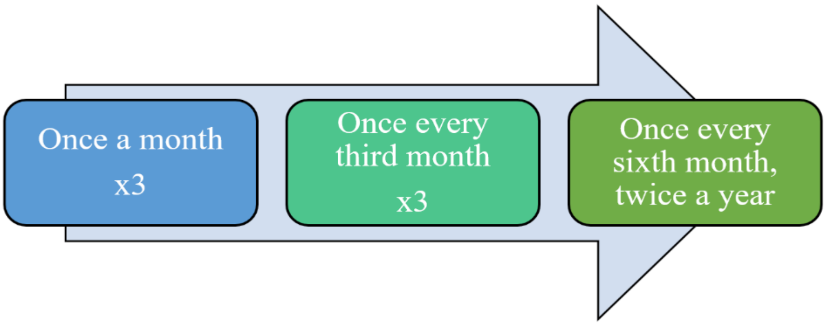

Figure 2.11 Periodic testing of DHSVs

(Page left intentionally blank)

3 Acceptance Criteria

Well barrier acceptance criteria is a concept included in NORSOK, API and ISO standards. On page 15 in the NORSOK D-010 rev 4 standard, acceptance criteria for well barrier elements are defined as “Technical and operational requirements and guidelines to be fulfilled in order to verify the well barrier element for its intended use.” [3]. In practical terms this means that the acceptance criteria is a way of ensuring and verifying that the different WBEs function properly. That the different WBEs can function together to create barrier envelopes. As mentioned, some WBEs have an acceptable leakage which it can be operated on. The DHSV is one of them. This chapter will therefore explain how the acceptance criteria is derived, calculated, and used today.

The different leakage rate criteria from mentioned standards are gathered in Table 3.1. The leakage criteria used in NORSOK D-010 and ISO 10417 are based on the API RP 14B leakage criteria. Leakage criteria from NORSOK D-010 will be used for all the calculations throughout the thesis. The leakage criteria will be converted from volume per time till pressure

Table 3.1 NORSOK, API and ISO standards leakage criteria for DHSV testing

	Gas	Liquid	Reference
NORSOK D-010	0.42 Sm^3/min 25.5 Sm^3/hr 900 scf/hr	0.4 l/min 6.3 gal/hr	[3]
API RP 14B	0.43 m^3/min 15 scf/min	400 cm^3/min	[14]
ISO 10417	0.43 m^3/min 15 scf/min	400 cm^3/min 13.5 oz/min	[16]

per time according to NORSOK D-010 [3]. This means that the acceptance criteria will be given as Equation (3.1):

$$AC = \Delta P/t \tag{0.1}$$

Where:

AC:	acceptance criteria [bar/min]
ΔP:	allowable pressure increase during test [bar]
t:	test duration [min]

By doing so, a pressure increase during a DHSV test can be measured directly and be evaluated against the precalculated acceptance criteria for that well. This makes it easier on site to check if the test is approved or failed.

Normally, the term used for the converted leakage criteria is just acceptance criteria. However, here it will be differentiated between Static Acceptance Criteria (SAC) and Dynamic Acceptance Criteria (DAC).

3.1 Static Acceptance Criteria vs. Dynamic Acceptance Criteria

The acceptance criteria used today has a fixed value. Due to this we refer to it as a Static Acceptance Criteria (SAC). It is calculated for each well or for each field depending on the similarity of the wells and will be used for each periodic DHSV test performed on that well. The calculations are based on the API leakage criteria in NORSOK D-010 and the result from both the test and the acceptance criteria will be given as Equation (3.1).

The acceptance criteria investigated in the thesis is capable of change. Due to this it is referred to as a Dynamic Acceptance Criteria (DAC). The DAC differs from SAC by being calculated for each test on each well. This means that DAC might have a different value for each test performed on the same well. The idea is that it eventually will be digitalized and calculated automatically while the test is performed. The goal in the end is that DAC will be more accurate and representative for the actual situation in the well and reduce the overall testing time. These are the problems of the thesis that will be investigate.

Figure 3.1 illustrates testing time today compared to testing time using DAC. The middle section represents typical testing time for different stages of the testing procedure, while the right section represents an imaginable testing time using digitalization and DAC. It is important to note that the typical testing times can have great variations. This is due to for instance difference in installation, crew and well type. The figure clearly shows that if the DAC is possible to use in the desired way, it can reduce the overall shut-in time of a well. Considering that DHSV leakage tests are performed a couple of thousand times each year, a large amount

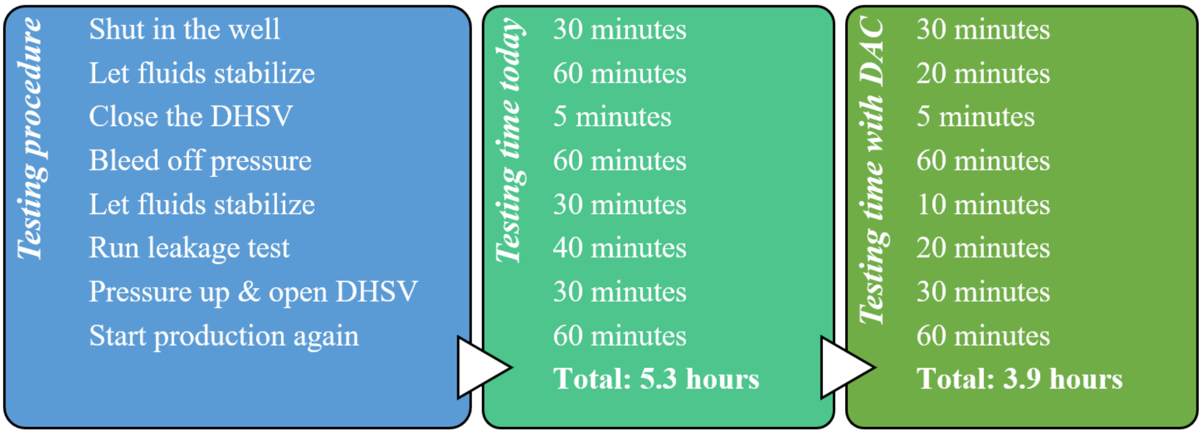

Figure 3.1 Testing time of DHSV with and without DAC

of production loss can be reduced. For Figure 3.1 it is important to note that the testing time of 40 minutes is based on a 30-minute testing time as mentioned in Chapter 2.4. Also, the 20-minute reduction in stabilization time is because the model using DAC should be able to use the ratio of gas and liquid. Therefore, there is no need to wait till the fluids in the well has segregated and most of the volume above the DHSV is gas.

3.2 Acceptance Criteria Calculations Today

The Acceptance criteria is supposed to be calculated based on the actual situation in the well [3]. However, this is not always the case. Normally it is calculated based on a 100% gas filled volume between the DHSV and the XT which is a conservative assumption. In order to calculate a more precise acceptance criteria, several parameters must be known. The calculations in this chapter are based on 100% gas filled volume for producers and 100% water filled volume for water injectors. The thesis will not focus on water injectors. However, understanding how to calculate acceptance criteria for water injectors are important to understand calculations regarding liquids later in the thesis.

When calculating an acceptance criteria, the volume must be known. Volume calculations are the same for both gas and liquid since it is based on a 100% gas filled volume for producers and a 100% water filled volume for water injectors. The formula will then be as Equation (3.2):

$$V = L * A = (d_{DHSV} - d_{TH}) * c \qquad (0.2)$$

Where:

V: volume of either gas or liquid [m^3]

L: length of volume between valves [m]

A: area [m^3]

d_{DHSV}: DHSV setting depth [m RKB]

d_{TH}: tubing hanger setting depth [m RKB]

c: tubing capacity [l/m]

Equation (3.2) is based on the setting depth of the DHSV and the tubing hanger. The volume between them represents the testing volume between the DHSV and the XT. When using tubing capacity, it is important to verify the units. For instance, if tubing capacity is given in l/m it must be divided by 1000 l/m^3 to get the volume in m^3.

The acceptance criteria calculations for gas and water are different. This is due to different properties of liquid and gas. These properties are explained further in Chapter 5. Formulas presented here are based on formulas given in ISO 16530-1 standard [17]. The formula in ISO 16530-1 for gas leaks is derived from the Formula of State, Equation (3.3). This derivation leads to Equation (3.4):

$$P * V = Z * n * R * T \tag{3.3}$$

$$P = \frac{n * R * T * Z}{V}, n * R \sim q * t$$

$$P = \frac{q * t * T * Z}{V * 2.84 * 10^3}, 2.84 * 10^3 \rightarrow \ to\ get\ SI\ units$$

$$\Delta P = \frac{q * t * T * Z}{V * 2.84 * 10^3} \tag{3.4}$$

Where:

P: pressure [MPa]

V: volume of gas [m^3]

Z: gas compressibility factor during test

n: number of gas moles [mol]

R: gas constant [J/mol*K]

T: temperature at the DHSV [K]

q: API gas leakage criteria [m^3/min]

t: test duration [min]

ΔP: allowable pressure increase during test [MPa]

$2.84*10^3$: factor to get SI units

Equation (3.4) gives the allowable pressure increase during the leakage test for that specific valve. The result shall be presented as pressure per time according to Equation (3.1). Hence, it shall be given as allowable pressure increase per 30 minutes, which corresponds to the testing time for DHSV [3]. If the leakage test of the DHSV gives a pressure increase lower than the acceptance criteria, the test is approved. However, if the pressure increase exceeds the calculated acceptance criteria, the test is failed.

The acceptance criteria for a 100% water filled volume is different from the 100% gas filled volume. The calculation is based on other and fewer parameters and the testing time is commonly only 10 min as explained in Chapter 2.4. This gives a less complicated equation. The liquid leak equation used here is also based on the given formula in ISO 16530-1 [17]. Equation (3.5) therefore forms the basis for the derivation of Equation (3.6):

$$q = c_w * V * \frac{dP}{t} \tag{3.5}$$

$$dp = \frac{q * t}{V * c_w}$$

$$\Delta P = \frac{q * t}{V * c_w} \tag{3.6}$$

Where:

q:	API liquid leakage criteria [m^3/min]
c_w:	water compressibility [MPa^{-1}]
V:	liquid volume [m^3]
t:	test duration [min]
dP:	change in pressure [MPa]
ΔP:	allowable pressure increase [MPa]

The allowable pressure increase gained in expression (3.6) must be given in bar per 30 minutes in the same way as Equation (3.4), which is gathered from Equation (3.1). It is also important to note that the API leakage criteria in expression (3.6) shall be given in m^3/min. From Table 3.1 the NORSOK D-010 liquid leakage criteria are given as 0.4l/min or 6.3gal/hr. A conversion must be done to achieve the right units:

$$0.4l = \frac{0.4l}{1000l/m^3} = 0.0004m^3 = 0.4 * 10^{-3}m^3$$

Therefore, 0.0004 m^3/min will be used as API leakage criteria for liquid calculations in the thesis.

3.2.1 Calculation Examples

To illustrate the usage of the equations given in Chapter 3.2 some examples are provided here. A summary of the results is provided in Table 3.2 together with an illustration of how to present the results. If the volume calculations, gas leak calculations and water leak calculations are based on these values:

d_{DHSV} = 250 m

d_{TH} = 30 m

c = 18.81 l/min

q_g = 0.42 m^3/min

q_l = 0.0004 m^3/min

t_g = 30 min

t_l = 10 min

T = 363 K

Z = 0.92

$C_w = 4.35 * 10^{-10}$ Pa^{-1}

Then the volume will be:

$$V = (d_{DHSV} - d_{TH}) * \frac{c}{1000} = (250\ m - 30\ m) * \frac{18.81\ l/min}{1000\ l/m^3} = 4.14m^3,$$

the maximum allowable pressure increase during a gas leak will be:

$$\Delta P = \frac{q_g * t * T * \Delta Z}{V * 2.84 * 10^3} = \frac{0.42m3/min * 30min * 363K * 0.92}{4.14m^3 * 2.84 * 10^3} = 0.357MPa$$
$$= 3.6 * 10^5 Pa = 3.6bar,$$

and the maximum allowable pressure increase during a water leak will be:

$$\Delta P = \frac{q * t}{V * C_w} = \frac{0.0004m3/min * 10min}{4.14m^3 * 4.35 * 10^{-4}MPa^{-1}} = 2.22MPa = 22.2 * 10^5 Pa = 22.2bar$$

The volume and the allowable pressure increases has now been calculated. Next step is to present the result in the right form. Table 3.2 is a summary of both calculation examples regarding the acceptance criteria. It illustrates the difference of testing time between the producer and the injector. The most important part of Table 3.2 is the acceptance criteria column to the right. This column illustrates the correct way of presenting the acceptance criteria. Remember that the DHSV test is evaluated against the result in this column. If the pressure increase during the test is above the calculated acceptance criteria, the test is failed. However, if the pressure increase is lower than the allowable calculated value, the test is approved.

Table 3.2 Acceptance Criteria Calculation Example Results

	Testing time	**Well type**	**Acceptance criteria**
100% gas filled volume	30 minutes	Producer	3.6 bar/30min
100% water filled volume	10 minutes	Water injector	22.2 bar/10min

The example calculations performed in this chapter is only based on one-phase fluid in the volume. However, what would change if there instead was a mixture of gas and liquid in the volume? When looking closer at the effect of including both gas and liquid to calculate DAC it is important to determine the fraction of each fluid. To determine these fractions, the liquid-gas interface in the well must be located. This can be done either by calculations or by measurements. The measurements include different measuring methods which allows the interface to be read of a monitor. Both calculations and the use of measurement methods are investigated in the thesis.

(Page left intentionally blank)

4 Measurement Methods

The measurement methods presented here are used to supplement the calculations. Two different methods are used for the measurements. They are Fiber Optics and Echo Sounding. These measurements are used to improve the calculations in Chapter 6. Their usage and relevance for the topic will be proven in Chapter 7. To understand their usage, it is important to understand their function. This will be explained here.

4.1 Fiber Optics

Fiber Optics is a technology that is more and more used today. Not only in the oil and gas industry, but also in everyday life. For instance, it is used for long telephone lines, for Local Area Network (LAN) connections, and for medical tools allowing internal examinations [18]. In the oil and gas industry similarly, it is used to transmit data from downhole to surface [19]. The data transmitted is real-time and through fiber optic cables. Since the downhole data is real-time, it can reduce the number of intervention runs needed on a well [19]. This can for instance be downhole data that normally is obtained using logging tools or gauges [20].

Fiber optic cables are built in layers. These layers are illustrated in Figure 4.1. The outer layer is a plastic coating for protection. The middle layer is a cladding layer that is reflecting. The inner layer is the core which is the transmitting part of the cable. The core is a thin fiber. In fact, the fiber core can have a diameter of only 10µm. [18]

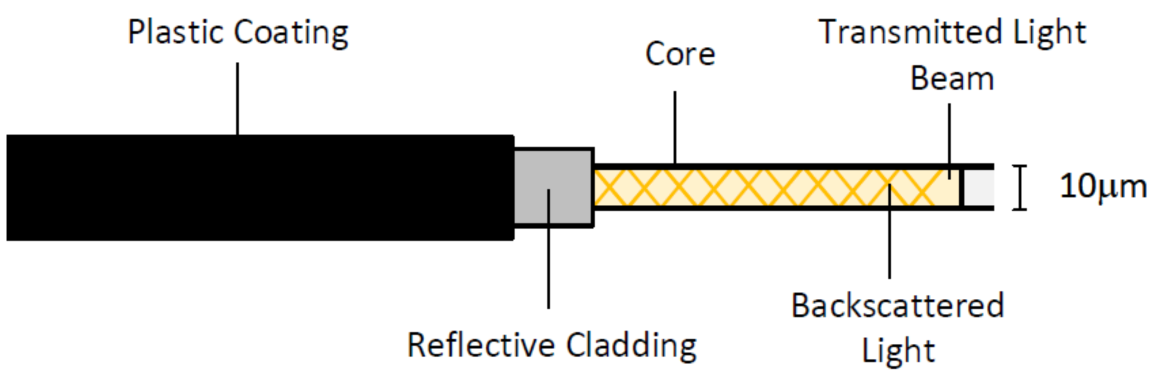

Figure 4.1 Fiber Optic cable

Figure 4.1 illustrates a light beam traveling along the fiber cable. As the light beam is transmitted into the fiber optic cable, the light will collide with the atoms that makes up the structure of the cable. These collisions will result in small light bursts that can have the same or a slightly different frequency. The light with then travel back to the recording instrument.

This returned light will be referred to as backscattered light. This backscattered light is affected by the state of the atoms at the point of reflection. This can be further used to derive properties such as temperature and sound. [13, 21]

The fiber cable can be placed in the well with different methods. It can be installed along the tubing and fastened with clamps, cemented on the outside of a casing, or it can be used temporary with a fiber rod [20]. Shorter fiber optic cables are usually made up of plastic while longer cables, like those used in a well, are usually made of glass [18]. Beams of light are transmitted into the cable. A beam is short and can have a duration down to 10 nanoseconds [21]. The light beams can be transmitted at a frequency up to 20,000 beams per second which corresponds to 20 kHz [20]. This is the measurement frequency. The fiber cable uses the two-way travel time of the light to determine at which depth the backscattered light is gathered from. This is possible because the light will have a constant velocity through the fiber optic cable.

The instrument that records the measurements are placed at one end of the fiber optic cable used in wells [21]. Hence, for a well it will be placed at the surface, and not downhole in the well. The measurements gathered using Fiber Optic cables are distributed. This means that the data are gathered along the entire fiber optic cable, and not just at given fixed points. Figure 4.2 illustrates a simple example of the differences of using point sensor or distributed sensor. The black dots illustrate the point sensors. From the figure it is clear to see that point sensors might lose important data that a distributed sensor can measure. For Fiber Optics, it is therefore

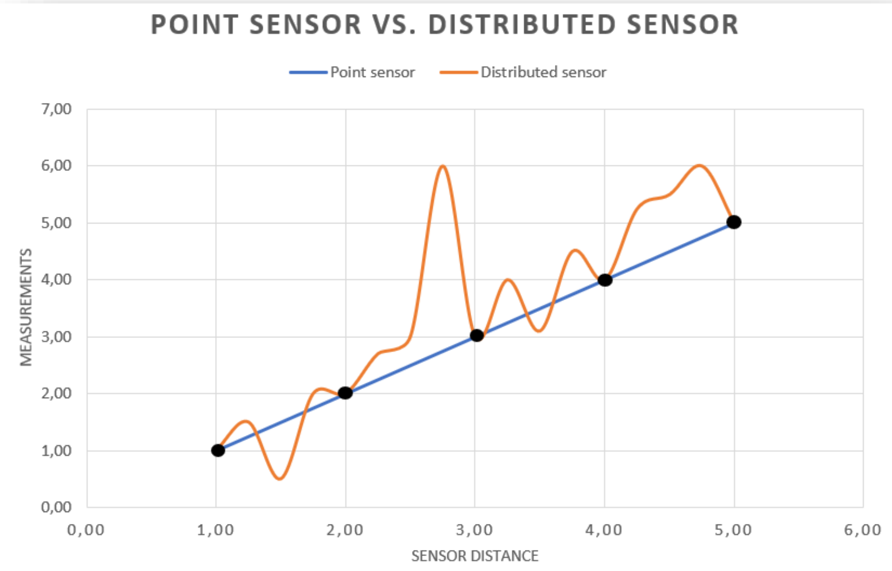

Figure 4.2 Point sensor vs. Distributed sensor

distinguished between Distributed Acoustic Sensing (DAS) and Distributed Temperature Sensing (DTS). Both are explained in this chapter.

4.1.1 Distributed Acoustic Sensing, DAS, and Distributed Temperature Sensing, DTS

Distributed Acoustic Sensing (DAS) is used to measure the acoustic frequency and amplitude of fluids in a well [22]. When a beam of light is transmitted into the Fiber Optic cable, DAS measures Rayleigh backscattering [19]. Rayleigh backscattering is elastic scattering of photons from the light beam. This means that the scattered photons will have the same energy before and after the scattering. The photons will only change direction. [23] When two light beams have been backscattered in the Fiber Optic cable, the differences in their properties are measured. The differences are then used to investigate the strain changes in the cable. Due to the high frequency of the light beams, the strain changes will be rapid and act as vibrations. Because of the high measurement frequency, these vibrations can be translated into a range that is audible. [19]

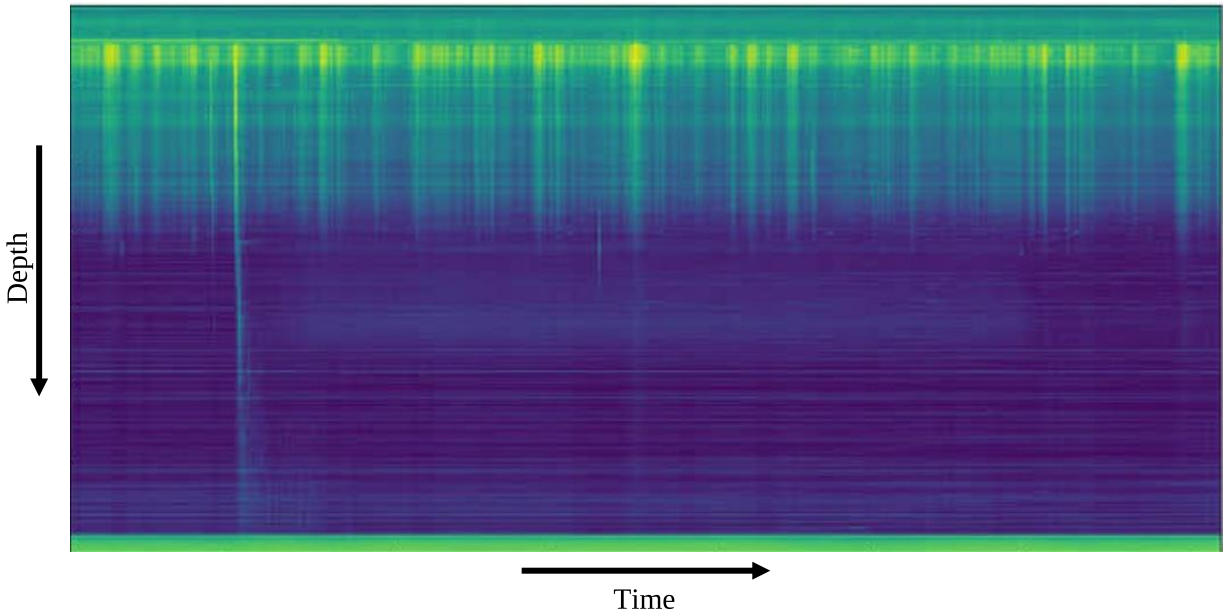

Figure 4.3 DAS measurement (reproduced with permission) [13]

Figure 4.3 illustrates a simple DAS measurement. The y-axis illustrates the depth, while the x-axis illustrates time. The colors in Figure 4.3 reflects the volume of sound. Hence, the bright colors are loud sounds, while the dark colors are quiet sounds. The figure shows sound energy. [13] The longer reflection to the left in the figure shows a DHSV being opened after an integrity test. It is seen as a short loud event that resounds in the entire well. As mentioned, Fiber Optics are included in the thesis to supplement the calculations later. It is mainly included to support the calculations for locating the gas-liquid interface in the well. However, using DAS for this has not shown to be an obvious choice. There are some doubts whether DAS can easily be used to detect the interface or not. Using DAS to detect the interface between gas and liquid in a well has not been investigated thoroughly yet. It is therefore too soon to conclude whether DAS can be used for this or not. Instead, DAS can be used to investigate the possibility of listening to leaks across a valve. Considering the good DHSV response in Figure 4.3, it might be reasonable to investigate how a leaking valve sounds depending on the size of the leak. If this turns out to be possible, it will reduce the shut-in time during the leakage test. This is method that has not been investigated in the thesis, since locating the interface between gas and liquid is the Fiber Optic focus. Due to this, DAS will not be used for further investigations in the thesis. Distributed Temperature Sensing (DTS) will be the focus on the Fiber Optic parts.

DTS is used to measure the absolute temperature in a well. DTS works in the same way as DAS, but DTS measures the Raman backscattering instead of the Rayleigh backscattering. Raman backscattering is the opposite of Rayleigh backscattering. It is inelastic. This means that the scattered photons from the light beam will not have the same energy before and after the scattering process. The scattered photon will either have more energy or less energy than the original photon. [23] The Raman backscattering is divided into two categories. These are known as anti-Stokes and Stokes. The difference between them is that Stokes refers to photons with larger wavelength after scattering and anti-Stokes refers to photons with smaller wavelength after scattering. This means that Stokes backscattering results in photons with lower energy than the original photons, and anti-Stokes results in photons with higher energy than the original. Another difference between them is that Stokes is less sensitive to temperature, while anti-Stokes is more sensitive. Due to the different backscattering energies and different temperature sensitivities, the measured signal must undergo averaging to gain a desired profile of the continuous temperature changes along the depth of the well. [21] Due to this, the DTS measurements are not real-time in the same way as DAS. DTS measurements are slightly shifted as they are plotted as degrees/min. Since the fiber cable often is installed on the outside of the tubing, the DTS measures the radial heat from the fluid flow inside the tubing. Hence, heat that propagates from the middle of the fluid flow. [13]

Figure 4.4 illustrates such a continuous temperature profile in a well. The figure shows an initial start-up of a well with a following short shut-in period. Like the DAS figure, the y-axis illustrates depth, while the x-axis illustrates time. The only difference from DAS is that the different colors for DTS represents the different temperatures. Red indicates heating, while blue illustrates cooling.

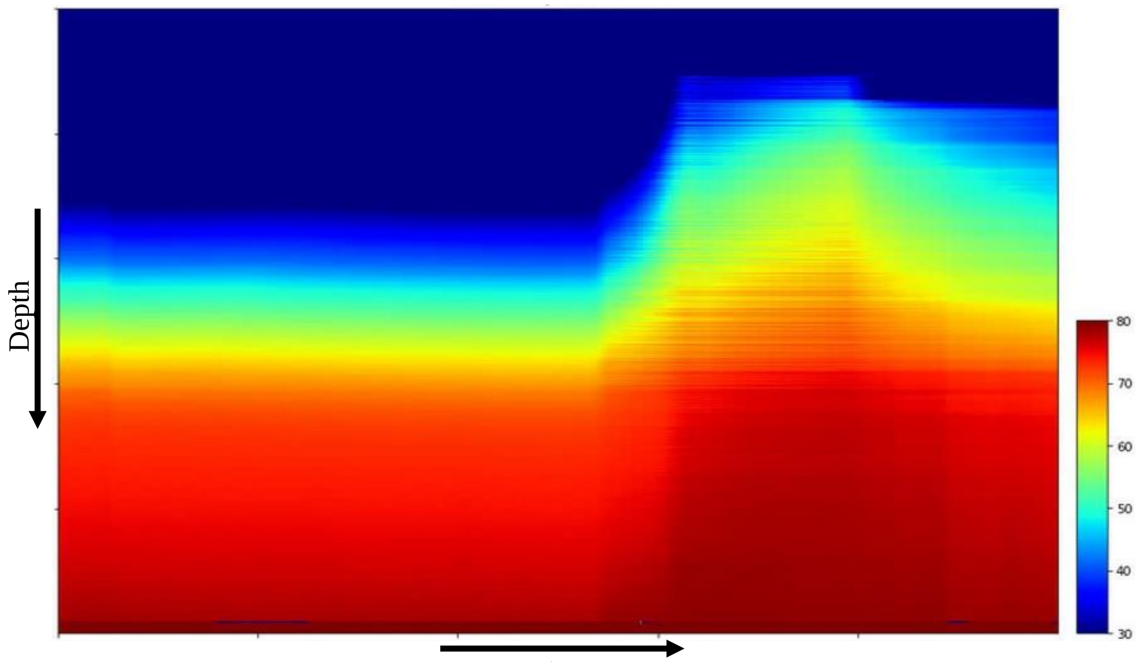

Figure 4.4 DTS measurement (reproduced with permission) [13]

The spatial resolution of both DAS and DTS can be down to half a meter, but it is usually one meter or higher [20, 22]. This means that measurements gathered using DAS or DTS can have an accuracy of ± half a meter, depending on the spatial resolution. This allows for quite accurate measurements considering the depth of some wells.

DAS and DTS can gather data on several things along the well. They can monitor the entire well profile and therefore provide information about the equipment in the well or about the processes in the well. For instance, they can detect whether a valve is active or not, if there are any leaks through a valve, or the depth of unloading [19]. Unloading is a process where one fluid is circulated out of the well using a different fluid. This can be used to initiate reservoir flow to start the production, or it can be used to initiate gas lift. [24] During unloading it is possible to follow the interface between the different fluids. Hence the unloading depth. Figure 4.5 illustrates an example of this using DTS. The figure shows unloading during initiation of gas lift. The difference between the interfaces are clearly shown by the temperature changes. This illustrates that DTS can track the interface accurately, which can lead to faster unloading operations. The reason for this response is the differences in temperature down in the well due to the temperature gradient. When a fluid moves up in the well, heating is measured since the formation is colder towards the top. In the unloading measurement in Figure 4.5, the temperature changes between the phases are also due to the heating capacity of the different

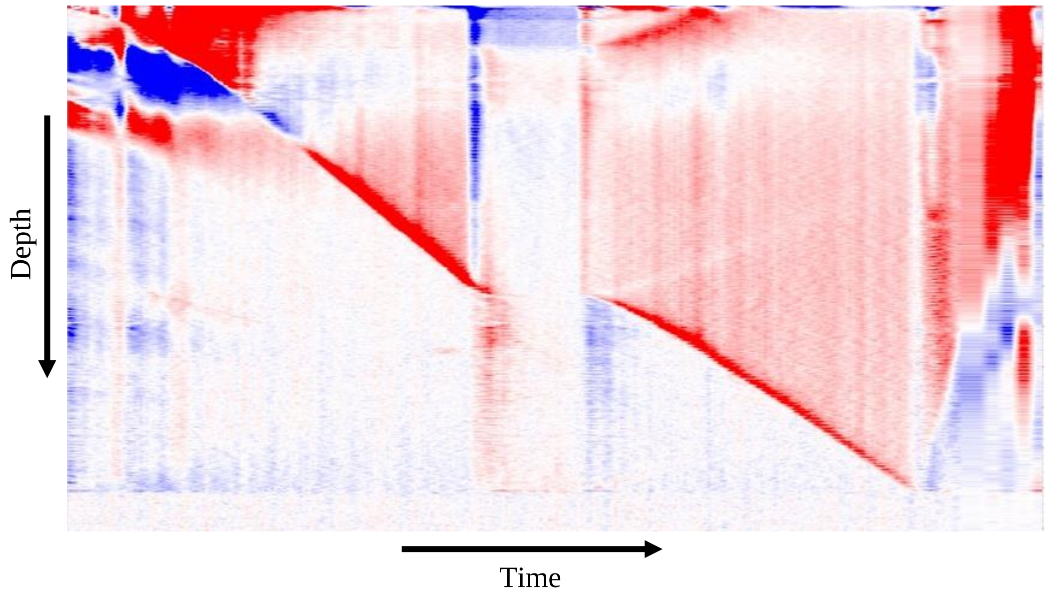

Figure 4.5 DTS unloading example (reproduced with permission) [13]

fluids. The heating capacity will determine the rate at which a fluid is heated up and cooled down. [13] This usage is also why it is believed that DTS can be used to detect the gas-liquid interface in a well during the DHSV test. However, there are some issues and uncertainties using DTS to locate the interface for this purpose. Figure 4.5 is accurate at tracking the interface if the fluids are moving. As soon as they stop moving, the interface is fading. This can be seen in the middle of Figure 4.5. This can indicate that if DTS is to be used for the desired purpose of the thesis, the interface depth must be measured as soon as the fluids stop moving.

4.2 Echo Sounding

Echo Sounder is a device that is commonly used to locate the seafloor to determine the water depth, or it is used to locate objects on the seafloor [25]. In this context, Echo Sounding is used to locate the interface between oil and gas in the tubing in a well.

The Echo Sounder works by emitting a strong electric energy pulse. A transducer is then used to convert this pulse into a pressure wave which is acoustic. [25] This pressure wave can propagate through liquids, solids and gases. [26] The pressure wave identifies all cross-sectional changes in the well [27]. When the pressure wave detects an interface, the pressure wave sends an echo back to a receiver on top. This is illustrated in Figure 4.6. The figure provides a simple illustration on how the pressure wave is transmitted, and how the echo is sent back to a receiver for each interface. When the echo is received it is transformed back into electric energy as it was initially. This electrical echo is enhanced and used as an indicator. [25] The result is then plotted to determine the interface depth.

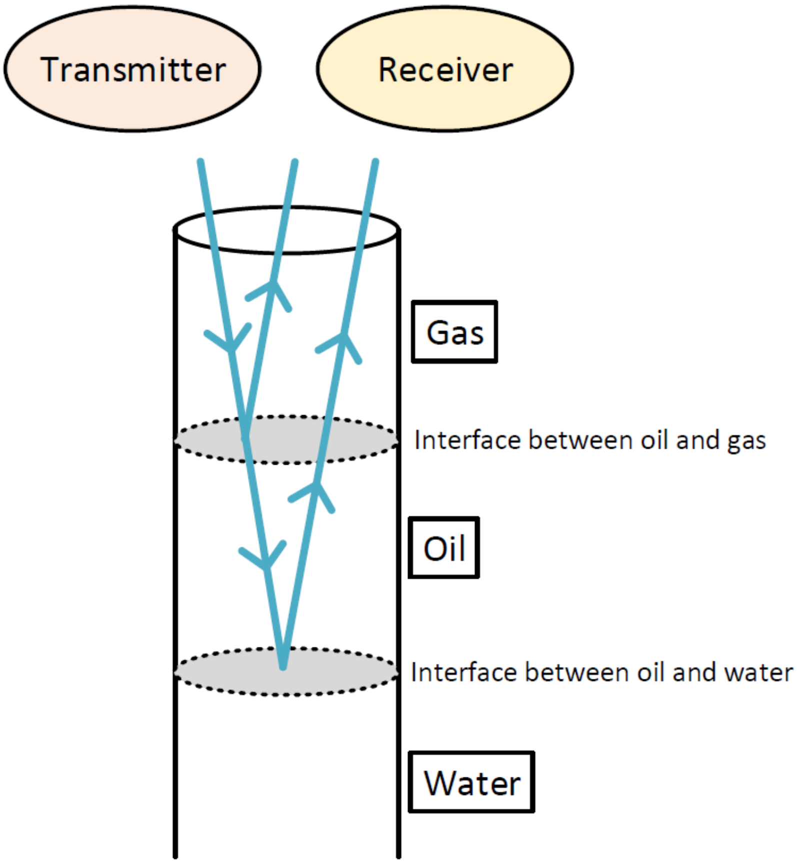

Figure 4.6 Echo Sounding in a tubing

The depth of the interface is determined by using some known depths of different equipment installed in the well. These equipment depths are used as reference depths to orient where the interface signal is coming from. Known depths can for instance be different valves installed in the well, like the DHSV. This means that Echo Sounding easily can determine if the interface is located above or below the DHSV in the well. This can be useful for DHSV leakage tests. As mentioned, the Echo Sounder measures all cross-sectional changes. This means that for the known component depths, the cross-sectional change in the tubing is recorded to verify where the signal is gathered from in the well. The measurements has an accuracy of ± 0.3 meters. [27]

A typical Echo Sounding measurement can take between one hour and two hours. A lot of the time goes into mobilization of the equipment and installing the equipment. It is more common to install the equipment for each job, rather than to install it permanently. However, if this technology were to be used each time a DHSV test is scheduled, it should be installed permanently to reduce time. By doing so, the equipment can be automated and controlled by a control room, and measurements can be gathered every 15 seconds. Although that might be the best option to reduce time spent on each measurement, the total cost of the installation against the need for measurements must be considered. [27]

5 Fluid Properties and Behaviors

The formation fluid from a well is rarely only one phase. It is usually a mix between oil, gas and water. Understanding how these phases behave together during production and during production stop is important when investigating a DAC. Therefore, some basic principles regarding fluid properties and behaviors are explained here.

5.1 Flow Regimes

Fluid flow is often referred to as either laminar flow or turbulent flow. Laminar flow is a smooth flow that often has low velocity and flows through narrow channels or tubes [28]. Turbulent flow is the opposite of laminar flow, but also the most common of them [28]. Turbulent flow involves mixing, fluctuations and has a velocity that is constantly changing [29]. Laminar and turbulent flow are the only flow regimes applicable for single phase flow. However, for two-phase flow there are other characteristics for fluid flow in addition to those listed above. [30]

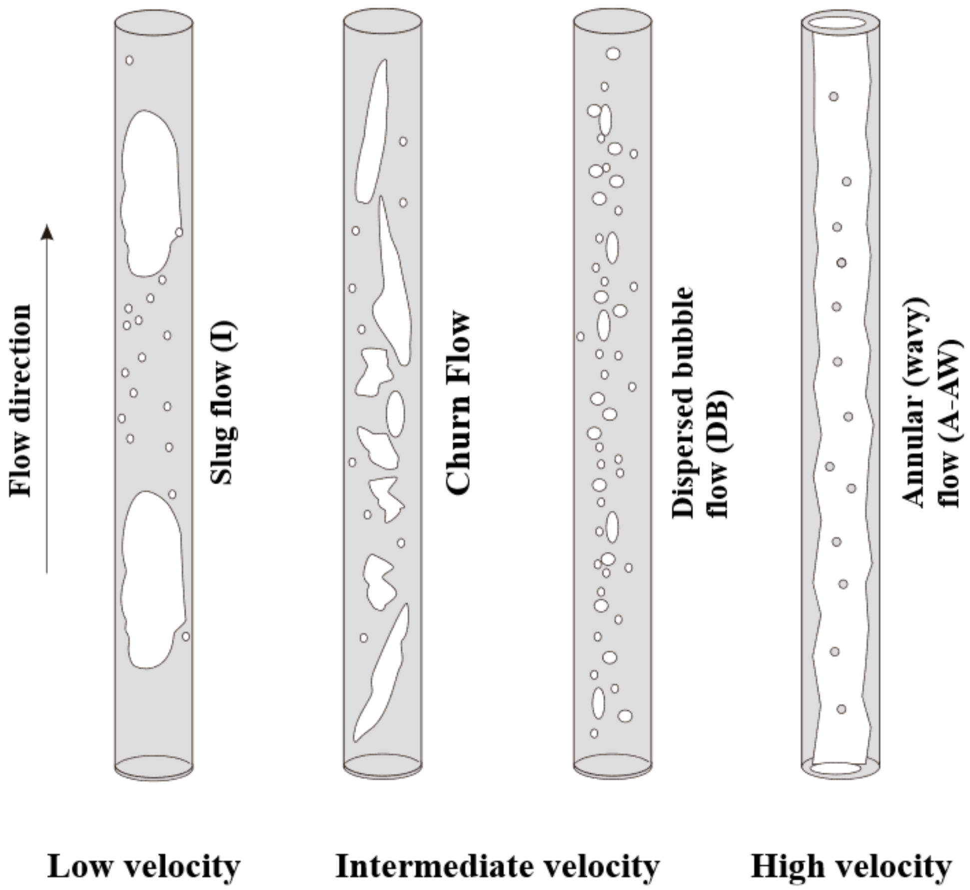

Figure 5.1 Flow regimes for vertical flow (reproduced with permission from author) [30]

For vertical flow there are four flow regimes. These are slug flow, churn flow, dispersed bubble flow and annular flow. The flow regimes evolve with increasing velocity of the flow. Slug flow for the lowest velocities and annular flow for higher velocities. Figure 5.1 illustrates the different flow regimes for vertical flow of a two-phase flow. The figure shows that the two phases, liquid and gas, are almost separated at lower velocities. This is the most separated the two phases will be for a vertical flow regime. At higher velocities the two phases are mixed together. [30]

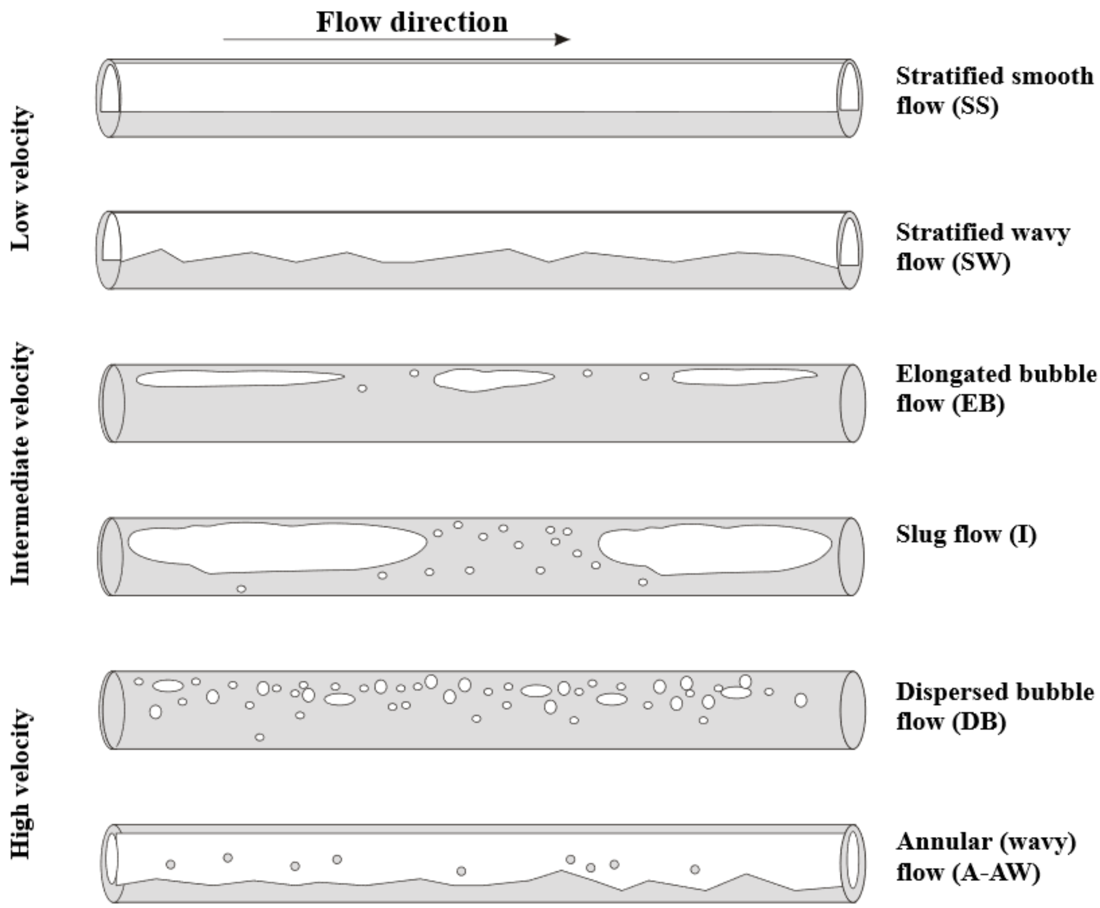

Figure 5.2 Flow regimes for horizontal flow (reproduced with permission from author) [30]

For horizontal flow there are six flow regimes. These are stratified smooth flow, stratified wavy flow, elongated bubble flow, slug flow, dispersed bubble flow and annular flow. The flow regimes are affected by flow velocity in the same way as for vertical flow with increasing flow velocity from stratified smooth flow to annular flow. Figure 5.2 illustrates the flow regimes of horizontal flow. The figure shows that for low velocities the flow regime is stratified smooth flow. Hence, for low velocities in a horizontal flow regime the two phases are completely separated. For high velocities the phases are mixed together as for vertical flow.

However, notice that slug flow occurs in intermediate flow velocities for horizontal flow. Not low velocities as for vertical flow. [30]

The investigations in the thesis are performed on a stationary process. It is natural to think that flow regimes during production is not applicable when considering this. However, understanding how the flow regimes behave before the test might help explain some of the phenomenon that occurs. For instance, during production the flow velocity is typically high. If the well is shut-in quickly it might, as mentioned earlier, “shock” the formation. However, it can also result in the two-phase fluid flow being completely mixed after the shut-in. This can result in a longer stabilization process before the test. If the well is shut-in slowly, the fluid flow will reduce its velocity and might start the separating process of the two phases before the stabilization process begins. This might help understand why it typically takes around 30 minutes to shut the well before the test.

5.2 Gravity Segregation

Segregation due to gravity results in fluids separating into different layers. This is the separation process that occurs during the stabilization step of the testing procedure of a DHSV. Heavier fluids will sink to the bottom while lighter fluids will accumulate at the top. [31] An example can be when oil and water are mixed. When the mixing stops, the gravity segregation begins. The oil will accumulate at the top due to lower density, while the water will sink to the bottom due to higher density. Figure 5.3 illustrates a simple gravity segregation of oil and water. This is the same basic principle used when a producing well is shut in. The fluids will come to

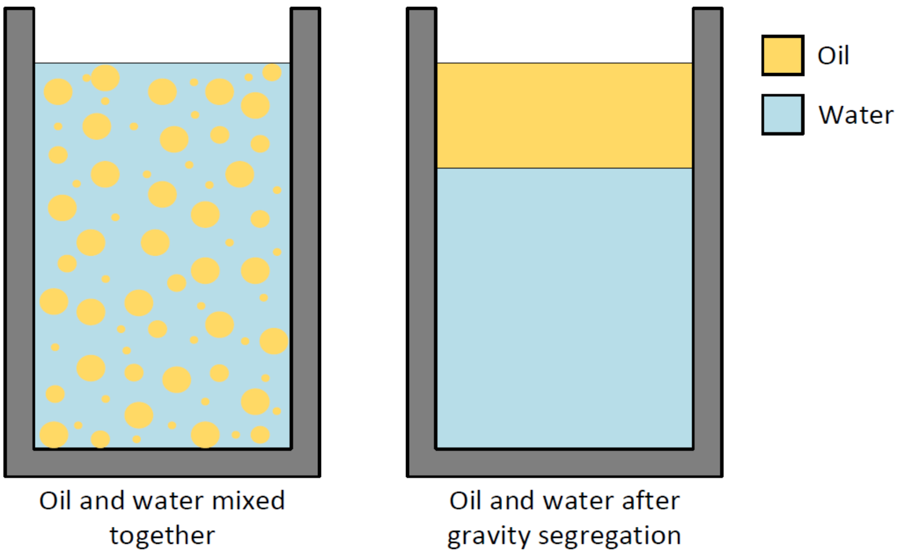

Figure 5.3 Gravity segregation

a rest and start segregating. This results in gas on the top and oil in the middle or bottom, depending on presence of water, which will accumulate at the bottom.

5.3 Bubble Point

When a reservoir fluid moves out of the reservoir and up in the well, it experiences great changes in pressure and temperature. Both pressure and temperature affect the density of the fluid and the state of the fluid itself. As the fluid moves up in the well, both the pressure and the temperature is gradually reduced. Since oil often is saturated with gas in the reservoir, this pressure and temperature reduction will cause gas to boil out of the oil. The exact point where this happens is dependent on the composition of the fluid. This point is called bubble point. It is the point where the first gas bubble is released from the oil. This process happens both in the reservoir as it is depleted, and in the well as the fluid is produced. Due to this, the gas content that accumulates in the top of the well can be from gas being produced together with the oil, from gas being boiled out of the oil, or it can be a combination of both. [32]

5.4 Pressure-Volume-Temperature (PVT) Data

Pressure, volume and temperature are three important parameters in the thesis. They can be used to evaluate different fluid properties [33]. For simplicity, only the relevant properties for the thesis will be explained.

Pressure is a parameter that affects different fluid properties. For instance, an increase in pressure results in a decrease in volume. If pressure instead is constant, then the volume is proportional to temperature. [34] By being proportional the ratio between the two parameters are constant. Pressure and Temperature also affects the liquid density. When temperature increases, the density decreases. When pressure increases, the density increases. As reservoir fluid moves up in the well, both pressure and temperature decreases. This results in a decreased density. [35] Pressure also affect the compressibility.

5.5 Compressibility

Compressibility is a measurement of how easy a fluid can be compressed. It is the ratio of change in volume per volume unit and the change in pressure [36]. The compression will therefore result in volume decrease due to an increase in pressure. The compressibility of gas and liquid is explained here. The gas compressibility can be calculated using this equation:

$$c_g = -\frac{1}{V} * \left(\frac{\partial V}{\partial P}\right)_T \tag{5.1}$$

Where:

c_g:	gas compressibility [Pa^{-1}]
V:	volume [m^3]
P:	pressure [Pa]

The T in the end of Equation (5.1) is not a parameter. It is only there to show what kind of process the compressibility is calculated under. In this case, the T shows that this is an isothermal process. An isothermal process is a process with constant temperature. Hence, the compressibility of gas is calculated under constant temperature.

Compared to the compressibility of gases the compressibility of liquids is very small. In fact, as pressure is increased 100 times, the properties might change with less than one percent [35]. This shows that the compressibility of a liquid usually will have a small impact on the total outcome in a mixture of gas and liquid. It is therefore often neglected, and liquids are considered incompressible fluids. The compressibility of oil is calculated as Equation (5.2) illustrates [37]:

$$c_o = -\frac{1}{V} * \left(\frac{\partial V}{\partial P}\right)_T \tag{5.2}$$

Where:

c_o:	oil compressibility [Pa^{-1}]
V:	volume [m^3]
P:	pressure [Pa]

Equation (5.2) can also be used for water compressibility, c_w. According to ISO 16530-1, the compressibility of water can be five times smaller than the compressibility of oil [17]. During the DAC calculations in Chapter 6, the impact and importance of liquid compressibility regarding the acceptance criteria is investigated. Same as for the gas compressibility, the liquid compressibility is here calculated under constant temperature.

To avoid confusion, it is important to note the difference between compressibility of gas and compressibility factor of gas, which is often referred to as the Z-factor. The Z-factor is a measurement of the difference between an ideal gas and a real gas [37]. It is used for all gases not considered ideal. Hence, for all real gases. The compressibility factor varies with each gas type. It can be higher, equal, or lower than one for real gases. For ideal gases it will always be equal to one. [35] The compressibility factor of a gas is defined as:

$$P * v = Z * R * T \tag{5.3}$$

$$Z = \frac{P * v}{R * T} \tag{5.4}$$

Where:

P:	pressure [MPa]
v:	specific volume [m^3/kg]
Z:	compressibility factor of gas
R:	gas constant [kPa*m^3/kg*K]
T:	temperature [K]

The compressibility factor given as Equation (5.4) is based on the real gas Equation (5.3) [35]. The gas constant is the parameter that will change depending on what type of gas it is. The gas compressibility factor can also be defined as this [37]:

$$Z = \frac{V_{actual}}{V_{ideal\ gas}} \tag{5.5}$$

Where:

Z:	compressibility factor of gas
V_{actual}:	actual gas volume at given pressure and temperature [m^3]
$V_{ideal\ gas}$:	ideal gas volume at given pressure and temperature [m^3]

All gases are considered real gases when calculating the acceptance criteria. Hence, the compressibility factor is used for all gas related calculations in the thesis. For simplicity, the Z-factor will be used in the thesis instead of the expression “compressibility factor for gas”. For simplicity, the compressibility of liquid and the Z-factor are assumed constant for all calculations in the thesis.

5.6 Joule-Thomson Effect

The Joule-Thomson effect describes the phenomenon where a gas changes temperature without losing heat to the surroundings. The temperature change will be caused by expansion or compression of a gas. It is important to note that the expansion or compression is not caused by performing work on the gas. Work on the gas can for instance be a piston that compresses the gas. The expansion or compression are rather caused by the gas moving through for instance a valve. One example can be when the pressure above the DHSV is reduced during a test. [38].

During a DHSV test, the pressure above the closed DHSV is reduced. The pressure is reduced by opening a valve and bleeding off a volume at the top of the well. Due to gravity segregation, the top portion of the well will consist of gas. Hence, gas is the medium being bled off. After the pressure has been reduced, there is room for expansion. As mentioned, liquids are often assumed incompressible because the compressibility impact is low. Due to this, the gas will be the fluid that expands the most. When it expands the temperature of the gas is reduced. The opposite will be the case when the pressure is increased above the DHSV after the test. The gas will then be compressed, and the temperature will increase.

(Page left intentionally blank)

6 Calculation of Dynamic Acceptance Criteria, DAC

Calculating the Dynamic Acceptance Criteria (DAC) can be a comprehensive task. There are many properties and parameters included. During this chapter, the thesis looks closer at calculating the DAC. The impact of different parameters and uncertainties during calculations are evaluated. The practicality of using DAC is also an important aspect that is considered.

6.1 Volume Calculations

The equations that form the basis for the DAC calculations are provided in Chapter 3. These equations are further used to formulate useful equations for the calculation of DAC. For instance, when considering Equation (3.2) for volume calculations, the calculations for two separate phases of gas and liquid can be done like this:

$$V_{tot} = V_l + V_g \tag{6.1}$$

$$V_l = L_l * A = L_l * c = V_{tot} * \varepsilon_l \tag{6.2}$$

$$V_g = L_g * A = L_g * c = V_{tot} * \varepsilon_g \tag{6.3}$$

Where:

V_{tot}:	total volume between DHSV and TH [m^3]
V_l and V_g:	liquid volume and gas volume [m^3]
L_l and L_g:	liquid level and gas level [m]
A:	area [m^2]
c:	tubing capacity [l/min]
ε_l and ε_g:	liquid fraction and gas fraction

Remember from Chapter 3 that when using the tubing capacity for volume calculations, it is important to keep track of the units. Equation (6.2) and (6.3) represents the volume calculations of the liquid phase and the gas phase respectively. The volume is calculated considering how much there is of each phase in the total volume. Hence, the equations either uses the length of the layer, or the volume fraction of the layer to calculate the representative volume for each phase. Equation (6.2) and Equation (6.3) is therefore used for the calculation of DAC.

6.2 DAC Calculations

When calculating the DAC, it might be an initial idea to combine the two acceptance criteria equations. Combining Equation (3.4) and (3.6) will result in this equation:

$$\Delta P = \frac{q_g * t * T * Z}{V_g * 2.84 * 10^3} + \frac{q_l * t}{V_W * c_W} \tag{6.4}$$

Where:

ΔP:	allowable pressure increase during test [MPa]
q_l and q_g:	API leakage criteria for liquid and gas [m^3/min]
t:	test duration [min]
T:	temperature at the DHSV [K]
Z:	gas compressibility factor during test
c_W:	water compressibility [MPa^{-1}]
V_w and V_g:	volume of liquid and volume of gas [m^3]
$2.84*10^3$:	conversion factor to get SI units

Although it might be a starting point to do it this way, it will not give a representative result. Equation (6.4) does not combine the volumes to calculate the leak rate through the DHSV. The equation calculates the maximum leakage into each of the volumes. Hence, it treats the total volume as two separate volumes. One with liquid and one with gas. By doing so, the equation

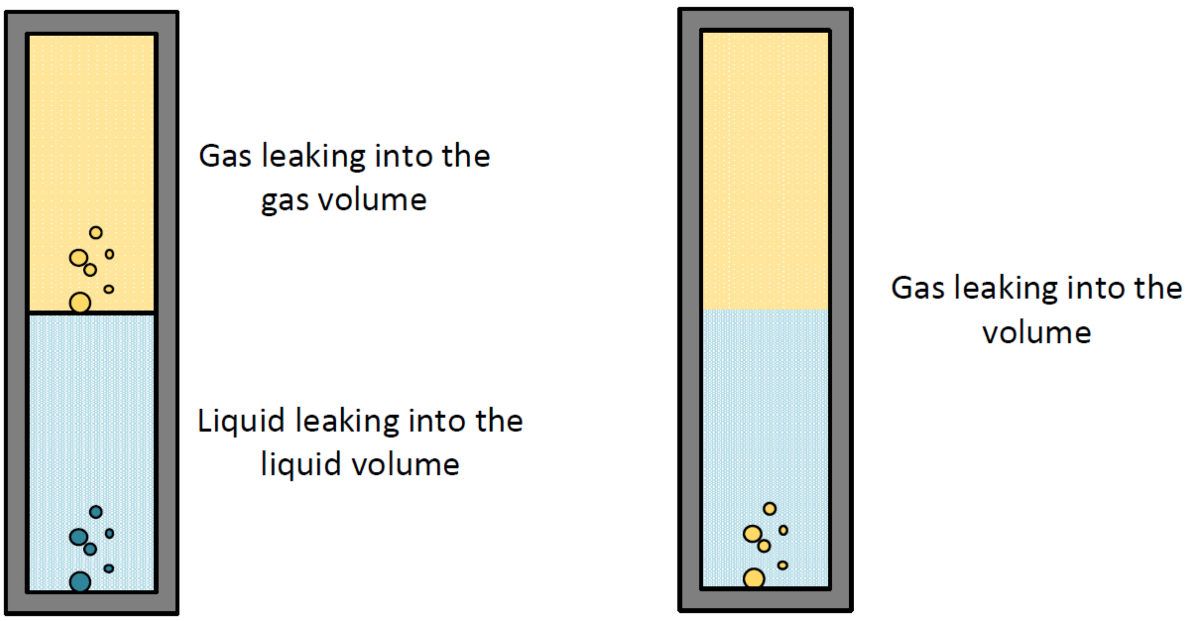

Figure 6.1 Separate volumes – left, Segregated volume – right

calculates the acceptance criteria based on maximum liquid leakage into the liquid volume and maximum gas leakage into the gas volume. The acceptance criteria for each volume is then added together. This is illustrated to the left in Figure 6.1. This method will not be representative since the DHSV is the only element to be tested in this situation. Hence the DHSV is assumed to be the only possible leakage point here. The volume between the DHSV and XT must therefore be treated as a segregated volume, not a separated volume, where it is assumed that the volume is fully segregated. This is illustrated to the right in Figure 6.1. Due to this, Equation (6.4) is not valid.

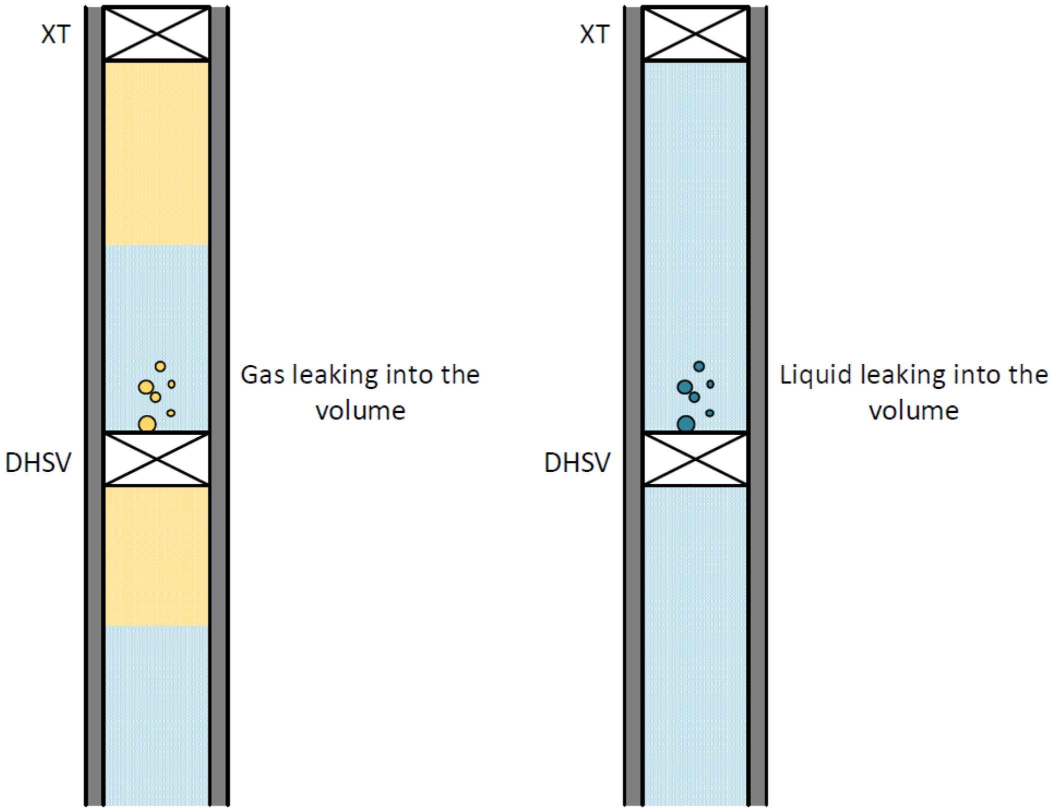

Figure 6.2 Actual situations in the well

The main problem with Equation (6.4) is the inclusion of both the gas and liquid leakage criteria. In order to treat the situation as one volume with one leakage point, only one leakage criteria can be used. The most realistic situations to occur in the well is illustrated in Figure 6.2. The figure illustrates two different possible scenarios to occur in the well during the leakage test. The well is shut-in and the DHSV is closed. For the scenario to the left in Figure 6.2, the well is left like this for a period to let the fluids segregate. However, the segregation process will not only occur between the DHSV and the XT. It will also occur below the DHSV. Gas will accumulate at the top just below the DHSV. Due to this it is reasonable to assume that gas will be the fluid leaking through the valve. The other scenario, the one to the right in Figure 6.2, illustrates a completely liquid filled well. Although it is more common to have a well with gas in the oil or gas boiled out of the oil, a completely oil filled well can be encountered. For this scenario, it is reasonable to assume that the leaking fluid through the DHSV is liquid. This results in two different calculations for these scenarios.

Since gas is assumed to be the leaking fluid through the valve in the first scenario in Figure 6.2, it is reasonable to assume that only the API leakage criteria for gas is to be used in the calculations. Equation (3.4) from Chapter 3 is used today for a 100% gas filled volume where the leaking fluid is gas. This equation will therefore form the basis of the DAC calculations for the first scenario. However, the equation does not include a parameter for the liquid phase. Hence, the impact of the liquid phase is not considered in this equation. It is already known from earlier that the liquid phase has a very low compressibility, while gas is highly compressible. In practical, this means that if there is gas in the volume, the gas will dominate and act as a spring. Therefore, the liquid is assumed to be incompressible in this case. Since the liquid is assumed incompressible, the volume is the only parameter in Equation (3.4) that can be affected by the presence of liquid. The volume in Equation (3.4) will therefore only represent the gas fraction of the total volume. Hence, the equation will be:

$$\Delta P_{DAC} = \frac{q_g * t * T * Z}{V_g * 2.84 * 10^3} = \frac{q_g * t * T * Z}{(V_{tot} * \varepsilon_g) * 2.84 * 10^3} \tag{6.5}$$

Where:

ΔP_{DAC}:	allowable pressure increase during test [MPa]
q_g:	API gas leakage criteria [m^3/min]
t:	test duration [min]
T:	temperature at the DHSV [K]
Z:	gas compressibility factor during test
V_g and V_{tot}:	volume of gas and total volume [m^3]
ε_g:	gas fraction
$2.84*10^3$:	conversion factor to get SI units

Equation (6.5) does not differ too much from the Equation (3.4) used to calculate SAC today. However, the calculation of the DAC requires the gas fraction to be known. This can either be measured or calculated. Both methods will be investigated in Chapter 7. For now, the different fractions will be given for the calculations.

To see how the DAC will change depending on the gas fraction, a plot is made. Figure 6.3 shows DAC vs. gas fraction. Equation (6.5) is used for the calculations in the figure and only the volume has been changed for the three graphs. The x-axis illustrates the gas fractions where 1.00 represents 100% gas and 0.50 represents 50% gas. The y-axis illustrates the DAC given in bar/30 min for the test. The figure shows that a lower volume results in an overall higher acceptance criteria. All three of the graphs have a slow increase in DAC as the volume fraction of gas decreases. This pattern of slow increase in DAC lasts until the gas fraction is around 30% - 40%. As the gas fraction falls below this, there is a rapid increase in the DAC.

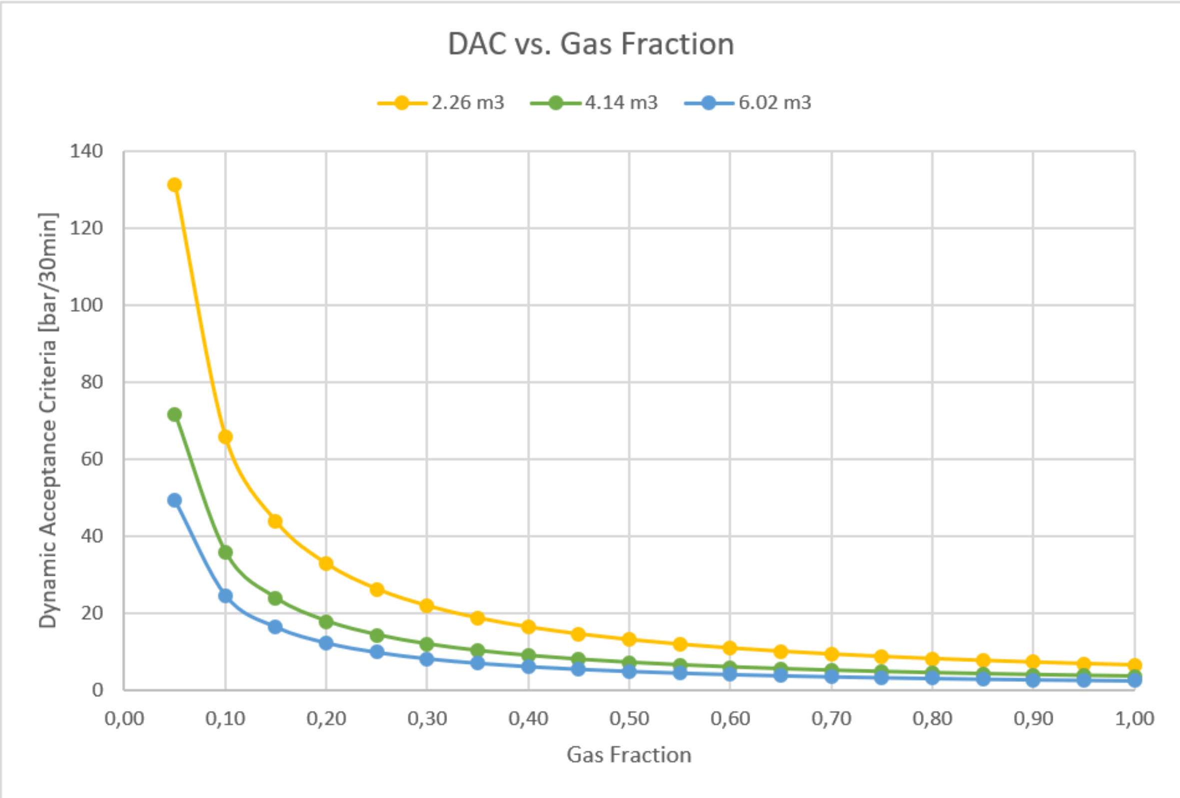

Figure 6.3 DAC vs. Gas fraction

This rapid increase questions the theory about the effect of the liquid. When the gas fraction falls below this level, there is only a small amount of gas in the total volume. A small gas leak through the DHSV and into the volume will therefore have a larger impact on the pressure. As the gas fraction gets smaller, the impact of the liquid compressibility might be significant. However, as stated earlier, liquid is assumed incompressible here. Furthermore, below 30% - 40% a gas leak will have a greater impact on the allowable pressure increase during the leakage test. This makes sense considering that most of the volume now is liquid. From the green graph in Figure 6.3 the DAC would be somewhere between 70 – 72 bar/30 min for a gas fraction of 0.05, while it is 3.6 for a gas fraction of 1.00. The standard way of calculating the acceptance criteria today is to assume that the entire volume is gas filled. This means that for this example, the SAC calculated today would be 3.6 bar/10 min. In a situation where the gas fraction is below 30% - 40%, the curves in Figure 6.3 clearly illustrates how highly erroneous the assumption of a complete gas filled volume in some cases could be.

For the second scenario, illustrated to the right in Figure 6.2, the calculation of DAC is different. In this scenario, it is assumed that the leaking fluid is liquid. The situation is for a producing well, and not an injector. Equation (3.6) for water leaks used for water injectors today, will therefore form the basis for this scenario:

$$\Delta P = \frac{q * t}{V_l * c_w} = \frac{q * t}{(V_{tot} * \varepsilon_l) * c_o} \tag{6.6}$$

Where:

ΔP:	allowable pressure increase [MPa]
q:	API liquid leakage criteria [m^3/min]
c_w:	water compressibility [MPa^{-1}]
c_o:	oil compressibility [MPa^{-1}]
ε_l:	liquid fraction
V_l and V_{tot}:	volume of liquid and total volume [m^3]
t:	test duration [min]

Equation (6.6) used for liquid leaks in producers is close to the equation used for water injectors today. The main difference is that the testing time is 30 minutes and not 10 minutes. Also, the equation uses oil compressibility and not water compressibility. For wells with high water cut, it might be useful to implement an oil compressibility that is close to the water compressibility. As mentioned earlier, the oil compressibility can be up to five times the water compressibility [17]. To be conservative an oil compressibility of three times the water compressibility is used for all calculations using Equation (6.6) in the thesis. Since the water compressibility is known to be $4.35 \times 10^{-4} MPa^{-1}$, then three times that value gives $1.3 \times 10^{-3} MPa^{-1}$, which is the oil compressibility used in the thesis. If the volume above the DHSV consists of mostly liquid, it might also be reasonable to assume that there is a liquid will leak through the DHSV. If the well is left stationary for a while, gas might start to form, and gas might leak through the valve. However, for simplicity, it is assumed that liquid is the leaking fluid here. It is also important to note that any gas in the volume is assumed incompressible when using Equation (6.6)

It has now been established that two equations can be used to calculate the DAC. To determine the limit of when one of the equations should be used instead of the other, a trial and error method is used. The fractions used for the different attempts are listed here:

1. Gas leak equation: 1.00 – 0.05
2. Gas leak equation: 1.00 – 0.05, Liquid leak equation: 0.00
3. Gas leak equation: 1.00 – 0.10, Liquid leak equation: 0.05 – 0.00
4. Gas leak equation: 1.00 – 0.15, Liquid leak equation: 0.10 – 0.00
5. Gas leak equation: 1.00 – 0.20, Liquid leak equation: 0.15 – 0.00

The results from this trial are presented in Figure 6.4 with corresponding fractions as in the list above. From the figure it is clear that the five different combinations provide quite different results. For attempt number one, only the gas leak equation is used. As the gas leak equation is only valid as long as there is gas in the volume, the equation is not valid for completely liquid filled volumes. Hence, attempt number one does not provide a method of calculating the final point on the curves. For attempt number two, the gas leak equation is used for the same fractions as in attempt number one. The only difference is that the liquid leak equation has now been used for fully liquid filled volumes. The shape of the curve does not make sense in a practical manner. The acceptance criteria is reduced when there is only liquid in the volume, between 5% gas down to the liquid filled volume. Attempt number three was therefore created. Here, the liquid leak equation is used for liquid filled volumes and for volumes with only 5% gas. This gives a curve with smaller deviation between the 0% and 5% gas when compared to attempt number two. However, it still does not make sense that the acceptance criteria for 5% gas is higher than for liquid filled volumes. Therefore, attempt number four was made. The fourth attempt used the same method as in attempt three. The only difference was that the liquid leak equation was used for 10% gas as well. From the curves in attempt number four, it is clear that the liquid leak equation increases the DAC values when the liquid fraction is reduced. Attempt number four results in another jump in DAC. Attempt number five was therefore created. This attempt shows the same trend on the curves as attempt number four. The reason for the shape of the curve can be because of the chosen compressibility for this example. With $1.3\text{x}10^{-3}\text{MPa}^{-1}$ for oil leaks and Z-factor of 0.92 for gas leaks. Changing the compressibility would most likely also change the graphs while at the same time keeping the trend as shown for the five examples here. From the curves, it is also reasonable to conclude that smaller volumes are more sensitive to changes.

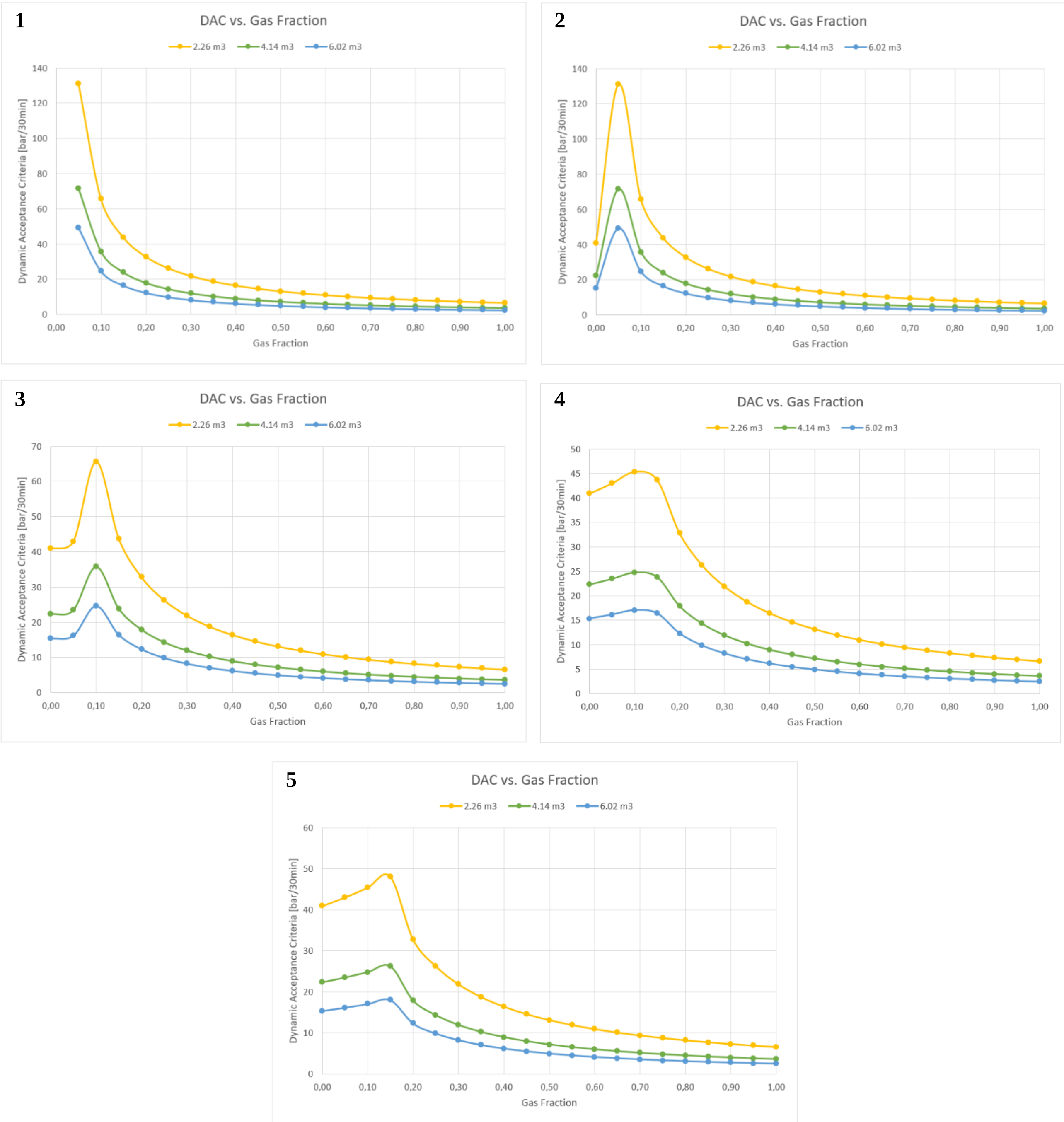

Figure 6.4 DAC vs. Gas fraction – including liquid leaks

The results gathered from the different conditions in Figure 6.4 does not make sense. Mathematically it is correct. However, practically something is not right. It is important to remember that the curves are plotted using two different equations. The results from the curves suggests that a combined equation could solve this problem. Although one common equation can solve the problem, the thesis uses the two equations already derived. Due to this, it is reasonable to choose attempt number four as foundation for the conditions of the equations. This is because attempt number four is the most conservative and less confusing of the five attempts here. Therefore, the gas leak equation will be used for all calculations in the thesis where the gas fraction is from 1.00 down to 0.10, and the liquid leak equation will be used for all gas fractions from 0.10 down to 0.00.

Incorporating DAC will in many cases give a more realistic acceptance criteria which might be more possible to achieve. This is because DAC removes the assumption of always having a gas filled testing volume, and instead uses all available information to include gas and liquid effects in the calculations. Hence, resulting in a lower failure fraction of DHSVs. Today it is common practice to include a longer segregation and stabilization time before the DHSV test. As the fluids segregate, the gas fraction above the valve will increase and go towards the condition that the acceptance criteria is based on today (100% gas filled), but this can be a time-consuming process. Introducing DAC can cause avoidance of the additional time for proper segregation of fluids which again results in reduced shut-in time of the well.

6.3 DAC Calculation Examples

This section investigates the sensitivity of different parameters in Equation (6.5) and Equation (6.6). Equation (6.5) for gas leaks consists of three constants and three variables. The constants are the API gas leakage criteria (q_g), the conversion factor and the testing time (t). Although the testing time can vary, it is assumed constant at 30 minutes in the thesis. The variables in the equation is then the remaining parameters. This is volume (V), Z-factor (Z) and temperature (T). Equation (6.6) for liquid leaks consists of two constants and two variables. The constants are the API liquid leakage criteria (q_l) and the testing time (t). The two variables are the volume (V) and the liquid compressibility (c_l). How these parameters affect the two DAC equations are investigated in five examples here. Three for the gas leak formula and two for the liquid leak formula.

6.3.1 Example 1: Change in Volume – Gas Leak

First parameter to be investigated is the volume. How will the DAC change if the volume change? The calculations here are based on four different volumes. These volumes are ranging from 4.00 m^3 to 7.00 m^3 with an increase of 1 m^3 per example from example 1.1 to example 1.4 in Table 6.1. The table provides some of the results from example 1. The table clearly illustrates that an increase in volume result in a decrease in DAC. This can also be seen in Figure 6.5. The four curved graphs represent the DAC, while the linear graphs represent the SAC. The dark blue graph, representing DAC with the smallest volume, gives a higher DAC than the orange

Table 6.1 Main results from example 1

	Example 1.1 4,00 m³		Example 1.2 5,00 m³		Example 1.3 6,00 m³		Example 1.4 7,00 m³	
εg	SAC	DAC	SAC	DAC	SAC	DAC	SAC	DAC
1,00	3,7	3,7	3,0	3,0	2,5	2,5	2,1	2,1
0,70	3,7	5,3	3,0	4,2	2,5	3,5	2,1	3,0
0,40	3,7	9,3	3,0	7,4	2,5	6,2	2,1	5,3
	Increasing Volume →							

graph which represents the greatest volume for DAC. The same trend can also be seen for SAC with the light blue and bright yellow graphs. More information regarding the base of these calculations and more results are provided in Appendix A.1.

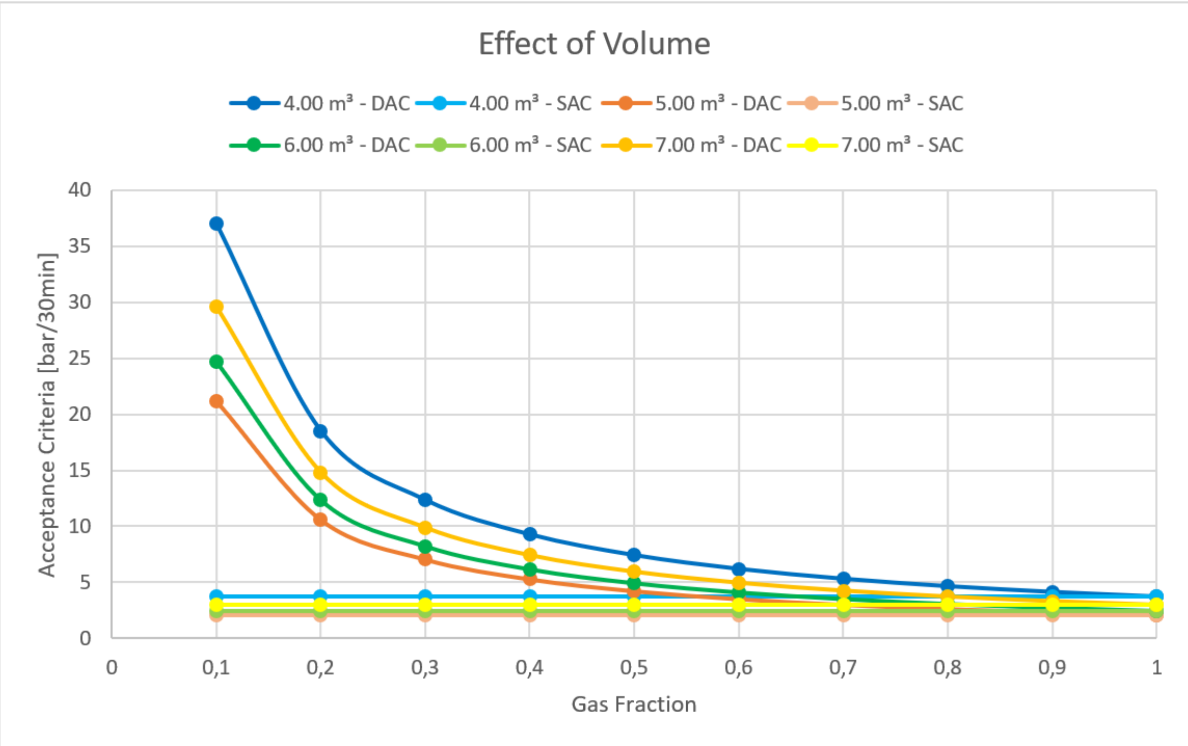

Figure 6.5 Effect of volume – gas leak

6.3.2 Example 2: Change in Temperature – Gas Leak

The second parameter to be investigated is the temperature. Here the temperature will range from 70°C to 100°C. This provides a temperature increase of 10°C per example provided in Table 6.2. The results in the table shows a clear 0.1 bar increase for every 10°C temperature increase for the 100% gas filled volume. However, for the other gas fractions the pattern is not so clear. For those the pressure changes ranges between 0.1 bar to 0.3 bar. Figure 6.6 illustrates the difference between DAC and SAC when the temperature changes. From the graphs it is reasonable to state that the change in acceptance criteria is smaller with every 10°C temperature

Table 6.2 Main results from example 2

	Example 2.1 70 °C		Example 2.2 80 °C		Example 2.3 90 °C		Example 2.4 100 °C	
εg	SAC	DAC	SAC	DAC	SAC	DAC	SAC	DAC
1,00	3,4	3,4	3,5	3,5	3,6	3,6	3,7	3,7
0,70	3,4	4,8	3,5	5,0	3,6	5,1	3,7	5,3
0,40	3,4	8,5	3,5	8,7	3,6	9,0	3,7	9,2
	Increasing Temperature →							

change than for every m^3 volume change. For more information regarding the calculations and to see more results, see Appendix A.2.

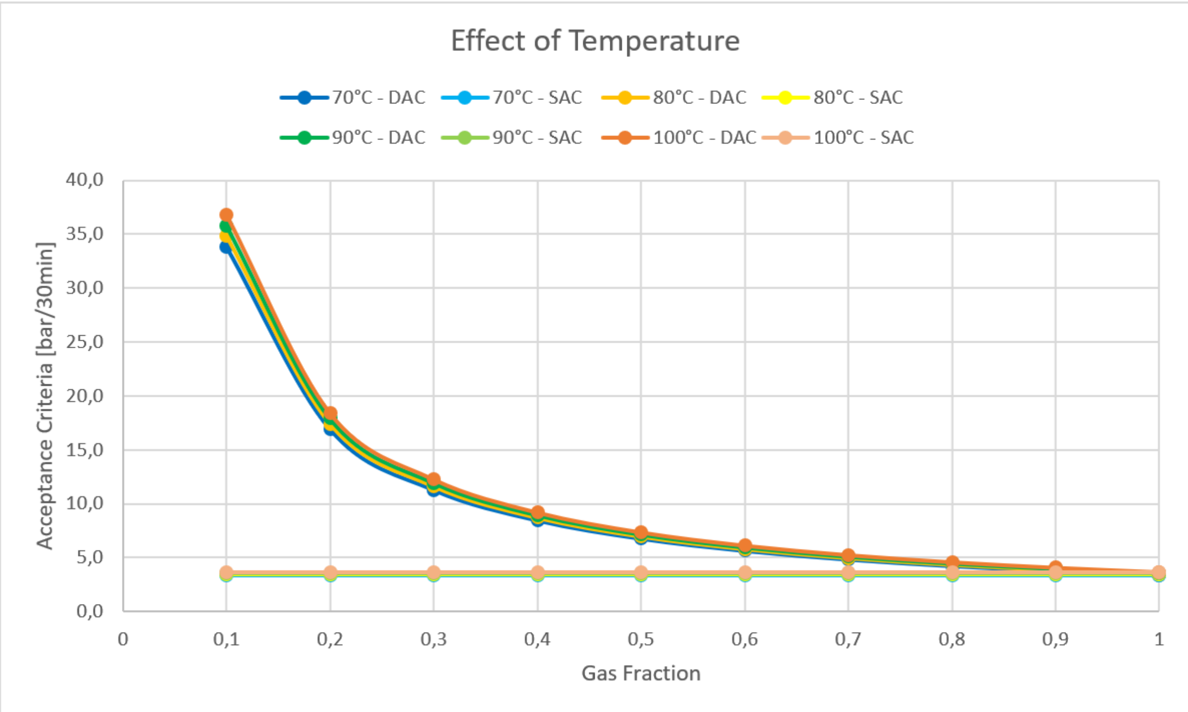

6.3.3 Example 3: Change in Z-factor – Gas Leak

The final parameter to be investigated is the Z-factor. The values of the different Z-factors used in this example ranges from 0.88 to 0.94 with an increase of 0.02 for each example. Table 6.3 presents some of the results from example 3. As the previous two examples the value

Table 6.3 Main results from example 3

	Example 3.1 0,88		Example 3.2 0,90		Example 3.3 0,92		Example 3.4 0,94	
εg	SAC	DAC	SAC	DAC	SAC	DAC	SAC	DAC
1,00	3,4	3,4	3,5	3,5	3,6	3,6	3,7	3,7
0,70	3,4	4,9	3,5	5,0	3,6	5,1	3,7	5,2
0,40	3,4	8,6	3,5	8,8	3,6	9,0	3,7	9,1
	Increasing Z-factor →							

of the parameter increases to the right in the table. It is clear to see that an increase in Z-factor results in an increase in DAC. The DAC for every 0.02 increase in Z-factor results in an increase of 0.1 bar when the gas fraction is 100%. For other gas fractions the increase ranges between 0.1 bar and 0.2 bar. The small change in acceptance criteria can be seen in Figure 6.7 in a similar way as for the temperature change in Figure 6.6. Can see that a change in Z-factor of 0.02 will have a smaller impact than a 1 m^3 volume change. For more information regarding the calculations, see Appendix A.3. More results are also presented there.

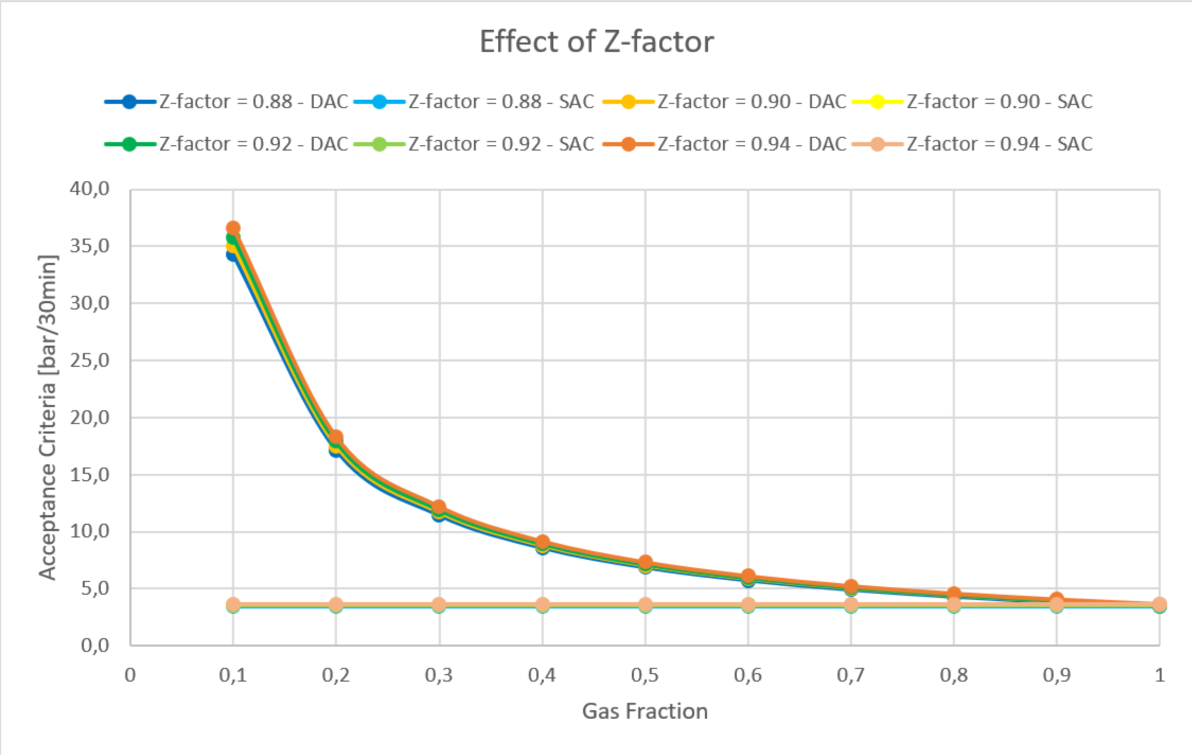

Figure 6.7 Effect of Z-factor – gas leak

6.3.4 Example 4: Change in Volume – Liquid Leak

For the liquid leak equation, the first variable to be investigated is the volume. Table 6.4 presents the main results from example 4. The rest of the results can be found in Appendix A.4 together with more information on the basis for the calculations. Example 4 investigates four

Table 6.4 Main results from example 4

	Example 4.1 4,00 m³		Example 4.2 5,00 m³		Example 4.3 6,00 m³		Example 4.4 7,00 m³	
εl	SAC	DAC	SAC	DAC	SAC	DAC	SAC	DAC
1,00	23,1	23,1	18,5	18,5	15,4	15,4	13,2	13,2
0,70	23,1	33,0	18,5	26,4	15,4	22,0	13,2	18,8
0,40	23,1	57,7	18,5	46,2	15,4	38,5	13,2	33,0
	Increasing Volume →							

different volumes. The volumes investigated ranges from 4.00 m^3 to 7.00 m^3, where the volume increases with 1 m^3 for each example. From the table it is clear to see that for a 100% liquid filled volume, both SAC and DAC are reduced as the volume is increased. This trend can also be seen in the plot in Figure 6.8. The figure is plotted in the same way as for the first three examples. It shows the effect of the change in volume against the DAC. Can see from the shapes of the graphs that they behave in the same manner as for the volume change when using the gas leak equation. This corresponds well with the two equations. In both equations, the volume is in the denominator. This causes an increase in DAC when the volume in the denominator is reduced. One important difference between the two plots for volume change, is that the DAC for the liquid leaks provide generally larger values of DAC. This can be seen very clearly when comparing the plot in Figure 6.5 with Figure 6.8 here.

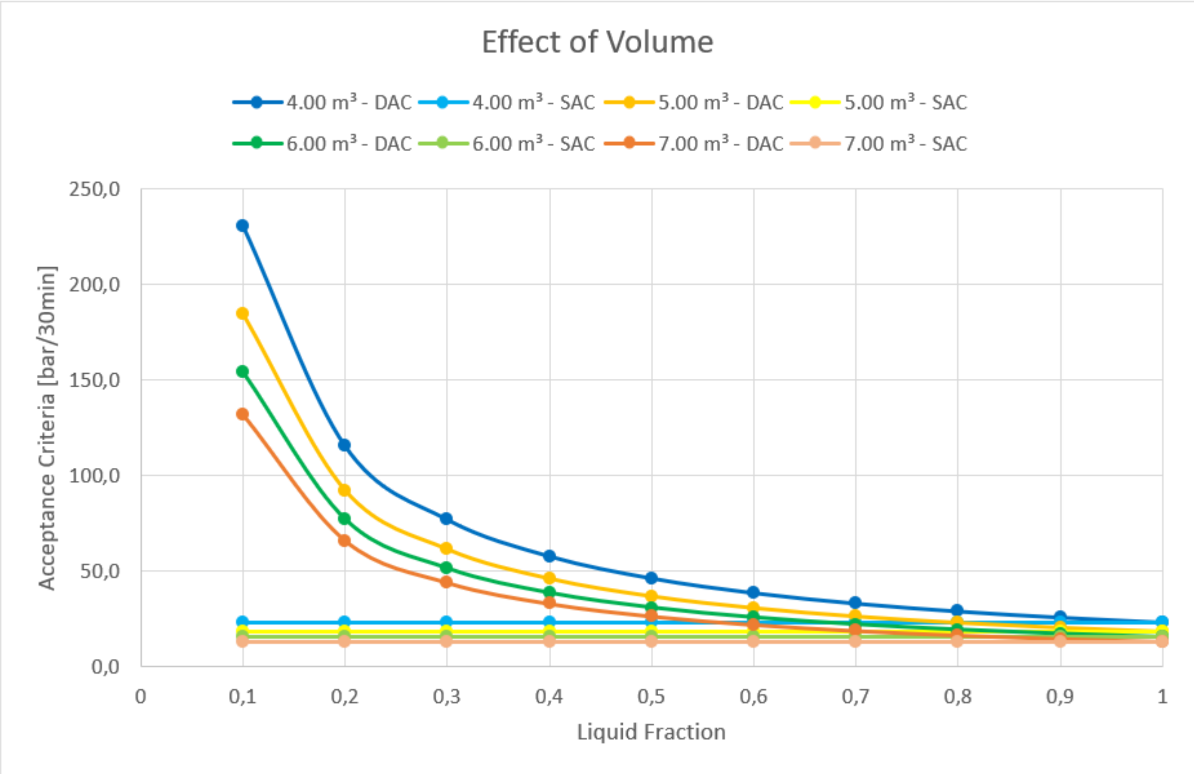

Figure 6.8 Effect of volume - liquid leak

6.3.5 Example 5: Change in Oil Compressibility – Liquid Leak

The final variable to be investigated for the liquid leak equation is the liquid compressibility. The main results from example 5 is found in Table 6.5, while the rest of them can be found in Appendix A.5 together with more information on the calculations. Four different values for compressibility are used. For example number 5.1, the compressibility is equal to the liquid compressibility of 4.35x10^{-4}MPa^{-1}. The second example are twice the water

Table 6.5 Main results from example 5

	Example 5.1 0,000435/MPa		Example 5.2 0,00087/MPa		Example 5.3 0,0013/MPa		Example 5.4 0,00218/MPa	
εl	SAC	DAC	SAC	DAC	SAC	DAC	SAC	DAC
1,00	66,7	66,7	33,3	33,3	22,3	22,3	13,3	13,3
0,70	66,7	95,2	33,3	47,6	22,3	31,9	13,3	19,0
0,40	66,7	166,7	33,3	83,3	22,3	55,8	13,3	33,3
	Increasing Oil compressibility →							

compressibility. The third example uses the compressibility chosen for the calculations in the thesis, $1.3x10^{-3}MPa^{-1}$, which corresponds to three times the water compressibility. The fourth and final example uses a compressibility that corresponds to five times the compressibility of water. The main results from these four examples are presented in Table 6.5. From the table an increase in compressibility results in a decrease in acceptance criteria. Results from example 5.1 are five times the result of 5.4, three times the result of 5.3 and twice the result from 5.2. this indicates that the DAC for liquid is proportional to compressibility. From the table it also is reasonable to conclude that DAC is sensitive to change in compressibility. DAC increases as the liquid fraction is decreases. This trend can also be seen in the plot in Figure 6.9. The graphs clearly show that a lower compressibility results in a higher acceptance criteria for the test. It can also be seen that the interval of different compressibility values provides a bigger variation

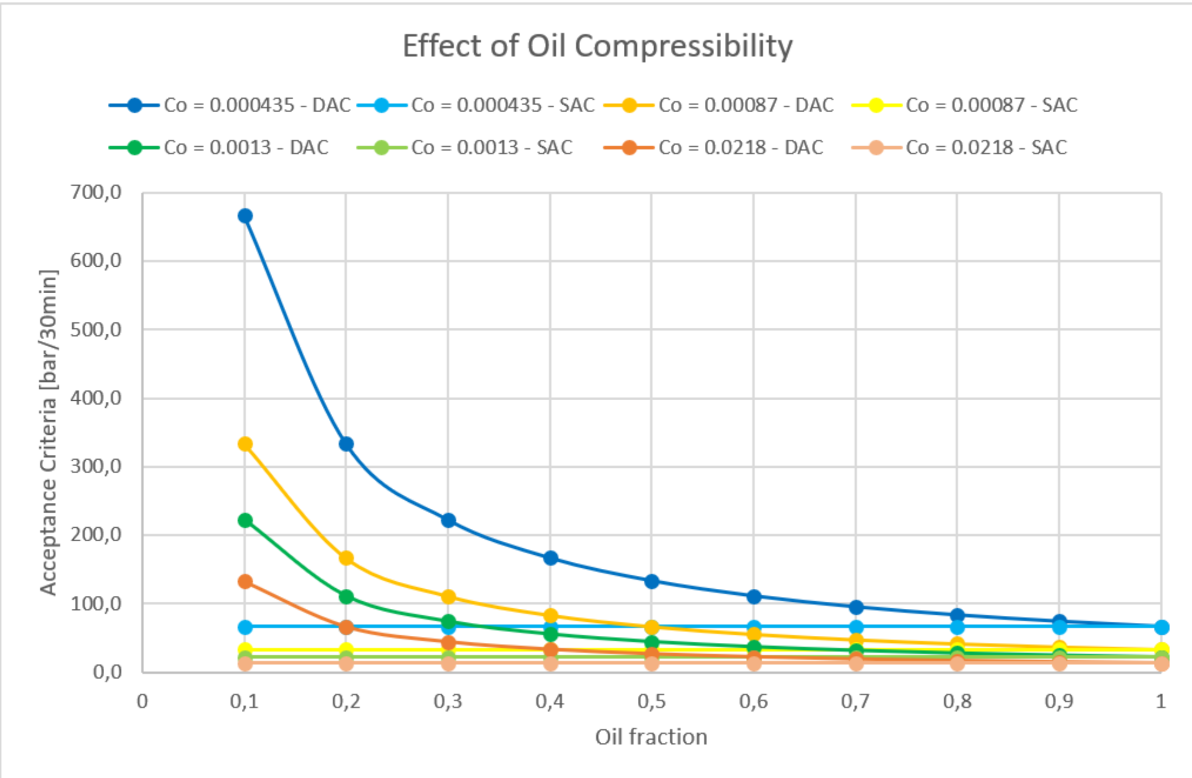

Figure 6.9 Effect of oil compressibility - liquid leak

of DAC for small liquid fractions. For values above 90% liquid, the DAC have smaller variations depending on compressibility. However, there are still variations in DAC values above 90% liquid fraction. This is not as clear in the figure as the y-axis stretches up to 700 bar/30 min, but it is clearer in Table 6.5. This causes great uncertainties when assuming a compressibility for the oil.

6.4 Excel Sheet for Calculations

Calculating the DAC will be more reliable if a standardized method is used. This can for instance be done using an Excel sheet. Using this method will provide faster calculations. It will make it easier for different people to use. Also, it ensures that the DAC is always calculated in the same way and thus mitigating possible human errors.

Parameter	Value	Unit	Description	Comment
D_{DHSV}	250	m RKB	Setting depth of DHSV	
D_{TH}	30	m RKB	Setting depth of tubing hanger	
c	18,81	l/m	Tubing capacity	
V_{tot}	**4,14**	**m³**	Total volume between DHSV and TH	Cell can be overwritten if value is known
ϵ_g	0,858	-	Gas fraction	Given as 1 = 100% gas, 0,50 = 50% gas etc.
V_g	**3,55**	**m³**	Gas volume	Cell can be overwritten if value is known
q	0,42	m³/min	API gas leakage criteria	Constant
t	30	min	Testing time	Should be minimum 30 min
T	90	°C	Temperature	Will automatically be converted to Kelvin during calculations
Z	0,92	-	Compressibility factor of gas	If unknown, use Z = 0,90
ΔP_{DAC}	**0,42**	**Mpa**	Allowable pressure increase during test	
ΔP_{DAC}	**4,2**	**bar**	Allowable pressure increase during test	

DAC = 3,6 bar / 30 min

Fill in **green** fields

$$\Delta P = \frac{q * t * T * Z}{V * 2.84 * 10^3}$$

Figure 6.10 Example on Excel sheet used for gas leak calculations

Figure 6.10 and Figure 6.11 illustrates both a simple way of doing this. Figure 6.10 shows an Excel sheet for the gas leak calculations, while Figure 6.11 shows an Excel sheet for the liquid leak calculations. The idea and layout of the excel sheets in the figures are gathered from similar excel sheets in Equinor [13]. However, the sheets provided here are modified versions of them, adapted to be used for both SAC and DAC. The excel sheets are created such that all the parameters are connected. If one parameter is changed the DAC in the yellow window will change accordingly. For simplicity it is only the cells marked green that should be changed.

Parameter	Value	Unit	Description	Comment
D_{DHSV}	250	m RKB	Setting depth of DHSV	
D_{TH}	30	m RKB	Setting depth of tubing hanger	
c	18,81	l/m	Tubing capacity	
V_{tot}	**4,14**	**m³**	Total volume between DHSV and TH	Cell can be overwritten if value is known
ϵ_o	1,000		Oil fraction	
V_{oil}	**4,14**	m³	Oil volume	
q	0,0004	m³/min	API liquid leakage criteria	Constant
t	30	min	Testing time	Should be minimum 30 min
C_o	0,0013	1/MPa	Oil compressibility	Cell can be overwritten if value is known
ΔP	**2,23**	**MPa**	Allowable pressure increase during test	
ΔP	**22,3**	**bar**	Allowable pressure increase during test	

DAC = 22,3 bar / 30 min

Fill in **green** fields

$$\Delta P = \frac{q * t}{V * c_o}$$

Figure 6.11 Example on Excel sheet used for liquid leak calculations

6.5 Summary of Assumptions and Uncertainties

There have been some assumptions made regarding the DAC equations and the DAC calculation examples provided in this chapter. These have been made to simplify the calculations and to make them more practical to use during an actual DHSV leakage test. These assumptions are:

- Gas leaking through the valve for gas fractions down to 0.10
- Liquid leaking through the valve for gas fractions from 0.10 and lower
- Assume DHSV is the only possible leakage point
- Incompressible liquid for gas leak calculations
- Incompressible gas for liquid leak calculations
- Constant testing time of 30 minutes
- Fully segregated volume
- Oil compressibility is 1.3×10^{-3} MPa^{-1}

There are also some uncertainties when using this method. These uncertainties are:

- The effect of liquid compressibility and gas compressibility combined
- Assuming gas leak down to 10% gas in the volume, then assuming liquid leak from 10% gas and up to 100% liquid filled volume

7 Locating the Interface Between Gas and Liquid

The main factor that differs DAC from SAC is the introduction of both gas and liquid. From Chapter 6 it has already been determined that the gas fraction is needed in order to calculate DAC for gas leaks, and the liquid fraction is needed to calculate DAC for liquid leaks. For the calculations in the thesis, the gas fraction is calculated and used to determine the liquid fraction. During production the fractions can be determined from separator data. However, when the well is shut-in and the volume is static, the fractions are unknown. This is the situation during the DHSV leakage test.

Being able to locate the interface between the liquid and the gas in the well is a crucial step in using DAC in a real DHSV leakage test. Until this point, the thesis has calculated DAC where the different fractions have been known. Now the interface must be determined from given data. Hence, data that is available during a DHSV test. It should be kept in mind that to implement DAC it must be practical to use during a real DHSV test, not just in theory. The methods must be based on available equipment and data and be performed within reasonable time. This is investigated throughout this chapter.

7.1 Calculation Using MATLAB

The idea of calculating the interface depth is based on an Equinor employee's idea (H. S. Bakka). The idea was to calculate the interface using a script. The script would use BHP, WHP and PVT data. It starts at the bottom (at the downhole pressure and temperature gauge) and calculates the liquid pressure in intervals up to a guessed interface depth. The guessed interface depth is the depth measured from the downhole pressure and temperature gauge, up to the depth where it is believed that the gas-liquid interface is located. At this interface depth, the script calculates the gas pressure up to the WH. If the WHP measured is equal to the WHP calculated the interface would be located at the guessed depth. If not, a new guess should be made, and calculations performed again. Based on this idea a MATLAB code is constructed to perform the calculations for the thesis. MATLAB was chosen because it has frequently been used at the University of Stavanger for several subjects. One of those subjects, *Computational Reservoir and Well Modeling*, forms the basis for the MATLAB code used here [39].

The MATLAB code used in the thesis is based on the idea from the Equinor employee. The code is based on the assumptions that the well is shut-in and the DHSV is open. The MATLAB code deviates from the original idea on some parts. For instance, the code does not guess a certain depth of the interface. Instead, the code guesses an interface interval. This interval is referred to as the Search Interval. The search interval should be specified such that the lower limit is 0, and the top limit is the depth of the bottom hole gauge. By doing this, the code will search for the interface in the whole well, and not just a small section. If this is done, the MATLAB code will have three possible solutions. These different solutions are illustrated in Table 7.1. The two columns to the right shows the different combinations of output values the code can have. The column to the right explain what these different combinations means.

Table 7.1 Possible MATLAB code result

Explanation of MATLAB code output	**error**	**solution**
No interface located in the well	= 1	= 0
Interface located above the TH, hence not in the well	= 1	≠ 0
Interface located in the well	= 0	≠ 0

Another part that differs from the original idea is that the MATLAB code calculates the average pressures. It does not calculate the pressure in given intervals. Instead it calculates the average liquid pressure up to the interface depth. At the interface depth the code uses a calculated temperature gradient to calculate an average temperature together with the average pressure up to the WH. The pressure and temperature above the interface are used to calculate the gas density. This means that the MATLAB code does not have an input for the gas density. For the liquid density, the code input is a reference density. Pressure and temperature will also affect the liquid density in the well. This means that the MATLAB code is differing from the original idea by using less accurate PVT data than those measured from the well.

The MATLAB code used in the thesis to locate the interface between gas and liquid consists of five files. All these files play an important part in locating the interface. The different files are named *main*, *bisection*, *func*, *rholiq* and *rhogas*. The *main* file is called a script, while the rest of the files are functions. This means that four of the files contain a separate function and are therefore more flexible [40]. The *main* script is simpler, as this part of the program uses the commands in the exact way they are written [40]. It is called *main* in this setting since it is the main part of the code than controls the whole program. To see what the code looks like, see Appendix B.

Figure 7.1 illustrates the build-up of the code. The *main* script calls upon the *bisection* function, the *bisection* function calls upon the *func* function, and the *func* function calls upon the *rholiq* and *rhogas* functions. Looking at the files in a reversed order can help explain how they work together. The *rholiq* and *rhogas* functions both calculate the densities with respect to pressure and temperature. These two are further used in the *func* function. The *func* function uses the given input and the values from *rholiq* and *rhogas* to calculate the WHP. The *bisection* function uses the *func* function to find out at which interface depth the WHP calculated is equal to the WHP measured. This part of the code has an accuracy of 100 Pa, which corresponds to 0.01 bar. To locate the interface and calculate the WHP, the *bisection* function implements the search interval which is given in the *main* script. Finally, the *main* script runs the whole program and display the result.

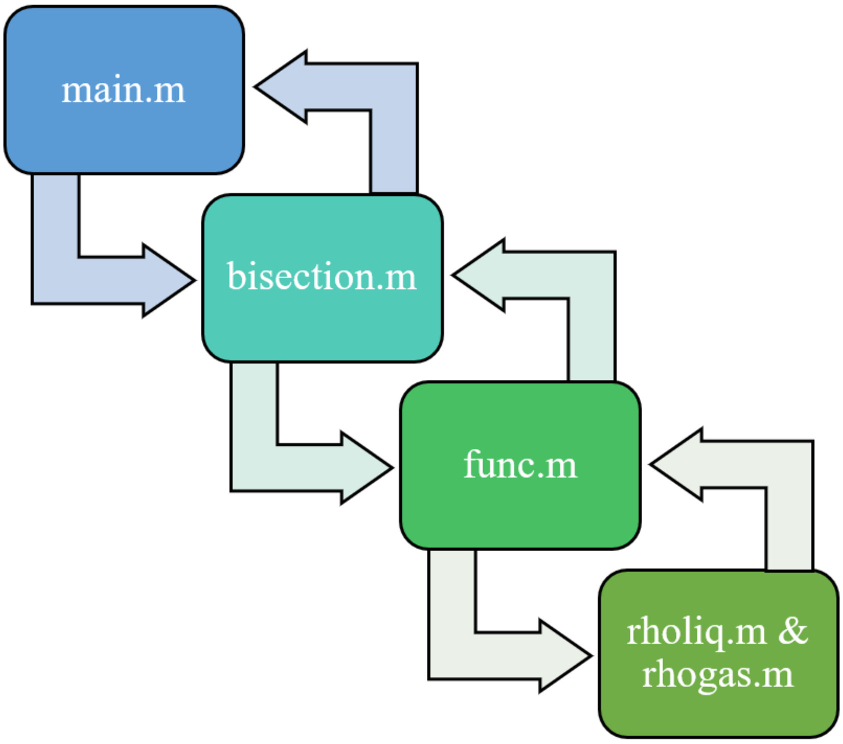

Figure 7.1 MATLAB code build-up

To make the program practical to use and at the same time more accurate, there are some input data needed for the code to run. The most important input data is given in Figure 7.2. The search interval, WHP, BHP, temperatures, TVD of the gauge, TVD of the tubing hanger, reference liquid density and Z-factor are all important data input needed for the code to function. It is important to note that TVD of the gauge means TVD of the bottom hole pressure and temperature gauge. This depth is specified in *main*, together with the search interval and the TH depth. It is also specified in *func*. TVD of the TH is a parameter that is included such that the code can tell the user if the interface found by the code is in the well or not. The reference liquid density refers to either the density at the bottom hole gauge depth, or an average density in the well. It is preferred to use the density at the gauge since the code uses the reference density at the bottom and includes temperature and pressure effects on the density for the remaining calculations in the code. The density is specified in *rholiq*. The Z-factor is specified in *rhogas*. If the value of the Z-factor is not known, it can be assumed to be 0.90. The remaining input data are all specified in *func*. In the MATLAB code located in Appendix B, there are also other input data than those illustrated in Figure 7.2, that can be changed. These inputs have a suggested value in the code (in the same way as the Z-factor) that can be changed if a more accurate value is known.

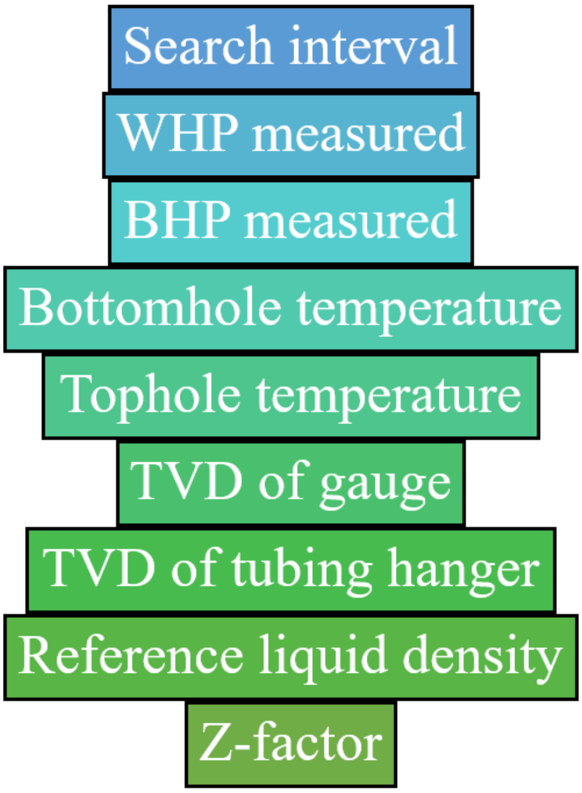

Figure 7.2 Input for MATLAB code

It is important to note that the MATLAB code has some uncertainties. For instance, the accurate PVT data along the well path is not used. For the liquid density, some water properties are used instead of oil properties. If more accurate oil properties are known they should be included since they would make the calculations more accurate. Also, the MATLAB code is based on simple calculations of the interface. To make the calculations more accurate, a more complex code should be made. This is not done for this thesis as the potential of using DAC for leakage tests are investigated. To illustrate how the MATLAB code used for the thesis can be used, and how it works, some basic examples are given.

7.1.1 Calculation Examples for the MATLAB Code

This section of the thesis illustrates the usage of the MATLAB code. The code in Appendix B will be tested using different values. The objective of the examples presented here is to illustrate how the code works with different input values in basic examples. Two of the examples will be used to illustrate the whole process from beginning to end, which starts at locating the interface and ends with obtaining the DAC.

Table 7.2 shows the input values for six examples. The green row present the interface depth gathered from the MATLAB code based on the given inputs for each example. The blue row tells if the interface is in the well or not. This is done by evaluating the code output. Remember the three possible solutions in Table 7.1 that the MATLAB code can provide. For example number 4 and 5, the MATLAB code did not find an interface. This can be seen from the output that displayed error = 1 and solution = 0. Hence, the interface is not in the well. For example number 1 and 6, the MATLAB code was able to locate an interface. However, this interface was found to be above the TH in the well. This can be seen from the output that displayed error = 1 and solution $\neq$0. Because of these results on these tests, it is concluded that there is no interface in these four wells. Therefore, it is reasonable to assume that these wells are liquid filled. The final two examples, example number 2 and 3, are the only two wells that have an interface in the well. This can be seen on their output being error = 0 and solution $\neq$ 0.

Table 7.2 MATLAB code examples

Example	1	2	3	4	5	6
BHP (bar)	170	180	190	170	190	190
WHP (bar)	30	40	50	20	20	50
TVD to gauge (m)	2000	2000	2500	2000	1800	1800
TVD to TH (m)	200	30	30	200	30	30
Temp. bottom (°C)	100	80	90	110	100	100
Temp. top (°C)	60	30	40	20	40	40
Liquid density (kg/m^3)	750	800	850	750	850	800
Z-factor	0.88	0.90	0.92	0.88	0.92	0.92
MATLAB error	1	0	0	1	1	1
MATLAB solution	**83.8**	**218.7**	**845.1**	0	0	**7.5**
Interface depth (m)	**N/A**	**218.7**	**845.1**	**error**	**error**	**N/A**
Interface in well?	**No**	**Yes**	**Yes**	**No**	**No**	**No**

Workspace

Name	Value
a	0
b	2000
error	1
solution	1.9162e+03
TH	200
TVD	2000
TVDint	83.8318

Example 1

Workspace

Name	Value
a	0
b	2000
error	0
solution	1.7813e+03
TH	30
TVD	2000
TVDint	218.7195

Example 2

Workspace

Name	Value
a	0
b	2500
error	0
solution	1.6549e+03
TH	30
TVD	2500
TVDint	845.0508

Example 3

Workspace

Name	Value
a	0
b	2000
error	1
solution	0
TH	200
TVD	2000
TVDint	2000

Example 4

Workspace

Name	Value
a	0
b	1800
error	1
solution	0
TH	30
TVD	1800
TVDint	1800

Example 5

Workspace

Name	Value
a	0
b	1800
error	1
solution	1.7925e+03
TH	30
TVD	1800
TVDint	7.4707

Example 6

Figure 7.3 Output of MATLAB code

The output and input values presented in Table 7.2 does not show how the results are displayed when using the code. The code has a *Workspace* that shows the input values specified in *main* and the output values from *bisection*. The results gathered from *bisection* are processed and presented by *main*. Figure 7.3 shows the *Workspace* of the six examples used here. There are seven values displayed for each example in the *Workspace*. The first two values displayed are a and b. They are the specified search interval measured from the bottom of the well. In Figure 7.3, the search interval starts at 0 (bottom) and ends at TVD of gauge (top). Since the search interval is specified as depth from bottom, the TVD of the gauge represents the length to the top of the well. The third value in the *Workspace* is called error. This value lets the user know if there is an interface in the well or not. The 0 means that there is an interface for the problem, while 1 means that there is either no interface in the well, or the code has calculated the interface to be above the TH. Which of these that is the case, is defined by the fourth output value in the *Workspace*, the solution. If the output shows solution = 0, then the code did not find an interface for the problem. However, if the solution ≠ 0, then the code have been able to calculate an interface depth. See Table 7.1 for a recap on the three possible solutions of the code. The interface depth given by solution is given m TVD from the bottom of the well. The next value in the Workspace is the TH depth. This depth is an input value that is only used to check if the interface found by the code is in the well or not. The next value is the TVD of the downhole gauge. This value is also the input value for the upper limit of the search interval (b).

Finally, the interface depth measured from the WH and down is calculated by subtracting the solution from the TVD of the downhole pressure gauge. This depth measured from the top is the depth used for further calculations of the DAC. To understand how this will be used to calculate the DAC, two examples will be looked closer at.

Example 2 and 3 will be used to calculate the DAC. First step in the calculations is to calculate the gas fraction by determining whether the interface is located above or below the DHSV. From the MATLAB code it has already been determined that the interface is located below the TH for these two examples. Next step is therefore to determine whether the interface is in the volume between the DHSV and the TH or not. For these two examples the DHSV is located at 250 m and the TH is located at 30 m (from Table 7.2). This means that for example number 3, where the interface is located at 845.1 m, the interface is located below the DHSV. Hence the volume above the valve is 100% gas filled and the gas fraction is 1.00. The acceptance criteria for example 3 can then be calculated using the same method as used today. However, in example number 2 the interface is located at 218.7 m and is therefore above the DHSV. This means that the gas fraction must be calculated using the DHSV depth, the TH depth, and the interface depth obtained from the MATLAB code:

$$\begin{aligned}\varepsilon_g = 1 - \varepsilon_l = 1 - \left(\frac{(d_{DHSV} - d_{TH}) - (d_{int} - d_{TH})}{d_{DHSV} - d_{TH}}\right) \\ = 1 - \left(\frac{(250m - 30m) - (218.7m - 30m)}{250m - 30m}\right) = 0.858\end{aligned}$$

From the calculation there is 85.8% gas in the volume above the DHSV in example 2. This gas fraction is then used in the final step of the DAC calculation. To perform the calculation, the Excel sheet in Figure 6.10 will be used. Figure 7.4 illustrates the calculations of both SAC and DAC for example number 2. The calculation on top in Figure 7.4 is the calculation for the SAC. Although the yellow window says DAC, it is the SAC calculation based on the gas fraction being equal to 1.00. The bottom calculation in the figure is therefore the DAC calculation. This can be seen by the gas fraction being equal to 0.858 and not 1.00. From these calculations it is clear to see that the DAC is 4.2 bar/30 min while the SAC is 3.6 bar/30 min. For this test this results in an increase of 0.6 bar/30 min on the acceptance criteria. The acceptance criteria has therefore gotten more spacious. If this well is now tested and has a pressure increase of 4,0 bar during the 30-minute test, the two different acceptance criteria provide different results. Using the SAC, which is the method used today, the test fails. This results in more shut-in time on the well to get a good test on the valve. However, if DAC is used the test is approved.

Parameter	Value	Unit	Description	Comment
D_{DHSV}	250	m RKB	Setting depth of DHSV	
D_{TH}	30	m RKB	Setting depth of tubung hanger	
c	18,81	l/m	Tubing capacity	
V_{tot}	**4,14**	m^3	Total volume between DHSV and TH	Cell can be overwritten if value is known
ϵ_g	1	-	Gas fraction	Given as 1 = 100% gas, 0,50 = 50% gas etc.
V_g	**4,14**	m^3	Gas volume	Cell can be overwritten if value is known
q	0,42	m^3/min	API gas leakage criteria	Constant
t	30	min	Testing time	Should be minimum 30 min
T	90	°C	Temperature	Will automatically be converted to Kelvin during calculations
Z	0,92	-	Compressibility factor of gas	If unknown, use Z = 0,90
ΔP_{DAC}	**0,36**	**Mpa**	Allowable pressure increase during test	
ΔP_{DAC}	**3,6**	**bar**	Allowable pressure increase during test	

DAC = 3,6 bar / 30 min

Parameter	Value	Unit	Description	Comment
D_{DHSV}	250	m RKB	Setting depth of DHSV	
D_{TH}	30	m RKB	Setting depth of tubung hanger	
c	18,81	l/m	Tubing capacity	
V_{tot}	**4,14**	m^3	Total volume between DHSV and TH	Cell can be overwritten if value is known
ϵ_g	0,858	-	Gas fraction	Given as 1 = 100% gas, 0,50 = 50% gas etc.
V_g	**3,55**	m^3	Gas volume	Cell can be overwritten if value is known
q	0,42	m^3/min	API gas leakage criteria	Constant
t	30	min	Testing time	Should be minimum 30 min
T	90	°C	Temperature	Will automatically be converted to Kelvin during calculations
Z	0,92	-	Compressibility factor of gas	If unknown, use Z = 0,90
ΔP_{DAC}	**0,42**	**Mpa**	Allowable pressure increase during test	
ΔP_{DAC}	**4,2**	**bar**	Allowable pressure increase during test	

DAC = 4,2 bar / 30 min

Figure 7.4 Comparison of SAC (top) and DAC (bottom)

How the interface is located using calculations in the MATLAB code has now been illustrated. However, calculating the interface depth is not the only method that can be used to locate the interface. Measurements using Fiber Optics or Echo Sounding can also be done to obtain the interface depth. How these two methods work was described in Chapter 4. Here, the practical use of the methods will be explained.

7.2 Using Fiber Optics

Fiber Optics is, as explained in Chapter 4, a technology that uses fiber optic cables along the well path which can measure fluid behavior. It is a technology that can be installed permanently or be installed for a single measurement. Fiber is not a technology that is common for all wells. The technology was first introduced to the oil and gas industry in the beginning of the 90's [41]. However, it is still far from all wells that have fiber installed. This means that Fiber Optics is a relatively new method that most likely can only be used for some wells.

The idea here is to use Fiber Optic measurements to locate the interface between gas and liquid for two different DHSV leakage tests. For these two tests, the interface will also be calculated using the MATLAB code. Finally, these results will be compared. Using Fiber Optics in this way, to measure the interface during a DHSV test, is a relatively new way of using the fiber. Due to this there are a lot of uncertainties that must be discussed. As stated in Chapter 4, only DTS will be used for this.

The first DHSV leakage test is illustrated in Figure 7.5. The y-axis represents the depth, while the x-axis illustrates time. The color represents the temperature gradient. This is the temperature change rate in degrees per minute (deg/min). Red are areas where the temperature is increasing, while blue areas are not. Note that the color scale in Figure 7.5 is clipped to only show the increasing temperatures. Hence only the heating. The measurements in Figure 7.5 shows three clear responses, a), b) and c). The first response, a), is the response measured when the lower master valve in the XT is opened after testing the XT before testing the DHSV. The second response, b), is for the pressure depletion above the DHSV before the DHSV leakage test. This is where the pressure above the DHSV is bled down to gain the desired 70 bar

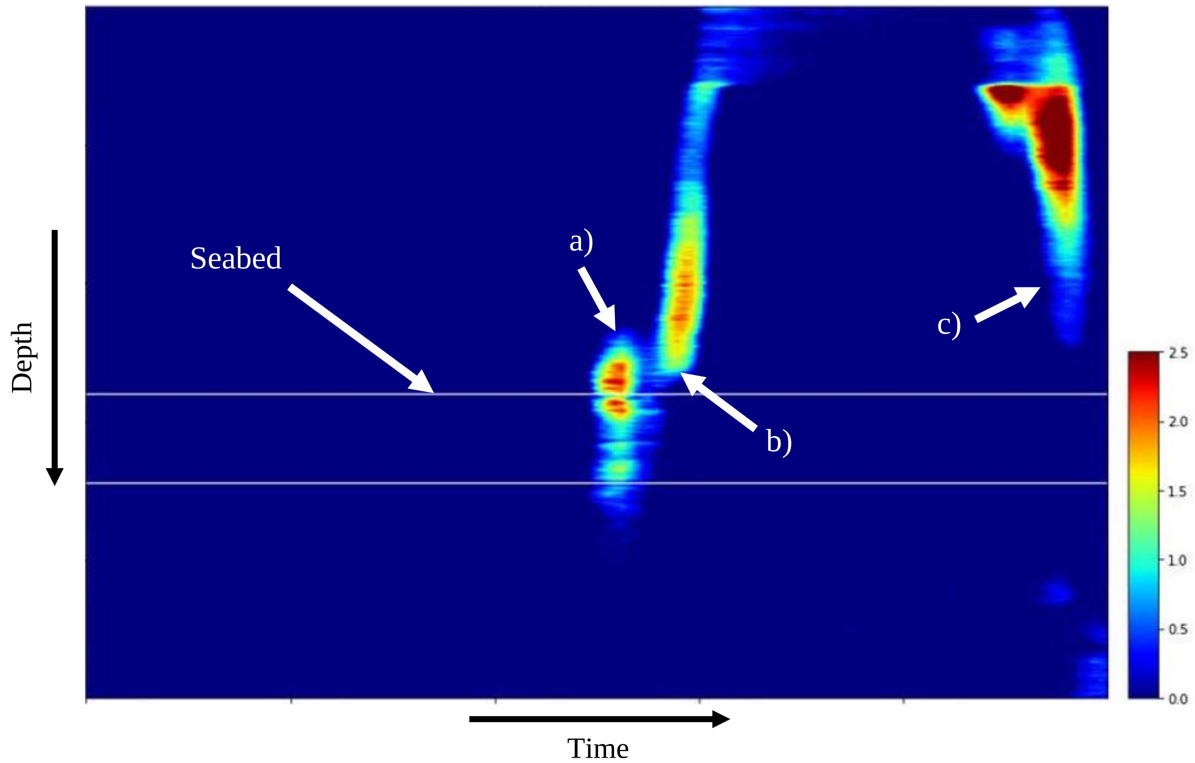

Figure 7.5 DTS interface level for the first DHSV leakage test (reproduced with permission) [13]

differential pressure across the DHSV. The DHSV is closed between these two responses. The third response, c), is the response gathered when the pressure above the DHSV is increased before opening the valve.

From the unloading example in Figure 4.5 in Chapter 4.1.1, it seemed that DTS was only able to see the interface clearly if the fluids where moving. Looking at Figure 7.5 that seems to be the case here as well. For all three responses, the fluids are moving. When the lower master valve is opened, when the pressure is bled off, and when pressure in equalized across the DHSV, the fluids are moving and DTS can measure the response. The difference in temperature at the top of a) and at the bottom of b) can therefore indicate the interface depth. Since response b) is gathered during the depletion procedure right before the DHSV test is performed, this might be the most accurate measurement to use as the interface depth. If this is the case, then the interface for the first DHSV test, gathered from the fiber, should be located at around 170-180 m TVD. To verify if this can be the case, the accurate data for this test will be used as input in the MATLAB code to calculate the interface depth. The data used for the calculations are not published in the thesis. Only the result from the code is included. The result from the code is summarized and compared to the result from the fiber measurements in Table 7.3, following the interpretation of the second DHSV test.

Before looking at the second DHSV test, it is also important to note that a) and b) are both located closely to the seabed in Figure 7.5. This causes uncertainty about this being the interface responses. As mentioned in Chapter 4.1.1, DTS measures heating as fluid are moving up in the well. Also, the interface gathered from the fiber measurements in Figure 7.5 are both located in a part of the well that is in the sea. Due to this, there is seawater with no clear temperature gradient outside the well. This makes it uncertain if the fiber measurements measures the interfaces or the fluids moving. Another uncertainty is response b). Here the pressure above the DHSV is reduced and the gas expands as the liquid is significantly less compressible. Due to the Joule-Thomson effect, it is expected that the expanded gas will cool down. However, the response in Figure 7.5 indicates heating. This response also contributes to the uncertainties around the interface depth being located in this area. [13]

The second DHSV test is illustrated in Figure 7.6. The y- and x-axis, and the colors are plotted in the same way as for Figure 7.5. The second DHSV test also has three clear responses in the figure, a), b) and c), in the same way as the first DHSV test. The procedure for both tests are the same. Hence, the first response, a), in Figure 7.6 is from opening the lower master valve

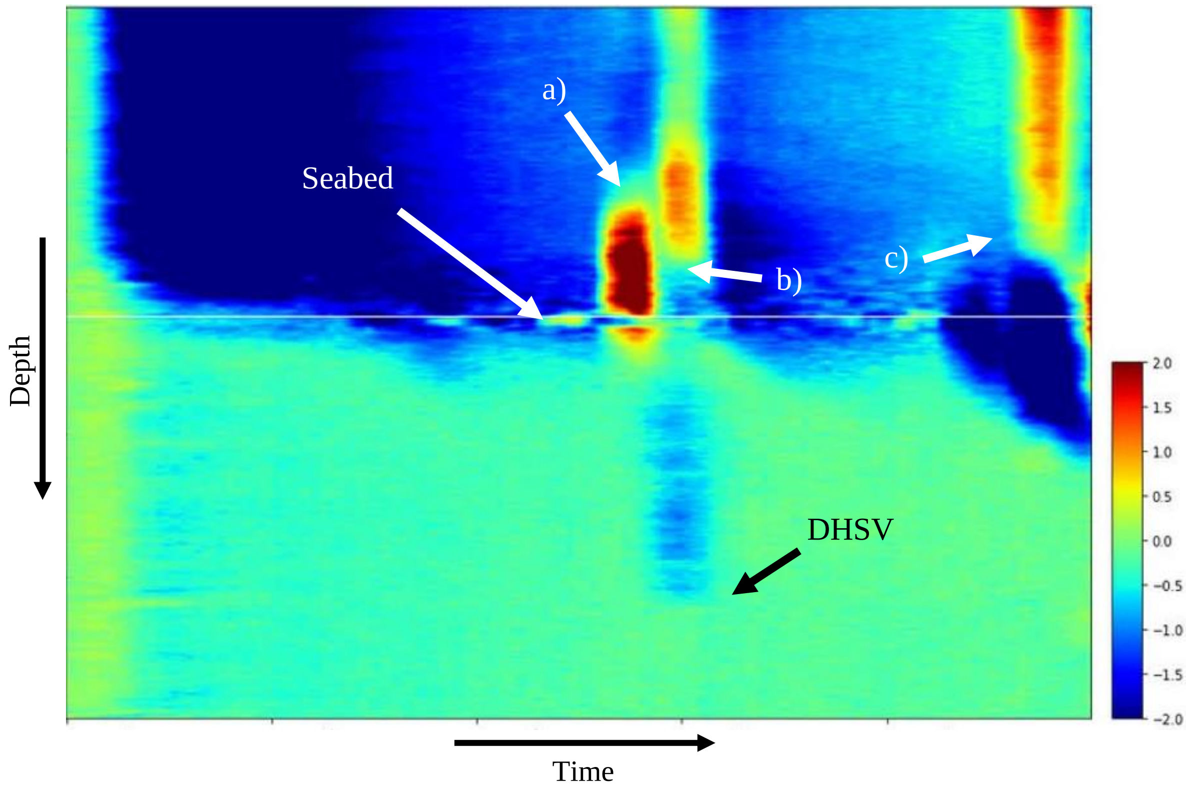

Figure 7.6 DTS interface level for the second DHSV leakage test (reproduced with permission) [13]

in the XT, while the second response, b), is from reducing the pressure above the DHSV to obtain 70 bar differential pressure across the valve before testing it. The third response, c), is from equalizing the pressure above the DHSV before opening the valve. The similarity in the response for the two DHSV tests demonstrates repeatability of the DTS measurements. However, Figure 7.5 and 7.6 does not look the same. This is because Figure 7.6 shows the cooling and heating, while Figure 7.5 only shows the heating. The temperature changes seen on top of a) and at the bottom of b) can indicate the depth of the interface. However, taking a closer look at the DHSV depth in Figure 7.6 might indicate something else. As the pressure is reduced above the DHSV, the lower part of the volume above the valve cools down, while the upper part heats up. This response might indicate that the fluids are moving up in the volume. This makes sense since the pressure reduction will cause gas to boil out of the liquid in the entire volume, or it can support the theory of the response being fluids that moves. The problem with this reaction is that this response makes it more uncertain to place the interface in this area. Due to this, it might be more reasonable to use response a) to locate the interface depth. By doing so, the interface will be located around 160 m TVD. Since the procedure is the same for both DHSV tests investigated here, it is reasonable to assume that the interface should be gathered at the same point in both fiber measurements. This means that using level at a) for the second test leads to also using a) for the first test. By doing this, the interface in the first test moves from around 180 m TVD to around 170 m TVD. These depths will be compared to the result gathered from the MATLAB code. It is important to note that the uncertainties around the seabed regarding whether the response shown interface or moving fluids are also applicable for the measurements in Figure 7.6. By further investigating response c) for both tests, these uncertainties might have been mitigated. This is however not done in the thesis. [13]

To run the MATLAB code, some internal data is used. These different values will, as mentioned, not be published in the thesis as their values are not important for the objective. Therefore, only the result from the code will be included here. It is important to note that for response a), which have been chosen to be used as liquid level here, the DHSV is still open. This means that the well is shut-in and the DHSV is open for both the interface depth gathered from the Fiber Optics and the data used in the MATLAB code.

Table 7.2 sums up and compares the interface depth results gathered from the fiber and the MATLAB code. From the table it is clear to see that the code and the fiber does not provide the same interface depths. The difference in interface between the fiber measurement and the MATLAB code is approximately 45 m in average for both tests. There are great uncertainties connected to these results. All the methods involved have their own uncertainties. From the fiber measurements, from the MATLAB code, and from the data gathering. They will all affect the total uncertainty for the result presented in Table 7.2. This might be the reason for the deviation in the results. However, it is uncertain if these uncertainties alone can contribute to the 30-50 m difference in interface depth. This needs to be further investigated.

Table 7.3 Interface depth from Fiber Optic vs. interface depth from MATLAB code

	Interface depth from fiber	**Interface depth calculated**	**Difference in interface depth**
First DHSV leakage test	~ 170 m TVD	134 m TVD	36 m
Second DHSV leakage test	~ 160 m TVD	107 m TVD	53 m

7.3 Using Echo Sounding

Echo Sounding is, as explained in Chapter 4, a technology that uses acoustic pressure waves to locate the interface in a well. It measures all cross-sectional changes that occurs along its path. Known reflections in the well are used as reference depths. This can for instance be the known depth of a valve. If unknown cross-sectional changes are measured, it can indicate casing collapse, or formation of scale, asphaltenes, wax or hydrates. However, the thesis only focuses on the measurements that locates the gas-liquid interface in the well. [27]

The measurements gathered from Echo Sounding has an accuracy of ± 0.3 meters. Considering the gas fraction calculations, and typical depths of DHSVs, 0.3 m will not affect the gas fraction noticeably. This means that using Echo Sounding to locate the interface will provide quite accurate results. Using it for all DHSV tests might not be cost efficient unless the equipment is installed permanent. However, if the equipment is not installed permanent, a solution can be to perform some measurements from time to time in order to update and improve the program used to calculate the interface. To show how Echo Sounding can be used, some examples are included here. [27]

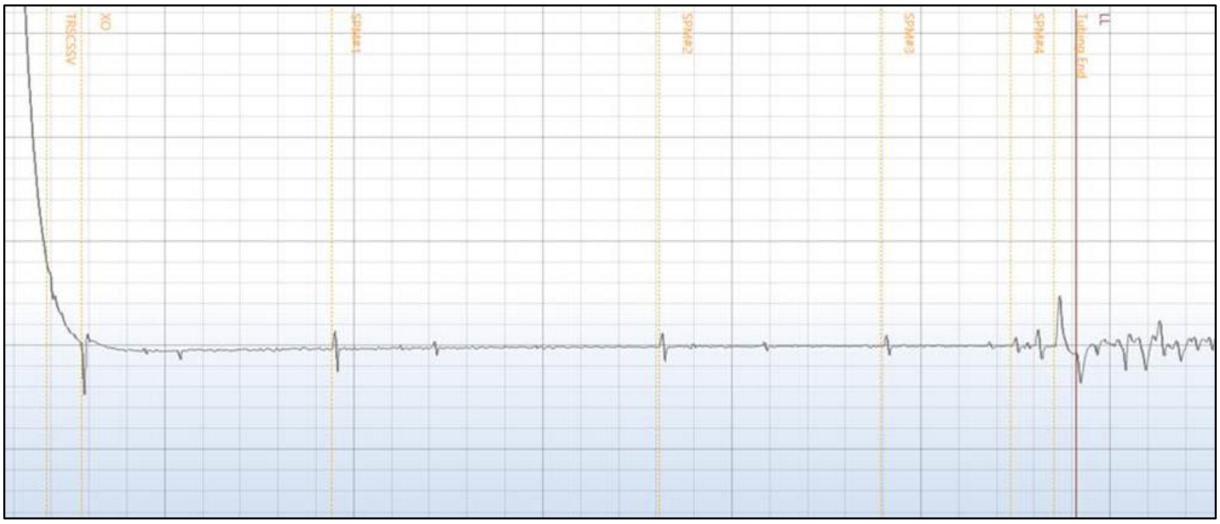

Figure 7.7 Liquid level in shut-in well (reproduced with permission) [27]

Figure 7.7 illustrates the first Echo Sounding example. These measurements are gathered from a shut-in well. As mentioned, the Echo Sounding measures the cross-sectional changes in a well using know depths for different equipment installed in the well. The equipment depth is marked in the figure with vertical, yellow lines. When a component causes an increase in cross-sectional diameter of the tubing, the signal jumps up. This can be seen in Figure 7.7 for SPM#1, SPM#2, SPM#3, and SPM#4. These are the Side Pocket Mandrels (SPMs) in the well. SPMs are pockets inside the tubing where for instance the gas lift valve can be installed [42]. The increased diameter of the tubing across the SPMs corresponds good with the small jumps in Figure 7.7. When the signal reacts the opposite way, by falling, it indicates a decrease in cross-sectional diameter. From Figure 7.7 this corresponds good with the known depth of the Crossover (XO). A XO is a device used to connect two pipes of different diameters or threads [43]. The greater the jump in signal, the greater the change in cross-sectional diameter. The DHSV to the left in Figure 7.7 only causes a small jump in the signal. This is because it is a TRSV. As mentioned, a TRSV is a part of the tubing. Hence, it does not change the ID of the tubing significantly. The red line to the right in Figure 7.7 is the Liquid Level (LL). Since the DHSV is located to the left in the figure, and depth moves to the right, this means that the interface for this well is located below the DHSV.

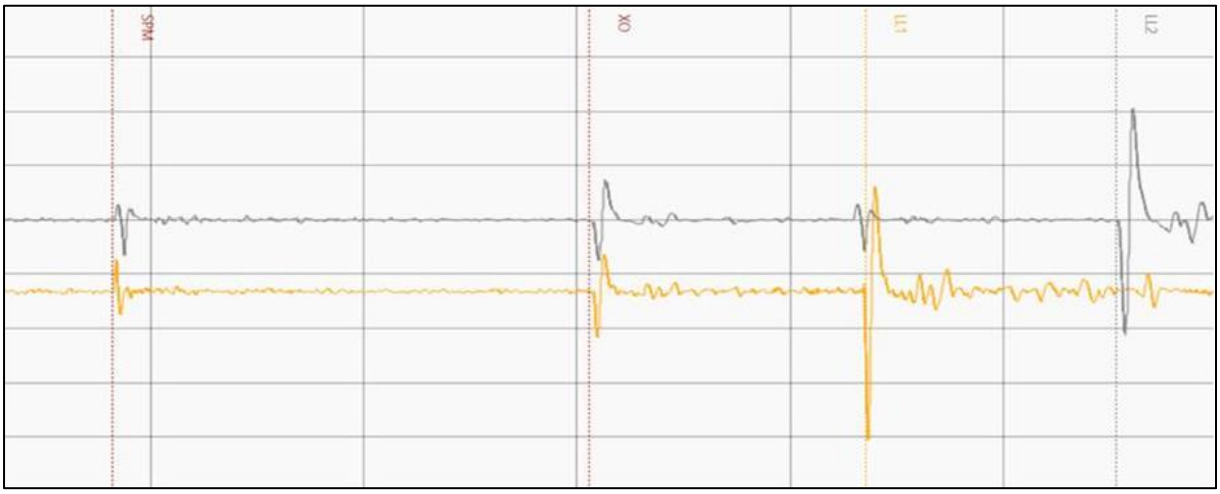

Figure 7.8 Liquid level measured twice in the same well (reproduced with permission) [27]

For the second example, in Figure 7.8, the situation is different. For this well, the LL is measured twice in the same well. The two measurements are then plotted in the same figure to see if the interface has moved. Here, the known component depths are marked with red, vertical lines, while the two LLs are marked by the yellow and the grey line to the right in the figure. LL2 is illustrated by the grey line and is the first liquid level measured. The yellow line, LL1, is the second level measured. From this figure it is clear to see that the interface moved higher up in the well from LL2 to LL1. Being able to see this as clearly as in Figure 7.8 shows that Echo Sounding can be used to measure how much liquid has been introduced into a volume. This means that Echo Sounding might be used to check for leaks during DHSV leakage tests. If Echo Sounding is used this way, the movement in the interface during the test can determine the leakage rate through the valve. [27]

As mentioned, the Echo Sounding has an accuracy of ± 0.3 meters. For some wells with a small tubing size and where it is only expected that liquid will leak through the DHSV, Echo Sounding could be used to determine if the leak is above or below the acceptance criteria. Take for instance a 5 ½" tubing with capacity of 11.57 l/m. Since liquid is the leaking fluid here, the acceptance criteria for liquid is used as leak rate. This corresponds to a liquid leak rate of 0.42 l/min from Table 3.1. If this leak is over the 30 min testing period, this would give 12.6 liters over 30 minutes. Since the tubing capacity is 11.57 l/m, it means that the liquid level will increase approximately 1 m in the volume above the DHSV. However, if the tubing size is bigger, for instance 7", the result is slightly different. A 7" tubing can have a capacity of 18.82 l/m. With the same leak rate here, the liquid level above the DHSV will increase with approximately 0.7 m. This level increase is still above, but closer to the uncertainty in the measurements and thereby more questionable to use to decide whether a test is good or not. It is also important to note, that this method would only be applicable if it were liquid leaking through the DHSV. This is not the case for many DHSV leakage tests. However, if using this method for DHSV leakage tests is proven accurate enough, it could reduce the testing time and further reduce the shut-in time of the well. However, this way of using Echo Sounding is not the focus in the thesis. [27]

7.4 Summary of Assumptions

To create the MATLAB code to locate the interface between gas and liquid in the well, some assumptions have been made. Some assumptions have also been made for the Fiber Optic measurements used to locate the interface. These assumptions are as follows:

- MATLAB code is based on shut-in well with DHSV open
- MATLAB code uses a reference liquid density in the well instead of accurate density profile along the well
- MATLAB code uses average pressure and temperature instead of accurate profiles along the well
- MATLAB code calculate gas density based on pressure and temperature. Does not use gas density profile along the well
- Interface depth gathered from Fiber Optics are gathered just before the pressure above the DHSV is being bled off.
- The well is shut-in and the DHSV is open for the interface depth gathered from Fiber Optics

7.5 DAC Study on Real DHSV Leakage Tests

Real DHSV leakage tests must be investigated to illustrate the practical usage of implementing DAC. The tests investigated are all gathered from different fields, different wells, and different years. The only common factor is that they all represent a failed DHSV leakage test on a producer, where the test failed due to a too high increase in pressure measured at the WH during the test. The study performed here evaluates these tests again, but this time using DAC. The equation for gas leaks is used for all volumes containing more than 10% gas. The equation for the liquid leaks is used for all tests where the volume is either 100% liquid filled, or the volume consist of 10% gas or less, as determined in Chapter 6.1.

To keep the tests anonymous, a test code will be given to each of the tests included here. The only relevant information needed to present the study properly is how big the pressure increase was during the test and what acceptance criteria the test was evaluated against. Relevant data from each test, that are needed for the MATLAB code and the DAC calculations, are used to make the study more accurate. This is internal data that will not be published here. Table 7.4 sums up the result of the study. The result column in the table uses red to illustrate tests that would still fail using DAC, while it uses green to illustrate those tests that would be approved using DAC. The final column gives a small comment for each of the tests. The comment includes what kind of volume it was just before the test, which equation was used for the calculations of DAC, and some comments on the results. [13]

Table 7.4 Results of SAC vs. DAC study

Test Code	Pressure increase during test *bar/30min*	SAC *bar/30min*	DAC *bar/30min*	Result	Comment
A	7.6	3.4	22.6	Approved	100% liquid filled volume **Liquid leak equation**
B	8.3	3.1	21.1	Approved	100% liquid filled volume **Liquid leak equation**
C	24.0	2.5	19.8	Failed	Less than 10% gas in the volume **Liquid leak equation** Pressure increase is higher than DAC

D	2.9	2.0	12.6	Approved	Less than 10% gas in the volume **Liquid leak equation**
E	13.0	2.0	14.8	Approved	Less than 10% gas in the volume **Liquid leak equation** DAC is close to the pressure increase
F	3.9	2.9	19.1	Approved	100% liquid filled volume **Liquid leak equation**
G	14.9	3.2	23.6	Approved	Less than 10% gas in the volume **Liquid leak equation**
H	37.0	9.3	69.4	Approved	100% liquid filled volume **Liquid leak equation** High DAC due to small volume
I	4.0	2.5	18.0	Approved	100% liquid filled volume **Liquid leak equation**
J	11.0	8.0	12.3	Approved	More than 10% gas in the volume **Gas leak equation** DAC is close to the pressure increase
K	9.0	2.0	14.9	Approved	Less than 10% gas in the volume **Liquid leak equation**
L	4.0	3.0	19.4	Approved	100% liquid filled volume **Liquid leak equation**
M	7.9	3.2	22.3	Approved	Less than 10% gas in the volume **Liquid leak equation**
N	8.2	3.0	19.9	Approved	100% liquid filled volume **Liquid leak equation**
O	5.9	2.5	18.4	Approved	100% liquid filled volume **Liquid leak equation**
P	8.0	2.0	15.3	Approved	Less than 10% gas in the volume **Liquid leak equation**
Q	11.1	3.1	13.2	Approved	More than 10% gas in the volume **Gas leak equation** DAC is close to the pressure increase
R	11.0	2.5	5.0	Failed	More than 10% gas in the volume **Gas leak equation** Pressure increase is higher than DAC

The results from the study presented in Table 7.4 showed that two tests would still fail using DAC, while the other 16 tests would be approved. The two failed tests are test C and R. This means that the overall result of the study is that 88.9% of these 18 tests would get a different result using DAC compared to using SAC. Using DAC could therefore decrease the overall failure rate of DHSV leakage tests significantly considering how many DHSV tests failes on the NCS each year. Although the results from the study in Table 7.3 looks great, ther are a lot of uncertainties concearning the study. These will be looked closer at here.

For instance, these 18 tests were randomly chosen for this study. If 18 other tests had been chosen, the results could have been completely different. Using only 18 tests for this study are too few tests investigated in order to present a statistically founded result. Out of the 18 tests, only three of them had more that 10% gas in the volume. This was test J, Q and R. This means that the remaining 15 tests had either 10% gas in the volume or less. Due to this high liquid amount, most of the tests have a spaseous DAC. Test H is the test with the largest DAC. The large DAC for test H can be explained by the well having a small volume between the DHSV and the TH. Test E, J and Q are the approved tests where the DAC is closest to the pressure increase during the test. If the volume composition in these tests had been different, then the overall result from the study would most likely have been different. If there had been mostly gas in the volumes, the DAC would have been smaller. Another uncertainty is connected to the gathering of data for the study. Gathering the data used for the DAC calculation and for the MATLAB code might not have been consistent. It was all individually gathered with great help from several employees. Although the data was supposed to be gathered just before the DHSV was closed, it is doubtfult that all of the data was gathered at the exact same time just before the valve closed. Also, all DHSV tests are not the same althoug they have the same basic testing procedure. For some tests, the DHSV or the PWV has been closed for a while, to test other elements in the well, before the DHSV is tested. This caused uncertainties on where the data should be gathered from for these tests. Another uncertainty is the densities used. It was stated, earlier in Chapter 7, that it was preffered to use the density at the downhole gauge, but that an average density could be used instead. For the study presented in Table 7.3, the average densities are used for all of the tests to ensure consistency in the results. After testing with different densities, it was shown that the MATLAB code is quite sensitive to density changes. Due to this, the density poses a great uncertainty in the study. It is also important to note that there are some uncertainties connected to the MATLAB code as well. These uncertainties was explained in section 7.1. A final and important uncertainty with the study in Table 7.3 is the oil compressibility. In section 6.2 concerning DAC calculations, it was stated that the oil compressibility to be used in the thesis is 1.3×10^{-3} MPa^{-1}. This compressibility value is an average value between high oil compressibility and water compressibility. What the real compressibility is for these tests are unknown, as this was not gathered during the data gathering for each test. Therefore, there are uncertainties regarding the effect of the oil compressibility on the results.

(Page left intentionally blank)

8 Results and Discussion

The thesis work investigated the possibility of including both gas and liquid into the acceptance criteria used for leak testing of DHSVs. The main goal was to see if this DAC could improve the accuracy of DHSV testing, if it could result in a more cost-effective operation, and if DAC could be more representative for each test than the SAC used today. After calculating and investigating different methods, the most important and relevant results obtained in Chapter 6 and 7 are highlighted here. The main results from investigating these methods are presented and discussed.

8.1 DAC Calculations – Results

The DAC calculations are based on the method used to calculate SAC today. The main difference is that any liquid in the volume above the DHSV is included for the DAC calculations. If there is no liquid in the volume, then DAC is equal to SAC. The DAC calculations from the thesis work resulted in two equations that are used under different conditions. The two equations are based on some similar parameters and some individual parameters. These parameters affected the DAC in different ways. The results from both equations are presented and discussed here.

8.1.1 Gas leak Calculations

The gas leak equation was the first equation to be investigated. The equation is based on the SAC calculations used today for gas leaks. The only difference now is that the gas fraction is used to include the effect of any liquid in the volume above the DHSV. The equation is referred to as Equation (6.5) in the thesis, and it is presented here:

$$\Delta P_{DAC} = \frac{q_g * t * T * Z}{V_g * 2.84 * 10^3} = \frac{q_g * t * T * Z}{(V_{tot} * \varepsilon_g) * 2.84 * 10^3} \tag{6.5}$$

See Chapter 6.1 for parameter description. The equation for gas leaks proved to be more sensitive to volume changes and less sensitive to temperature and Z-factor changes. The remaining parameters in the equation are constant for producers. This means that the DAC is mostly affected by changes in volume. Since the DAC is based on using the gas fraction, which changes the volume, the DAC will be spacious compared to SAC.

For the DAC calculations using the gas leak equation, the liquid phase is assumed incompressible until a liquid fraction of 0.9 (90%). This makes the calculations simpler than if it was included. Furthermore, the compressibility of liquids is generally a lot less than the gas, which makes it reasonable to dismiss this effect for the liquid phase. Also, it was stated earlier in the thesis that the gas will dominate if it is present in the volume. If the liquid compressibility had been included for the gas leak calculations, it would most likely not change the DAC significantly. Although dismissing the liquid compressibility makes the gas leak calculations simpler, it might also make the calculations less accurate.

It has also been stated in the thesis that the gas leak equation is to be used for gas fractions higher than 0.10 to make the calculations with smaller gas fractions more accurate. Since the DAC increased rapidly for the smallest gas fractions, it was reasonable to assume that the compressibility of liquid should be taken into account in addition to the gas compressibility. It was therefore assumed that the liquid leak equation was more accurate to use in this section, to ensure the inclusion of the liquid effects. The graph that illustrates this is seen in Figure 8.1. This is the same figure as attempt number 4 presented in Chapter 6.1 in Figure 6.4. Although the liquid leak equation for the smaller gas fractions resulted in a more conservative DAC, it still provides a quite spacious DAC.

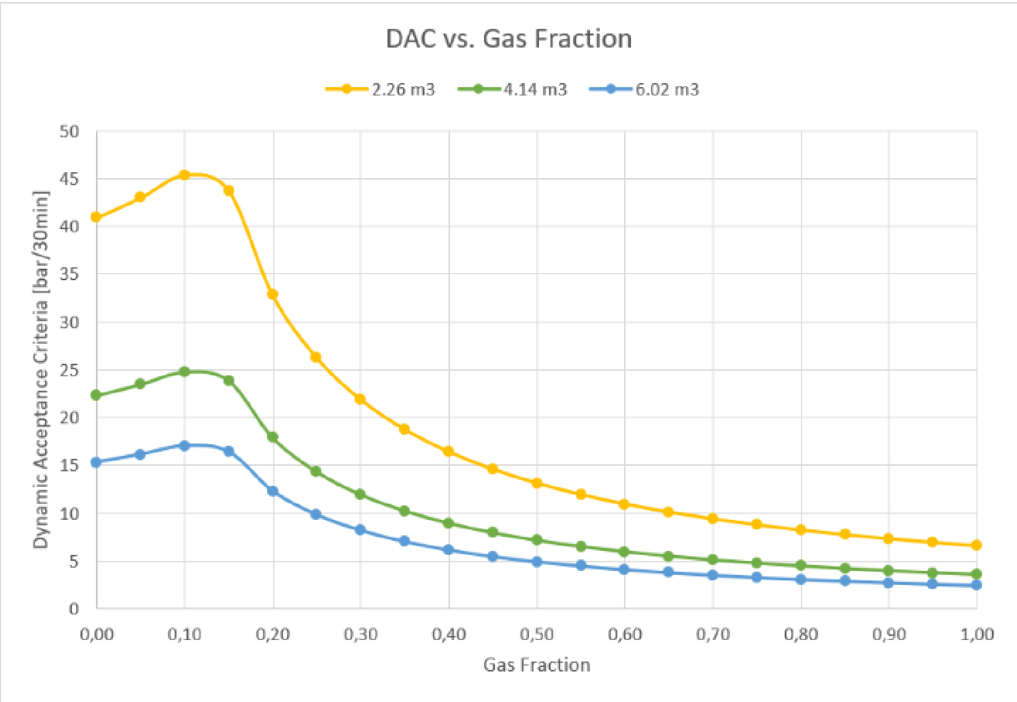

Figure 8.1 DAC vs. Gas fraction

8.1.2 Liquid Leak Calculations

The liquid leak equation mentioned above was developed to fill the gap of gas fractions from 0.10 to 0.00. The equation is therefore either used for liquid filled producers, or for volumes with 10% gas or less. The same equation can also be used for water injectors. For water injectors the equation uses water compressibility and the total volume between the DHSV and the TH. For oil filled producers it uses the oil volume and oil compressibility. The two ways of using the liquid leak Equation (6.6) is presented here:

$$\Delta P = \frac{q * t}{V_{tot} * c_w} = \frac{q * t}{(V_{tot} * \varepsilon_l) * c_o} \tag{6.6}$$

See Chapter 6.1 for parameter description. The thesis only focused on liquid leaks where oil was the leaking fluid, and not water. When investigating the sensitivity of the variables, the equation proved to be more sensitive to changes in oil compressibility and less sensitive to changes in volume. The last two parameters are constant for producers. Although oil compressibility is the more sensitive variable, it is still the volume that causes the deviation between SAC and DAC for liquid leaks with liquid fraction less than 1.00. The DAC will therefore be larger than the SAC as the denominator in the equation is reduced for DAC.

When using the liquid leak equation in the thesis, oil is assumed to be the only leaking fluid through the valve. This is reasonable since a liquid filled volume above the DHSV will result in liquid below the valve as well. Although this is a reasonable assumption, it might not be representative for all situations. For some situations, the liquid might start to segregate immediately. If this is the case, the liquid filled volume might gradually fill up with gas from the segregation process above the valve, and potentially from a leak through the valve. For these situations, the liquid leak equation will not be representative.

In the liquid leak equation, the oil compressibility is assumed to be $1.3x10^{-3}MPa^{-1}$. This value was chosen because it is a conservative value of the average oil compressibility. Since it was stated earlier that the oil compressibility can be up to five times the water compressibility, this value chosen for the thesis as it was three times the water compressibility. Although this value seems reasonable, the equation for liquid leaks was proven to be highly sensitive for changes in oil compressibility. This means that the average value used for all the thesis calculations can deviate greatly from the real value. Hence, result in a DAC that highly deviates from what it should have been with the correct compressibility. Real data on this was unfortunately not gathered for the thesis calculations, which leads to great uncertainties regarding this.

The liquid leak formula is only used for liquid fractions from 0.90 to 1.00, which corresponds to gas fractions from 0.10 to 0.00. This result in a more conservative DAC than if the gas leak equation had been used. This increases the reliability of the DAC for volumes with large amounts of liquid. Although it increases the reliability, it is still a spacious acceptance criteria compared to those used today, which questions the total reliability of the acceptance criteria.

Implementing DAC can result in reduced waiting time for the well to stabilize before the DHSV test is performed. For some wells with a high liquid fraction, it might be beneficial to let the well stabilize before the DHSV is closed and the leakage test is performed. By doing this, more gas can build above the DHSV. This will result in a more conservative DAC and increase the reliability of the test. However, there are also some wells that struggles to build gas above the DHSV. For these cases, the DAC will most likely reduce the time spent on the test, as these tests must stabilize for a longer period today before the test can be performed. For these wells, using the liquid leak equation might be the best option after all.

8.2 Locating the Interface – Results

To locate the interface between gas and liquid in a well, the thesis investigated three different methods. The first method is using the MATLAB code that calculates the interface depth. The final two methods are Fiber Optics and Echo Sounding. These two measurement methods measures the interface depth in the well. The three methods investigated have their own uncertainties when locating the interface. The results provided by the three methods will therefore be presented and discussed here.

8.2.1 MATLAB Code Calculations

The first method to be investigated was the MATLAB code calculations. The code needed several input variables for each test to calculate the interface between gas and liquid in the well. The code proved to be highly sensitive especially for density changes. This means that using a density from the bottom of the well or using an average density for the well will provide quite different results. For simplicity, the thesis used average densities for all the DHSV tests investigated in the SAC vs. DAC study in Chapter 7, and a more accurate density from the bottom of the well for the comparison of the interface results obtained from the code and the Fiber Optics. This means that the interface depths calculated for the Fiber Optics vs. MATLAB code comparison were more accurate than the interfaces obtained from the code and used for the DAC calculations in the SAC vs. DAC study.

The MATLAB code has a lot of uncertainties regarding the calculation of the interface between gas and liquid. One of these uncertainties are connected to the densities. The code uses one value for the density of the liquid, and only a constant value for the Z-factor for the gas density. This causes the code to use the liquid density as the bottom hole density and use this density with regards to temperature and pressure effects for the interface calculations up in the well. The gas density only uses a constant Z-factor and calculates the gas density based on pressure and temperature calculated by the code. This causes the code to be simpler and easier to use. For the thesis purpose it also made the data collection easier. Although it is a simpler method, it is also a less accurate method. Using the accurate PVT data gathered from the well for both density calculations would have made the code significantly more accurate.

The MATLAB code is based on several input values. Pressure and temperature at the top and at the bottom of the well are important inputs. These pressure and temperature inputs are used by the code to calculate average pressure and temperature variations along the well path. This made it easier when constructing the code, and it was thought to be accurate enough for the thesis prospects. Although it might have been accurate enough for the thesis, it would not have been accurate enough to be used for real tests. It that case, the MATLAB code should have been made more complex such that it calculated the variations in shorter intervals along the well. This would have made the code more accurate.

The real data collected to be used in the thesis was mostly gathered just before the DHSV was closed, and when the PWV already was closed. This resulted in consistency when gathering this data. Also, it satisfied the condition that the MATLAB code was built on, namely that the well is shut-in, and the DHSV is open. Collecting the data should therefore be straight forward. However, that was not the case. For some tests is was not clear where the data should be gathered, for other tests the DHSV was already closed and had been closed for a while, and for some tests the data was gathered just before the DHSV closed and the well was shut in. This variation in data collection questions the statement of consistency in the pressure and temperature data used. It also causes some uncertainty to the interface depth used for the thesis calculations.

8.2.2 Fiber Optic Measurements

The Fiber Optic measurements in the thesis consisted of two measurements. One was the DAS and the other one was the DTS. DAS was included in the thesis to mention that it might be possible to use for listening after leaks. As DAS has not been investigated enough to be used for this purpose or to be used to locate the interface in the well, it is too soon to say anything about its potential of usage. Therefore, the DTS measurements was the focus for the Fiber Optic measurement parts of the thesis and DTS is the only Fiber Optical part with results to discuss.

The Fiber Optical part of the thesis used to locate the interface between oil and gas in the well provided two examples on this. These two examples represented two different DHSV tests with the same testing procedure. This can be seen on the responses in the two fiber measurements in Figure 8.2. These two figures are the same as Figure 7.5 and Figure 7.6 in Chapter 7.2. Here it is important to remember that the fiber measurement to the left in Figure 8.2 only shows heating, while the fiber measurements to the right shows heating and cooling.

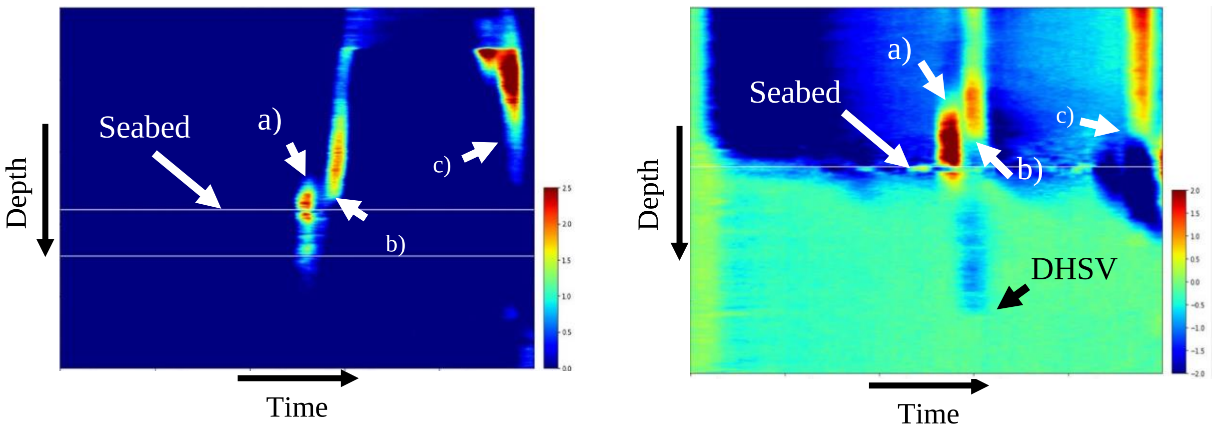

Figure 8.2 Fiber Optic measurements used to locate the interface [13]

From these fiber measurements, there were some uncertainties mentioned. One of these were the location of the seabed. As seen in Figure 8.2, the seabed is located close to the measured interface at the top of response b), just before the pressure was reduced above the DHSV. Since the seawater just above the seabed has lower temperature than the formation just below the seabed, this resulted in some uncertainties regarding whether this response shows the interface or if it just shows the fluids moving. The fiber measurements have some clear temperature changes at the top of a) and at the bottom of b). These changes support the theory about the location of the interface in these two spots. Although it looks clear according to the temperature changes, it is still uncertain what effect the seabed has on these measurements. Due to this, it is hard to say certain that this is the interface moving from a) to b).

Regarding the temperature changes in the measurements, there are also some uncertainties. From both measurements, it is seen that the fluid at the top heats up as pressure is bled off at b). From the measurement to the right in Figure 8.2 the fluid cools down closer to the DHSV. Due to segregation theory, gas should be the top fluid, while the liquid should be the lower fluid. It is assumed that the interface is located between these two, in b). This response does not correspond with the theory. According to the Joule Thomson effect, the gas should have cooled down as the pressure was reduced in b). The cooling measured below the seabed can indicate that more gas is bled out of the liquid. The heating and cooling response in b) can therefore indicate that the fluids are moving, and that it is not the interface. Hence, they are not stabilized in two different phases. This uncertain and unclear reason for this response questions the idea that the interface located at b) can be used as interface for further calculations. Due to this, a) is used as point of measurement for the interface gathered from Fiber Optics, as the results are more precise in this area. Choosing this point makes the interface depth more accurate than the one gathered at a later stage where the response is confusing. Also, using this earlier stage results in less time spent on the stabilization process. Although it is the point which seems most reasonable to use, there are still uncertainties regarding whether this is the interface or not. Due to the additional uncertainty from the seabed, it is hard to argument that this simply is the interface.

To further investigate the chosen interface depth from the Fiber Optic measurements, the MATLAB code was run to calculate the interface for these two tests. The results showed that the interface depth from the MATLAB code was located 30-50 m higher in the well than the depth measured with the fiber. It was suggested that this difference was due to the combined uncertainty of the Fiber Optic measurements, the MATLAB code, and the data gathering. However, 30-50 m seems to be quite a big change due to the uncertainties alone. Remember that the volume, affected by the interface depth, is sensitive for the DAC calculations. This is therefore an uncertainty that should be mitigated before it can be used for real tests.

8.2.3 Echo Sounding Measurements

For the Echo Sounding measurements, no real DHSV test was used to investigate the method. The method was included in the thesis to show that Echo Sounding can be a method used to locate the interface during a DHSV leakage test, or to determine the leakage rate through the valve during the test. Therefore, only the uncertainty in the method itself is discussed.

It was stated in Chapter 4.2 and in Chapter 7.3 that the Echo Sounding measurements has an accuracy of ± 0.3 meters. This small interval makes it reasonable to claim that the Echo Sounding measurements are quite accurate when locating the interface between gas and liquid in a well. When Echo Sounding is used to locate the interface used for DAC calculations, the ± 0.3 meters will not impact the gas or liquid fractions noticeably. Although ± 0.3 meters is a small interval that does not impact the DAC significantly, it can still impact it enough to make the acceptance criteria just below the pressure increase during the test. Hence, resulting in a failed test.

If Echo Sounding is to be used to determine the leakage rate during a DHSV test, it is uncertain if it can provide a satisfactory accuracy. For this usage, the Echo Sounder will provide the same accuracy measurement as for all measurements. The Eco Sounder will measure the change in interface above the DHSV during the test. This means that the Echo Sounder can only be used like this for wells that experience liquid leaks. This usage was discussed in Chapter 7.3. It was stated that if Echo sounder were to be used for this purpose, it would decrease the testing time of the DHSV. Hence reduce the shut-in time of the well. Although it might reduce the time spent on the test, it might not provide a satisfactory accurate result. The ± 0.3 meters might cause a too high uncertainty for this usage.

8.3 Practicality and Reliability of Methods Investigated

When testing DHSV today, the gas and liquid fraction are not known. Wells with a high liquid fraction still uses the gas leaking criteria for 100% gas filled volume. This means that a valve can be deemed as a leaking valve even though the valve is not leaking above the API leakage criteria. This can be one of the reasons for the high failure fraction of DHSVs on the NCS. Using DAC calculations and different methods to locate the interface have already been discussed. However, the discussion regarding the practicality and reliability of implementing a new method of calculating the acceptance criteria has not been discussed. This will be done here.

The thesis performed a SAC vs. DAC study to combine the methods investigated in the thesis. This study showed great potential for reducing the failure fraction of DHSVs. By using DAC, the testing time can be reduced, and the number of failed tests performed before an approved test is achieved, can be reduced. This results in an overall shorter shut-in time for a well when leakage testing the DHSV. Although the method showed great potential, it also consists of many uncertainties. For instance, most of the wells used for the study was wells with less than 10% gas in the volume. Had there been more tests with a higher gas fraction in the volume, the result might have been different. Also, using only 18 tests are too few to perform a representative study. Using 18 different tests than those used in the thesis might also have given a completely different result. The overall result is that the DAC provide a more spacious acceptance criteria than the conservative acceptance criteria used today. From all of this it is reasonable to believe that implementing DAC has potential to be an effective method to reduce the failure rate and to reduce the shut-in time. However, the method must be further tested and developed before it can be implemented for real DHSV tests.

For this to be implemented, it must also be practical to use. It was shown that several input values are needed for the MATLAB code to function. All these input values can be found before the DHSV test and implemented into the code. The best way of doing this might be to make a separate code either for each field or each well, depending on the similarities of the properties. By doing so, the code can be constructed with accurate data for that specific test, where for instance only the pressure and temperature values are input values. The code can also be constructed to calculate the gas fraction and further calculate the DAC. By doing this, the code can do all the calculations needed. This will mitigate human errors and provide the DHSV test with a representative acceptance criteria for each test. However, implementing this will be quite time consuming. It is a large task to create a code or a program like this for every well or field.

The initial idea was to implement the use of DAC in a digitalized method. The thesis work shows a clear potential of reaching this goal. The MATLAB code can be further developed into a program (does not have to be MATLAB) where the only input values are the measured pressure and temperature. These input values are available as live data in different systems today and can also potentially be captured automatically by the program. The program can then do all calculations needed as the DHSV is leakage tested. Further, it could also be implemented that the program evaluates the result and report the results. This will mitigate human errors in several steps of the operation. It will also ensure consistency in how and what is reported for all tests performed. For some wells, a part of the program can be switched out for one of the measurement methods investigated in the thesis. Although this seems promising, there is much work remaining to implement this. Before this method can replace the method used today, it must be proven that the safety of the barrier is not compromised due to a more spacious acceptance criteria. It is important that the reliability of the DHSV is not reduced by using DAC. The DHSV is a safety critical element, which makes it even more important that is can perform its intended purpose.

(Page left intentionally blank)

9 Summary and Conclusion

The Downhole Safety Valves (DHSVs) used on the Norwegian Continental Shelf (NCS) have shown over the last years to have too high failure rate than what is accepted. The Dynamic Acceptance Criteria (DAC) was therefore introduced. The DAC includes the effect caused by variations of gas and liquid fractions in the testing volume. This is different from the more Static Acceptance Criteria (SAC) used today where the volume is always assumed gas filled. Therefore, the DAC was researched to see if it could make the acceptance criteria, used to evaluate the periodic leak test results today, more accurate, more representative and reduce the overall time spent on the testing today.

From the research performed for this thesis it cannot simply be concluded whether DAC improves the accuracy of the periodic testing of DHSVs or not. DAC is generally more spacious than SAC, but it is recommended that further investigations should be performed to investigate how the accuracy of the acceptance criteria is affected when implementing DAC.

From the thesis work is was shown that using DAC will reduce the shut-in time of a well. Hence, make the operation more cost-effective. DAC can be used for gas volumes, liquid volumes or for mixed volumes. This means that there is generally no time needed to let the fluids segregate and let gas build up above the valve before the test. This might not be possible to do for all wells, but for most wells. From this it is concluded that using the DAC instead of the SAC will reduce the overall time spent on each periodic DHSV leakage test.

The research proved that using DAC would make the acceptance criteria more representative for each test. In the SAC vs. DAC study, some of the tests were gathered from the same well. From those 18 different tests, none of them had the same DAC. This proves that the DAC can have a different value for different tests performed on the same well. From this it is concluded that the DAC is more representative for each periodic DHSV leakage test compared to the SAC used today.

Although implementing DAC shows great potential of improving the method for calculating acceptance criteria used today, further research should be performed. For instance, the thesis work showed a need of researching the accuracy of the DAC to ensure that it does not compromise the barrier function of the DHSV. The thesis also suggested that the possibility of deriving one equation to calculate the DAC should be researched. In addition to this, the effect of compressibility should be further investigated. Also, the different methods used to locate the interface should be further investigated. For instance the MATLAB code should be made more complex such that it can perform more calculations with more accurate Pressure-Volume-Temperature (PVT) data to be more representative. For the Fiber Optic measurement method using Distributed Temperature Sensing (DTS), there were a lot of uncertainties connected to transition zone around the seabed and the cooling effect from seawater outside the well from seabed to surface. Due to this, it is recommended that further investigations should take place to mitigate these uncertainties. This can for instance be done by forcing the interface further down in the well, or by testing a shut-in well for fluid movements over time. For the Echo Sounding, the measurements can be used to improve the accuracy of the code used to calculate the interface depth. If it is further investigated, it might also be able to use the Echo Sounding technology in connection to the periodic DHSV leakage test to improve the accuracy and reduce time on the operation.

Finally, it has been proven by the thesis work that implementing DAC results in a more time-efficient operation and it gives a more representative acceptance criteria for each leakage test performed. Although there are still a need for further research before the DAC can be implemented for real periodic DHSV leakage tests, the method shows great potential.

References

1. Standard Norway. *NORSOK standards*. Online 2019, [cited 13/04/2020]. Available from: https://www.standard.no/fagomrader/energi-og-klima/petroleum/norsok-standards/#.XpRAh25uLXA.
2. H.-E.B. Torbergsen, et al. *An Introduction to Well Integrity*. Rev. 0. 2012, Norway: NTNU Trondheim, Norsk Olje og Gass, University of Stavanger. (pp. 45-48).
3. *Well integrity in drilling and well operations*, NORSOK D-010, June 2013, (pp. 15, 63, 71, 72, 74 & 162).
4. Petroleum Safety Authority Norway. *Role and area of responsibility* Online 2020, [cited 13/04/2020]. Available from: https://www.ptil.no/en/about-us/role-and-area-of-responsibility/.
5. Petroleum Safety Authority Norway. *What is Trends in risk level in the petroleum activity (RNNP)?* . Online 2019, [cited 13/04/2020]. Available from: https://www.ptil.no/en/technical-competence/rnnp/about-rnnp/.
6. Petroleum Safety Authority Norway (PSA). *RNNP 2019 Hovedrapport*. Online report (in Norwegian), 2020. rev. 1, (p. 128) Available from: https://www.ptil.no/contentassets/1a88cd8a426b44808897e284ae3ca42a/1.4-rnnp-2019-sokkelrapport.pdf
7. Schlumberger. *subsurface safety valve (SSSV)*. Oilfield Glossary. Online 2020, [cited 04/02/2020]. Available from: https://www.glossary.oilfield.slb.com/en/Terms/s/subsurface_safety_valve_sssv.aspx.
8. H. Crumpton. *Well Control for Completions and Interventions*. 1. ed. 2018, Isle of Skye, Scotland: Gulf Professional Publishing. (pp. 125-130).
9. Baker Hughes Inc. *DHSV, ASV, SPM, SS, PBR med seal stem, og produksjonspakning for øvre komplettering*. Online figure (license CC BY-SA 4.0) 2018, [cited 12/06/2020]. (in Norwegian). Available from: https://ndla.no/nb/subjects/subject:6/topic:1:182061/topic:1:151959/resource:1:181784.
10. Nasjonal Digital Læringsarena (NDLA). *Standardutstyr i øvre komplettering*. Online 2018, [cited 17/03/2020]. (in Norwegian). Available from: https://ndla.no/nb/subjects/subject:6/topic:1:182061/topic:1:151959/resource:1:181812/310.
11. T. Schwerdtfeger, B. Scott, and J.v.d. Akker. *World-First All-Electric Subsea Well*. Offshore Technology Conference, OTC-27701-MS, May 2017. vol. 4, (pp. 11-12 & 17). Available from: https://doi.org/10.4043/27701-MS
12. Nasjonal Digital Læringsarena (NDLA). *Standardutstyr i øvre komplettering*. Online 2018, [cited 09/02/2020]. (in Norwegian). Available from: https://ndla.no/nb/subjects/subject:6/topic:1:182061/topic:1:151959/resource:1:181812/310.
13. T. Paulsen. *Equinor - Internal document/communication*. Unpublished 2020.
14. *Design, Installation, Operation, Test, and Redress of Subsurface Safety Valve Systems*, API RP 14B, September 2015, (p. 19).
15. WIF/Jan Krokeide. *NORSOK D-010: Section 7 Completion*. Online 2012, [cited 28/03/2020]. Comments/Suggestions to NORSOK D-010 Section 7. Available from: https://www.standard.no/Global/PDF/Petroleum/D-010%20Comments/Sect.%207%20_%20comments%20rev.4.%2015.8.12.pdf.
16. *Petroleum and natural gas industries - Subsurface safety valve systems - Design, installation, operation and redress*, ISO 10417, July 2004, (p. 8).
17. *Petroleum and natural gas industries - Well integrity - Part 1: Life cycle governance*, ISO 16530-1, March 2017, (pp. 100-102).

18. The Editors of Encyclopaedia Britannica. *fiber optics*. Encyclopaedia Britannica. Online 2020, [cited 19/02/2020]. Available from: https://www.britannica.com/science/fiber-optics.
19. G. Hemink and J.v.d. Horst. *On the Use of Distributed Temperature Sensing and Distributed Acoustic Sensing for the Application of Gas Lift Surveillance*. Society of Petroleum Engineers, SPE-191130-PA, Nov. 2018. vol. 33 (no. 04), (pp. 896-897). Available from: https://doi.org/10.2118/191130-PA
20. P.I. Panhuis, et al. *Flow Monitoring and Production Profiling Using DAS*. Society of Petroleum Engineers, SPE-170917-MS, Oct. 2014. vol. 6, (p. 1). Available from: https://doi.org/10.2118/170917-MS
21. J.J. Smolen and A.v.d. Spek. *Distributed Temperature Sensing: A DTS Primer for Oil & Gas Production*. Shell International Exploration and Production B.V., May 2003. (pp. 1 & 6). Available from: http://w3.energistics.org/schema/witsml_v1.3.1_data/doc/Shell_DTS_Primer.pdf
22. S. Fitzel, et al. *Gas Injection EOR Optimization Using Fiber-Optic Logging with DTS and DAS for Remedial Work*. Society of Petroleum Engineers, SPE-175891-MS, Oct. 2015. (pp. 1 & 3). Available from: https://doi.org/10.2118/175891-MS
23. Verivin Instruments. *Rayleigh and Raman Scattering*. Online 2020, [cited 24/05/2020]. Available from: https://www.verivin.com/2016/10/rayleigh-and-raman-scattering/.
24. Schlumberger. *unload*. Oilfield Glossary. Online 2020, [cited 25/03/2020]. Available from: https://www.glossary.oilfield.slb.com/en/Terms/u/unload.aspx.
25. The Editors of Encyclopaedia Britannica. *Depth finder*. Encyclopaedia Britannica. Online 2020, [cited 27/02/2020]. Available from: https://www.britannica.com/technology/depth-finder.
26. Society of Petroleum Engineers. *Acoustic logging*. PetroWiki. Online 2020, [cited 03/03/2020]. Available from: https://petrowiki.org/Acoustic_logging.
27. M. Kvernvold - CEO ScanWell. *Echo Sounding*. E-mail conversation, May 2020.
28. The Editors of Encyclopaedia Britannica. *Laminar flow*. Encyclopaedia Britannica. Online 2018, [cited 01/06/2020]. Available from: https://www.britannica.com/science/laminar-flow.
29. The Editors of Encyclopaedia Britannica. *Turbulent flow*. Encyclopaedia Britannica. Online 2020, [cited 01/06/2020]. Available from: https://www.britannica.com/science/turbulent-flow.
30. R.W. Time. *Two-Phase Flow in Pipelines*. Course Compendium. 2017, Department of Petroleum Engineering, Faculty of Science and Technology, University of Stavanger. (pp. 26-29).
31. Schlumberger. *gravity segregation*. Oilfield Glossary. Online 2020, [cited 01/03/2020]. Available from: https://www.glossary.oilfield.slb.com/en/Terms/g/gravity_segregation.aspx.
32. Schlumberger. *bubble point*. Online 2020, [cited 04/06/2020]. Available from: https://www.glossary.oilfield.slb.com/en/Terms/b/bubble_point.aspx.
33. Schlumberger. *PVT*. Oilfield Glossary. Online 2020, [cited 24/03/2020]. Available from: https://www.glossary.oilfield.slb.com/en/Terms/p/pvt.aspx.
34. B.A. Averill and P. Eldredge. *Principles of General Chemistry*. Online Book, v. 1.0, Unknown year, [cited 11/06/2020]. Available from: https://2012books.lardbucket.org/books/principles-of-general-chemistry-v1.0/s14-03-relationships-among-pressure-t.html.
35. Y.A. Cengel, J.M. Cimbala, and R.H. Turner. *Fundamentals of Thermal-Fluid Sciences*. 4. ed. 2012, New York: McGraw-Hill Education. (pp. 28, 123 & 130).
36. Schlumberger. *compressibility*. Oilfield Glossary. Online 2020, [cited 05/03/2020]. Available from: https://www.glossary.oilfield.slb.com/en/Terms/c/compressibility.aspx.
37. B. Guo, X. Liu, and X. Tan. *Petroleum Production Engineering*. 2. ed. 2017: Gulf Professional Publishing. (pp. 22 & 27).

38. The Editors of Encyclopaedia Britannica. *Joule-Thomson effect*. Encyclopaedia Britannica. Online 2020, [cited 27/02/2020]. Available from: https://www.britannica.com/science/Joule-Thomson-effect.
39. K.K. Fjelde. *Modelling of Well Flow*. Course Compendium. Unknown year, Department of Petroleum Engineering, Faculty of Science and Technology, University of Stavanger. (29 pages).
40. MathWorks. *Scripts vs. Functions*. Help Center. Online 2020, [cited 28/05/2020]. Available from: https://se.mathworks.com/help/matlab/matlab_prog/scripts-and-functions.html.
41. E. Hurtig, et al. *Borehole temperature measurements using distributed fiber optic sensing.* Scientific Drilling - Geophysics, Geochemistry, and Technology, June 1993. vol. 3 (no. 6), (p. 283).
42. Society of Petroleum Engineers. *Side pocket mandrel*. PetroWiki - Glossary. Online 2020, [cited 25/05/2020]. Available from: https://petrowiki.org/Glossary:Side_pocket_mandrel.
43. Schlumberger. *crossover*. Oilfield Glossary. Online 2020, [cited 25/05/2020]. Available from: https://www.glossary.oilfield.slb.com/en/Terms/c/crossover.aspx.

(Page left intentionally blank)

Appendix A – DAC Calculations

This section contains all the results and information used for the calculations in Chapter 6.3. The graphs for the five examples in Chapter 6.3 are based on the data provided here.

A.1 Change in Volume – Gas Leak

T	90	°C
Z	0,92	
Vtot	4,00	m³

Constants:		
qg	0,42	m³/min
t	30	min

εg	1	0,9	0,8	0,7	0,6	0,5	0,4	0,3	0,2	0,1	0
SAC (bar/30 min)	3,7	3,7	3,7	3,7	3,7	3,7	3,7	3,7	3,7	3,7	N/A
DAC (bar/30 min)	3,7	4,1	4,6	5,3	6,2	7,4	9,3	12,3	18,5	37,0	N/A

Figure A.1 Data from example 1.1

T	90	°C
Z	0,92	
Vtot	5,00	m³

Constants:		
qg	0,42	m³/min
t	30	min

εg	1	0,9	0,8	0,7	0,6	0,5	0,4	0,3	0,2	0,1	0
SAC (bar/30 min)	3,0	3,0	3,0	3,0	3,0	3,0	3,0	3,0	3,0	3,0	N/A
DAC (bar/30 min)	3,0	3,3	3,7	4,2	4,9	5,9	7,4	9,9	14,8	29,6	N/A

Figure A.2 Data from example 1.2

T	90	°C
Z	0,92	
Vtot	6,00	m³

Constants:		
qg	0,42	m³/min
t	30	min

εg	1	0,9	0,8	0,7	0,6	0,5	0,4	0,3	0,2	0,1	0
SAC (bar/30 min)	2,5	2,5	2,5	2,5	2,5	2,5	2,5	2,5	2,5	2,5	N/A
DAC (bar/30 min)	2,5	2,7	3,1	3,5	4,1	4,9	6,2	8,2	12,3	24,7	N/A

Figure A.3 Data from example 1.3

T	90	°C
Z	0,92	
Vtot	7,00	m³

Constants:		
qg	0,42	m³/min
t	30	min

εg	1	0,9	0,8	0,7	0,6	0,5	0,4	0,3	0,2	0,1	0
SAC (bar/30 min)	2,1	2,1	2,1	2,1	2,1	2,1	2,1	2,1	2,1	2,1	N/A
DAC (bar/30 min)	2,1	2,4	2,6	3,0	3,5	4,2	5,3	7,1	10,6	21,2	N/A

Figure A.4 Data from example 1.4

A.2 Change in Temperature – Gas Leak

T	70	°C
Z	0,92	
V_{tot}	4,14	m³

Constants:		
q_g	0,42	m³/min
t	30	min

ε_g	1	0,9	0,8	0,7	0,6	0,5	0,4	0,3	0,2	0,1	0
SAC (bar/30 min)	3,4	3,4	3,4	3,4	3,4	3,4	3,4	3,4	3,4	3,4	N/A
DAC (bar/30 min)	3,4	3,8	4,2	4,8	5,6	6,8	8,5	11,3	16,9	33,8	N/A

Figure A.5 Data from example 2.1

T	80	°C
Z	0,92	
V_{tot}	4,14	m³

Constants:		
q_g	0,42	m³/min
t	30	min

ε_g	1	0,9	0,8	0,7	0,6	0,5	0,4	0,3	0,2	0,1	0
SAC (bar/30 min)	3,5	3,5	3,5	3,5	3,5	3,5	3,5	3,5	3,5	3,5	N/A
DAC (bar/30 min)	3,5	3,9	4,4	5,0	5,8	7,0	8,7	11,6	17,4	34,8	N/A

Figure A.6 Data from example 2.2

T	90	°C
Z	0,92	
V_{tot}	4,14	m³

Constants:		
q_g	0,42	m³/min
t	30	min

ε_g	1	0,9	0,8	0,7	0,6	0,5	0,4	0,3	0,2	0,1	0
SAC (bar/30 min)	3,6	3,6	3,6	3,6	3,6	3,6	3,6	3,6	3,6	3,6	N/A
DAC (bar/30 min)	3,6	4,0	4,5	5,1	6,0	7,2	9,0	11,9	17,9	35,8	N/A

Figure A.7 Data from example 2.3

T	100	°C
Z	0,92	
V_{tot}	4,14	m3

Constants:		
q_g	0,42	m³/min
t	30	min

ε_g	1	0,9	0,8	0,7	0,6	0,5	0,4	0,3	0,2	0,1	0
SAC (bar/30 min)	3,7	3,7	3,7	3,7	3,7	3,7	3,7	3,7	3,7	3,7	N/A
DAC (bar/30 min)	3,7	4,1	4,6	5,3	6,1	7,4	9,2	12,3	18,4	36,8	N/A

Figure A.8 Data from example 2.4

A.3 Change in Z-Factor – Gas Leak

T	90	°C
Z	0,88	
Vtot	4,14	m³

Constants:		
qg	0,42	m³/min
t	30	min

εg	1	0,9	0,8	0,7	0,6	0,5	0,4	0,3	0,2	0,1	0
SAC (bar/30 min)	3,4	3,4	3,4	3,4	3,4	3,4	3,4	3,4	3,4	3,4	N/A
DAC (bar/30 min)	3,4	3,8	4,3	4,9	5,7	6,8	8,6	11,4	17,1	34,2	N/A

Figure A.9 Data from example 3.1

T	90	°C
Z	0,90	
Vtot	4,14	m³

Constants:		
qg	0,42	m³/min
t	30	min

εg	1	0,9	0,8	0,7	0,6	0,5	0,4	0,3	0,2	0,1	0
SAC (bar/30 min)	3,5	3,5	3,5	3,5	3,5	3,5	3,5	3,5	3,5	3,5	N/A
DAC (bar/30 min)	3,5	3,9	4,4	5,0	5,8	7,0	8,8	11,7	17,5	35,0	N/A

Figure A.10 Data from example 3.2

T	90	°C
Z	0,92	
Vtot	4,14	m³

Constants:		
qg	0,42	m³/min
t	30	min

εg	1	0,9	0,8	0,7	0,6	0,5	0,4	0,3	0,2	0,1	0
SAC (bar/30 min)	3,6	3,6	3,6	3,6	3,6	3,6	3,6	3,6	3,6	3,6	N/A
DAC (bar/30 min)	3,6	4,0	4,5	5,1	6,0	7,2	9,0	11,9	17,9	35,8	N/A

Figure A.11 Data from example 3.3

T	90	°C
Z	0,94	
Vtot	4,14	m³

Constants:		
qg	0,42	m³/min
t	30	min

εg	1	0,9	0,8	0,7	0,6	0,5	0,4	0,3	0,2	0,1	0
SAC (bar/30 min)	3,7	3,7	3,7	3,7	3,7	3,7	3,7	3,7	3,7	3,7	N/A
DAC (bar/30 min)	3,7	4,1	4,6	5,2	6,1	7,3	9,1	12,2	18,3	36,6	N/A

Figure A.12 Data from example 3.4

A.4 Change in Volume – Liquid Leak

Co	0,0013	MPa^{-1}			
Vtot	4,00	m³			

Constants:		
qg	0,0004	m³/min
t	30	min

εl	1	0,9	0,8	0,7	0,6	0,5	0,4	0,3	0,2	0,1	0
SAC (bar/30 min)	23,1	23,1	23,1	23,1	23,1	23,1	23,1	23,1	23,1	23,1	N/A
DAC (bar/30 min)	23,1	25,6	28,8	33,0	38,5	46,2	57,7	76,9	115,4	230,8	N/A

Figure A.13 Data from example 4.1

Co	0,0013	MPa^{-1}
Vtot	5,00	m³

Constants:		
qg	0,0004	m³/min
t	30	min

εl	1	0,9	0,8	0,7	0,6	0,5	0,4	0,3	0,2	0,1	0
SAC (bar/30 min)	18,5	18,5	18,5	18,5	18,5	18,5	18,5	18,5	18,5	18,5	N/A
DAC (bar/30 min)	18,5	20,5	23,1	26,4	30,8	36,9	46,2	61,5	92,3	184,6	N/A

Figure A.14 Data from example 4.2

Co	0,0013	MPa^{-1}
Vtot	6,00	m³

Constants:		
qg	0,0004	m³/min
t	30	min

εg	1	0,9	0,8	0,7	0,6	0,5	0,4	0,3	0,2	0,1	0
SAC (bar/30 min)	15,4	15,4	15,4	15,4	15,4	15,4	15,4	15,4	15,4	15,4	N/A
DAC (bar/30 min)	15,4	17,1	19,2	22,0	25,6	30,8	38,5	51,3	76,9	153,8	N/A

Figure A.15 Data from example 4.3

Co	0,0013	MPa^{-1}
Vtot	7,00	m³

Constants:		
qg	0,0004	m³/min
t	30	min

εg	1	0,9	0,8	0,7	0,6	0,5	0,4	0,3	0,2	0,1	0
SAC (bar/30 min)	13,2	13,2	13,2	13,2	13,2	13,2	13,2	13,2	13,2	13,2	N/A
DAC (bar/30 min)	13,2	14,7	16,5	18,8	22,0	26,4	33,0	44,0	65,9	131,9	N/A

Figure A.16 Data from example 4.4

A.5 Change in Oil Compressibility – Liquid Leak

Co	0,00044	MPa^{-1}
Vtot	4,14	m^3

Constants:		
ql	0,0004	m^3/min
t	30	min

εl	1	0,9	0,8	0,7	0,6	0,5	0,4	0,3	0,2	0,1	0
SAC (bar/30 min)	66,7	66,7	66,7	66,7	66,7	66,7	66,7	66,7	66,7	66,7	N/A
DAC (bar/30 min)	66,7	74,1	83,3	95,2	111,1	133,3	166,7	222,2	333,3	666,6	N/A

Figure A.17 Data from example 5.1

Co	0,0008	MPa^{-1}
Vtot	4,14	m^3

Constants:		
ql	0,0004	m^3/min
t	30	min

εl	1	0,9	0,8	0,7	0,6	0,5	0,4	0,3	0,2	0,1	0
SAC (bar/30 min)	36,2	36,2	36,2	36,2	36,2	36,2	36,2	36,2	36,2	36,2	N/A
DAC (bar/30 min)	36,2	40,3	45,3	51,8	60,4	72,5	90,6	120,8	181,2	362,5	N/A

Figure A.18 Data from example 5.2

Co	0,0013	MPa^{-1}
Vtot	4,14	m^3

Constants:		
ql	0,0004	m^3/min
t	30	min

εl	1	0,9	0,8	0,7	0,6	0,5	0,4	0,3	0,2	0,1	0
SAC (bar/30 min)	22,3	22,3	22,3	22,3	22,3	22,3	22,3	22,3	22,3	22,3	N/A
DAC (bar/30 min)	22,3	24,8	27,9	31,9	37,2	44,6	55,8	74,4	111,5	223,1	N/A

Figure A.19 Data from example 5.3

Co	0,00218	MPa^{-1}
Vtot	4,14	m^3

Constants:		
ql	0,0004	m^3/min
t	30	min

εl	1	0,9	0,8	0,7	0,6	0,5	0,4	0,3	0,2	0,1	0
SAC (bar/30 min)	13,3	13,3	13,3	13,3	13,3	13,3	13,3	13,3	13,3	13,3	N/A
DAC (bar/30 min)	13,3	14,8	16,6	19,0	22,2	26,6	33,3	44,3	66,5	133,0	N/A

Figure A.20 data from example 5.4

(Page left intentionally blank)

Appendix B – MATLAB Code

The MATLAB code provided here is the code developed in Chapter 7.1 The code provided has example values from example 1 in Chapter 7.1.1 inserted. See green comments in figure for explanations.

B.1 The Main Script

```
%----------------------------------%
% GAS/LIQUID INTERFACE CALCULATION %
%----------------------------------%

clear   %% Clear the MATLAB Workspace
clc     %% Clear the MATLAB Command Window

% Main is a program that is developed to locate the interface between gas
% and liquid in a well. The program calls upon the bisection function to
% find a solution to the problem f(x) = 0. The bisection function calls
% upon the func function, which again calls upon the roliq and rogas
% functions.

% The search interval [a,b] and the well depth are specified in the main
% program. a and b represent the lower (a) and upper (b) limit of the
% guessed interface search depth. The search interval is sendt into the
% bisection function. If a = 0 and b = TVD, then the whole well is
% investigated to locate the interface. If specified like this, there is no
% need to adjust the search interval.

% If error = 1 and there is a solution, it means that the interface is
% located above the tubing hanger.
% If error = 1 and solution = 0, it means that there is no interface
% located in the well, and f(a) x f(b) < 0 is not fulfilled.
% For both cases it is assumed that the well is liquid filled.
% If error = 0 and there is a solution, an interface has been located in
% the well.
% Specify depths:
 TVD = 2000; %% total depth of downhole gauge in m
 TH = 200; %% total depth of tubing hanger in m

% Search interval:
 a = 0; %% lower limit measured from bottom of the well
 b = TVD; %% upper limit measured from bottom of the well

% The bisection function returns the result to main. The results are
% defined by the variables "solution" and "error".
 [solution,error] = bisection(a,b);

% Interface depth measured from top of the well is defined by this:
 TVDint = TVD-solution;

% Determine if interface is above or below the TH depth:
 if TVDint > TH
     TVDint = TVD-solution;
 else
     error = 1;
 end

% Written to screen:
 TVDint                    % Interface depth from top of the well.
 solution                  % Interface depth from bottom of the well.
 error                     % Indicates no interface, interface above search
                           % interval or interface in the well. Can also
                           % indicate need to adjust search interval if this
                           % is specified in smaller interval than
                           % illustrated here
```

Figure B.1 main.m

B.2 The Bisection Function

```
function [solution,error] = bisection(a,b)

% The numerical solver implemented here for solving the equation f(x)= 0
% is called Method of Halving the Interval also known as Bisection Method.

% There will not be an exact match for f(x)= 0, but maybe there is a match
% for f(x) = 0.0001.
% If abs(f(x)) < ftol the result is satisfying. The ftol marks the
% tolerance value for the accuracy of the result. This might be changed
% depending on the problem. The iteration can also end if the search
% interval [a,b] is satisfactory small.

% Specify the tolerance:
 ftol = 100;  %% accuracy of 100 Pa


% Number of iterations (noit) is set to zero. This number will tell how
% many iterations are required to find a solution with the specified
% accuracy.

  noit = 0;

  x1 = a;
  x2 = b;


  f1 = func(x1);
  f2 = func(x2);


% Before the iteration process begins, check whether f1 x f2 < 0 or not. If
% not, then error = 1 and solution = 0 will be displayed. Then the initial
% search interval in main must be adjusted such that error = 0 and a
% solution is presented.
```

```
 if (f1*f2)>=0 %% check if search interval is correct
     error = 1;
     solution = 0;
 else  %% start iterating
     x3 = (x1+x2)/2.0
     f3 = func(x3)

     while (f3>ftol | f3 < -ftol)
        noit = noit +1 ;

        if (f3*f1) < 0
           x2 = x3;
        else
           x1 = x3;
        end

        x3 = (x1+x2)/2.0
        f3 = func(x3)
        f1 = func(x1);

     end
     error = 0;
     solution = x3;
     noit %% writes out the number of iterations to the screen
 end
```

Figure B.2 bisection.m

B.3 The Function Script

```
function f = func(depth)

% Specify pressures and depth of the well:
  realWHP = 3000000; %% measured wellhead pressure in Pa
  BHP = 17000000; %% measured bottomhole pressure in Pa
  TVD = 2000; %% total depth to downhole gauge in m (same as in main)
  Tbot = 273.15+100; %% temperature at the bottom of the well
  Ttop = 273.15+60; %% temperature at the top of the well
  % Specify the two temperatures above in Celcius. The code adds 273.15 to
  % convert them to Kelvin.

  Tempgrad = (Tbot-Ttop)/TVD; %% calc. temperature gradient
  Pint = BHP-9.81*rholiq(BHP,Tbot)*depth; %% calc. pressure at interface
  Pavg = (Pint+BHP)/2; %% calc. the average pressure up to interface
  Tint = Tbot-depth*Tempgrad; %% calc. temperature at interface
  Tavg = (Tint+Tbot)/2; %% calc. average temperature up to interface
  Pint = BHP-9.81*rholiq(Pavg,Tavg)*depth; %% calc. new interface pressure

  gasDens = rhogas(Pint,Tint); %% calc. gas density using rhogas
  calcWHP = Pint-9.81*gasDens*(TVD-depth); %% calc. wellhead pressure
  pavg = (Pint+calcWHP)/2; %% calc. average pressure above interface
  tempavg = (Tint+Ttop)/2; %% calc. average temp. above interface
  gasDens = rhogas(pavg,tempavg); %% calc. new gas density using rhogas
  calcWHP= Pint-9.81*gasDens*(TVD-depth); %% calc. new wellhead pressure

% This function calculates the difference between the calculated and
% measured wellhead pressure.
  f = calcWHP-realWHP;

% Remove ";" to display values to screen.
```

Figure B.3 func.m

B.4 The Liquid and Gas Density Scripts

```
function rhol = rholiq(pressure,temp)

% A simple liquid density model which takes pressure and temperature
% variations into consideration.

% Specify reference density for the liquid. Also specify B and alpha. If B
% and alpha are unknown, use water values in comments:
  rhoref = 750; %% reference density in kg/m3
  B = 2.2*10^9; %% bulk modulus of the liquid (2.2*10^9 Pa)
  a = 0.000207; %% volumetric thermal expansion coefficient (0.000207 K^-1)

  rhol = rhoref+(rhoref/B)*(pressure-100000)-(rhoref*a*(temp-293));
```

Figure B.4 rholiq.m

```
function rhog = rhogas(pressure,temp)

% Specify values or use values in comments:
  M = 16.04; %% molar mass methane (16.04 g/mol)
  R = 8.314;   %% universal gas constant in (8.314 J/(mol*K))
  zgas = 0.88;  %% z-factor for gas (0.90)

  rhog = M/(R*temp)*pressure/zgas;  %% desity of gas in g/m3
  rhog = rhog/1000; %% density of gas in kg/m3
```

Figure B.5 rhogas.m

Appendix C – MATLAB Output from SAC vs. DAC Study

This section contains all the MATLAB code output values from the SAC vs. DAC study in Chapter 7.5. The output values was used for further calculations.

Workspace

Name	Value
a	0
b	2.6962e+03
error	1
solution	2.6667e+03
TH	36.8000
TVD	2.6962e+03
TVDint	29.4979

Test A

Workspace

Name	Value
a	0
b	2.8624e+03
error	1
solution	2.8547e+03
TH	38.5000
TVD	2.8624e+03
TVDint	7.6871

Test B

Workspace

Name	Value
a	0
b	1703
error	0
solution	1.6573e+03
TH	26.6000
TVD	1703
TVDint	45.7349

Test C

Workspace

Name	Value
a	0
b	2.4166e+03
error	0
solution	2.3886e+03
TH	23.4000
TVD	2.4166e+03
TVDint	28.0245

Test D

Workspace

Name	Value
a	0
b	2395
error	0
solution	2.1065e+03
TH	276
TVD	2395
TVDint	288.4664

Test E

Workspace

Name	Value
a	0
b	1.7986e+03
error	1
solution	1.7714e+03
TH	38.6000
TVD	1.7986e+03
TVDint	27.2249

Test F

Figure C.1 Output A – F for SAC vs. DAC study

Workspace

Name	Value
a	0
b	2.3018e+03
error	0
solution	2.2445e+03
TH	36.9000
TVD	2.3018e+03
TVDint	57.3202

Test G

N/A

Know the volume is filled with liquid

Test H

Workspace

Name	Value
a	0
b	2.3379e+03
error	1
solution	2.3143e+03
TH	26.6000
TVD	2.3379e+03
TVDint	23.6159

Test I

Workspace

Name	Value
a	0
b	2.3082e+03
error	0
solution	1.8738e+03
TH	380.7000
TVD	2.3082e+03
TVDint	434.4429

Test J

Workspace

Name	Value
a	0
b	2395
error	0
solution	2.1037e+03
TH	276
TVD	2395
TVDint	291.3169

Test K

Workspace

Name	Value
a	0
b	1.7533e+03
error	1
solution	1.7187e+03
TH	38.6000
TVD	1.7533e+03
TVDint	34.6187

Test L

Figure C.2 Output G – L for SAC vs. DAC study

Workspace

Name	Value
a	0
b	2.3018e+03
error	0
solution	2.2566e+03
TH	36.9000
TVD	2.3018e+03
TVDint	45.1678

Test M

Workspace

Name	Value
a	0
b	2.4704e+03
error	1
solution	2.4520e+03
TH	38.5000
TVD	2.4704e+03
TVDint	18.3953

Test N

Workspace

Name	Value
a	0
b	1703
error	1
solution	1.6830e+03
TH	26.6000
TVD	1703
TVDint	20.0090

Test O

Workspace

Name	Value
a	0
b	2395
error	0
solution	2.0951e+03
TH	276
TVD	2395
TVDint	299.8501

Test P

Workspace

Name	Value
a	0
b	2.8624e+03
error	0
solution	2.7723e+03
TH	38.5000
TVD	2.8624e+03
TVDint	90.1488

Test Q

Workspace

Name	Value
a	0
b	2049
error	0
solution	1.8909e+03
TH	26.7000
TVD	2049
TVDint	158.0771

Test R

Figure C.3 Output M – R for SAC vs. DAC study